Differential Modulation of Trunk Muscle Activation using Thoracic Epidural Spinal Stimulation

by

Sydney Schadan

A thesis submitted in partial fulfillment of the requirements for the degree of

Master of Science

Department of Mechanical Engineering
University of Alberta

Abstract

Trunk stability and control in a world of gravitational forces and perturbations requires coordinated trunk muscle activation through involvement of control mechanisms within the neuromuscular system. Individuals with spinal cord injury (SCI) often suffer under impaired trunk control and posture, which may lead to physical limitations, including the inability to sit upright and perform common reaching tasks. Such impairment can also result in secondary health complications, particularly pressure sores, kyphosis, or compromised internal organ function. Epidural spinal stimulation (ESS) delivers electrical current to the dorsal spine to selectively activate motor pools within the spine, allowing for targeted muscle activation and improved functional outcomes following SCI. ESS has been used to evoke trunk muscle responses and demonstrated promising functional improvements in trunk control and posture following SCI, including improved trunk extension, and forward and lateral reaching. Current anatomical knowledge suggests that trunk muscles are innervated within the upper and lower thoracic regions of the spine. In spite of this, previous studies employing ESS for the purpose of trunk muscle activation have been limited to stimulation above the twelfth thoracic (T12) to first lumbar (L1) vertebral levels. Moreover, the majority of work to date has focused on characterizing functional outcomes, with less emphasis given to advancing our systematic understanding of the muscle responses to ESS. Therefore, the objective of this thesis was to further our understanding of the relationship between epidural spinal stimulation and activation of spinal circuitry and muscle activation in the domain of trunk stability and control. Within this domain, a study was performed to investigate trunk muscle activation in response to ESS at varying stimulation locations above the thoracic spine. A 16- or 32- electrode array was implanted above two adjacent vertebra levels within the fourth thoracic (T4) to tenth thoracic (T10) vertebral range of 13 participants. Data from 11 participants were analyzed.

Electromyography data were collected bilaterally from the external obliques, internal obliques, and rectus abdominis, as well as unilaterally from the erector spinae muscles at one thoracic (T7) and one lumbar level (L3). The amplitude and timing of evoked muscle responses were quantified while stimulation location along both the rostrocaudal and mediolateral axes of the spine was systematically manipulated. ESS delivered between the T6 and T10 vertebrae evoked responses in all trunk muscles resulting in average motor thresholds and onset latencies of abdominal muscles from ipsilateral stimulation ranging from 1.5 to 2.0 μC and 7.4 to 9.2 ms, respectively; however, stimulation between the T8 and T10 vertebrae demonstrated lower motor thresholds and shorter onset latencies. ESS evoked responses in both ipsilateral and contralateral muscles; however, on average 2.4 times greater maximum response amplitudes, 30% lower motor thresholds, and 0.9 ms shorter onset latencies were seen for ipsilateral stimulation compared to contralateral stimulation. All abdominal muscles demonstrated constant onset latencies with increasing charge applied, which is consistent with activation of afferent pathways. The presence of shorter onset latencies at higher applied charges in the responses recorded in the erector spinae muscles provided evidence for activation of both afferent and efferent pathways. The results from this study demonstrate the influence of stimulation location on trunk muscle activation via thoracic ESS. The results may guide electrode placement for future rehabilitative applications aiming to improve trunk control and posture following SCI via ESS. Future work is required to determine the transferability of results to less-invasive spinal stimulation approaches.

Preface

The following work is a collaboration between the University of Alberta (Edmonton, Alberta, Canada) and Houston Methodist Research Institute (Houston, Texas, United States). The research objective was formulated by Dr. Dimitry Sayenko and Dr. Albert Vette in the context of their ongoing research collaboration. The experimental protocols were designed by myself in collaboration with Dr. Dimitry Sayenko and Dr. Albert Vette. Experimental data were collected at Houston Methodist Hospital, led by Dr. Amir Faraji and assisted by Dr. Dimitry Sayenko and Dr. Alexander Steele. The literature review, data processing and reduction, data analysis, data conceptualization and visualization, as well as result interpretation and discussion were my original work under the supervision of Dr. Albert Vette. I also wrote the original drafts of both the thesis and manuscript, which were reviewed by Dr. Albert Vette and Dr. Dimitry Sayenko. The work presented in this thesis, including the experimental protocols, primary findings, and discussions, has been submitted as an original research article titled "Differential modulation of trunk muscle activation using thoracic epidural spinal stimulation" to the journal Scientific Reports. The primary findings and discussions presented in this thesis are coherent with the content of this manuscript, with certain paragraphs included verbatim. In addition, I have contributed to the following conference submissions that are associated with the work in this thesis:

- Wedemeier, K., Shaik Gadda, A., **Schadan, S.**, Steele, A., Faraji, A., Sayenko, D. & Vette, A.H. Modeling the dynamics between single-pulse epidural spinal stimulation and trunk muscle activity: a system identification study. *16th World Congress of the International Neuromodulation Society* (Vancouver, British Columbia, Canada, May 11–16, 2024).
- **Schadan, S.M**., Steele, A., Faraji, A., Sayenko, D.G. & Vette, A.H. Stimulation-dependent characterization of trunk muscle responses to single-pulse epidural spinal stimulation. *2023 Annual Meeting of the Society for the Neural Control of Movement* (Victoria, British Columbia, Canada, April 17–21, 2023).
- **Schadan, S.M**., Rouhani, H., Sayenko, D.G. & Vette, A.H. Stimulation-dependent quantification of trunk muscle responses to single-pulse epidural spinal stimulation. *23rd Annual Alberta Biomedical Engineering Conference* (Banff, Alberta, Canada, October 21–22, 2022).

This project was partially funded through a Discovery Grant (RGPIN-2021-04041), a Discovery Grants Accelerator Supplement (RGPAS-2021-00043), and a Canada Graduate Scholarship (CGS-M), all from the Natural Sciences and Engineering Research Council of Canada (NSERC). All participants provided informed consent to experimental procedures which were approved by the Institutional Review Board of Houston Methodist Research Institute under protocol Pro00023336.

Acknowledgments

It is with a great honour that I have had the opportunity to work with my supervisor, Dr. Albert Vette. My journey with Albert began during my undergraduate summer research and continued into my MSc studies. Albert has been a truly exceptional leader and mentor who has inspired my passion for research. Albert, I cannot thank you enough for the countless hours you've invested in meetings and thesis revisions, no matter the time zone you were in. I aspire to carry forward your meticulous attention to detail, ensuring that no spelling or grammar mistake goes unnoticed – and I hope I've mastered the difference between 'effect' and 'affect'. Your support has been invaluable throughout my journey as a MSc student, not only academically but also in shaping my professional career path.

I would also like to extend my gratitude to our collaborator, Dr. Dimitry Sayenko. Your willingness to teach and share your knowledge in the medical field, particularly on concepts that were new to me as someone with an engineering background, has been invaluable. Your field of research has inspired me, and I look forward to seeing the future of this research field. I would also like to acknowledge our project collaborators Dr. Alexander Steele and Dr. Amir Faraji, without whom this project would not have been possible.

I am incredibly grateful to my family for their unwavering support, cheering me on at every step of this journey. I couldn't have done it without you. Finally, I am deeply grateful for my fiancée, Gavin, for his endless support and patience as I talked for hours about my research. Gavin, you provided the encouragement and motivation to keep me going throughout it all.

Table of Contents

List of Tables

List of Figures

1 Introduction

1.1 Trunk Stability and Control

Maintaining a balanced and stable body posture is essential for coordinated and controlled movements which minimize required effort during daily activities. However, in a dynamic world full of gravitational forces and disturbances, even seemingly simple tasks, such as reaching to grab a glass on the table or remaining upright on a bus that suddenly stops, can challenge one's postural stability. The trunk, being the body segment with the greatest mass, plays a pivotal role in maintaining postural control and stability of the human body. Control and stability of the trunk is crucial even for seemingly unrelated tasks. For example, the trunk must remain stable while running to prevent falling or remain upright to enable proper expansion of the lungs. Thus, trunk stability and control take on a pivotal functional role in daily life.

The neuromuscular system within the human body serves as a network of neurons relaying electrical and chemical signals to transmit information between muscles and the central nervous system. It is through these complex networks that the human body can contract muscles enabling voluntary movement, such as walking or running, or involuntarily movement, such as reflexively pulling your hand away from a hot stove. Similarly, the neuromuscular system can maintain, through a series of passive and active control mechanisms[1], a stable trunk posture in a world full of perturbations challenging this stability. Through voluntary and/or involuntary coordinated trunk muscle activation, the neuromuscular system can increase trunk stiffness and facilitate trunk movement to maintain trunk stability and control[1,2].

1.2 Impaired Trunk Stability and Control Following Spinal Cord Injury

Neuromuscular impairment, such as chronic spinal cord injury (SCI), can affect sensory and motor functions below the site of injury. Among other consequences, individuals with cervical or thoracic SCI often face impaired muscle function in the lower and upper limbs as well as the trunk. Impairment to trunk muscle activation can impair one's trunk stability and control[3]. A lack of trunk stability and control jeopardizes one's ability to sit upright and perform routine tasks which require a stable upright posture, such as reaching tasks. Furthermore, such impairment can also result in severe secondary health complications, such as pressure sores, spasticity, and compromised

internal organ function[4]. Since such consequences can greatly impact independence and quality of life, it is not surprising that affected individuals view restoring trunk stability as a top priority in their rehabilitation objectives[5].

1.3 Technologies for Improving Trunk Stability and Control

Some conventional technologies, including tilted wheelchairs, belts, or braces, aim to passively increase trunk stability following SCI. Alternatively, active technologies emerged to purposefully engage the neuromuscular system to activate relevant skeletal muscles and enhance mobility and posture. Transcutaneous spinal stimulation (TSS) is one of such approaches, which non-invasively delivers electrical pulses to the dorsal spinal cord activating spinal circuitry projecting to targeted muscles[6]. Spinal stimulation can produce motor responses via Ia afferents synapsing on α-motoneurons, but can also activate other neural entities within the spinal cord, including interneurons, ascending sensory fibers, and descending motor tracts[7–16]. In the domain of upper body function, TSS has demonstrated promising functional outcomes following SCI, including improved trunk control and upright posture[17,18]. Moreover, TSS in combination with physical therapy has shown immediate and sustained improvements in upper body sensory and motor function in SCI populations, demonstrating the potential for neuroplastic changes within spinal networks[19,20].

TSS can induce muscle responses depending on stimulation location, frequency, intensity, and pulse width. The objective quantification of these muscle responses using electromyography (EMG) serves as a valuable tool to guide parameter selection for stimulation applications. Recent data demonstrate that TSS can differentially activate upper[15,16] and lower limb muscles[21–23], based on the anatomical arrangements of targeted motor pools located along the rostrocaudal and mediolateral axes within the cervical and lumbosacral enlargements, respectively. The configuration of optimized stimulation can direct electric fields toward specific subsets of dorsal root entry zones, thereby modulating selected ensembles of motor neuron pools. Such approach aids in promoting specific motor functions with greater precision and objectivity, aligning with the priorities of targeted neurorehabilitation[24]. In this context, spatial mapping of spinal motor pools within the thoracic spinal cord projecting to trunk muscles holds significant clinical and electrophysiological implications. At the same time, spatial mapping of thoracic motoneurons

using TSS poses challenges due to relatively high stimulation intensities required for the electrical current to activate the motoneurons and the proximity of the stimulation site to the recorded muscles. Consequently, due to the brief latency between the stimulation event and the onset of the evoked motor response, the evoked motor responses are frequently obscured by stimulation artifacts in the EMG recordings. This poses difficulties not only in evaluating response latency, but also in discerning small evoked responses from substantial artifacts. In this light, epidural spinal stimulation (ESS) can offer a viable solution for mapping the motor pools located in the thoracic spinal cord. The proximity of stimulating electrodes during ESS to the dorsal roots entering the spinal cord results in significantly smaller electrical current requirements for activating the Ia afferents compared to TSS. Consequently, this mitigates the issue of large stimulation artifacts obscuring the evoked responses. Importantly, findings from ESS studies are transferable to and suggest similar outcomes for TSS applications[10,22,25,26].

In the context of trunk control and stability, ESS has been used to investigate EMG responses in select trunk muscles[27]. Such studies have been limited to stimulation locations within the lower thoracic (T11) to upper lumbosacral (L1) levels, although Rowald et al. suggested stimulating additional thoracic dorsal roots for improved trunk muscle activation and postural stability[28]. Furthermore, individuals with low thoracic SCI demonstrate better dynamic sitting stability than high thoracic SCI, implying that trunk muscle innervation for trunk stability is more likely occurring in the high thoracic region[29]. This is in line with current neuroanatomical knowledge of the thoracic innervation of several trunk muscles relevant for trunk stability and control[30,31], e.g., the rectus abdominis, internal obliques, and external obliques.

1.4 Thesis Objectives

Spinal stimulation, as a relatively novel and promising technique, still holds questions regarding targeted spinal structures and the mechanisms by which spinal network activation enables selective muscle activation and improved functional outcomes, and this in dependence of stimulation location relative to the spine. The objective of this thesis was to further our understanding of the complex relationship between spinal stimulation and the neuromuscular system as it relates to trunk control and stability. Within this domain, and based on the considerations above, a study was performed with the objective of systematically investigating the relative recruitment selectivity of

different motor pools projecting to trunk muscles, using ESS along the rostrocaudal and mediolateral axes of the thoracic spinal cord. Spatial mapping of trunk muscles from thoracic ESS may guide future targeted spinal stimulation applications, both invasive and non-invasive, for restoring trunk stability and control following neuromuscular impairment.

1.5 Thesis Outline

Chapter 2 provides background knowledge of relevant anatomy and physiology of the neuromuscular system. EMG as a measurement tool of the neuromuscular activity is also described. These topics are then linked to postural control and stability through discussion of neuromuscular involvement. An overview of the literature investigating ESS as a technique for facilitating muscle function following SCI, and more specifically, trunk control and stability, is also provided. Chapter 3 describes an experimental study investigating the effect of manipulating ESS stimulation location along the thoracic spine on trunk muscle activation. Chapter 4 presents results from the experimental study, and Chapter 5 discusses them in the context of existing literature. Chapter 6 summarizes the significance of the key findings in the context of improving trunk control and stability following neuromuscular impairment, such as SCI.

2 Literature Review

ESS delivers electrical current to the dorsal spinal cord to activate targeted spinal networks. This chapter provides a deeper understanding into the mechanisms by which ESS can improve muscle function, including trunk control and stability, following SCI through exploration of three domains: (1) relevant anatomy and physiology of the neuromuscular system and EMG as a measurement tool, (2) the involvement of the musculoskeletal system in trunk control and stability, and (3) current literature involving ESS for improved muscle function following SCI.

2.1 Anatomy of the Spine

2.1.1 The Neuron

A neuron is a specialized cell found within nervous tissue and can be divided into four main components: the cell body, dendrites, axon or nerve fibre, and axon terminal or nerve ending[32,33]. The cell body contains the nucleus and other organelles important for cell life. A dendrite is a branch protruding from the cell body that receives chemical or electrical signals from nearby cells. An axon is a conducting structure that can transmit electrical signals within the body, sometimes over distances greater than one metre[34]. Lastly, an axon terminal is used to transmit signals to nearby structures, such as another neuron or muscle cell, through the release of chemicals known as neurotransmitters[32,33].

Neurons have an excitable membrane that can rapidly alter ion flow, enabling transmission of electrical and/or chemical signals to relay information within the nervous system[33,35]. Neurons are often grouped according to function and location. Neurons transmitting sensory information from sense organs (e.g., skin receptors) toward the central nervous system are known as afferent or sensory neurons[33]. Neurons carrying information from the central nervous system to the peripheral nervous system are known as efferent or motor neurons. Efferent neurons can be classified as somatic (i.e., targeting skeletal muscles) or visceral/autonomic (i.e., targeting internal organs)[33]. Interneurons relay information between motor and sensory neurons and are located within the spinal cord[33]. Bundles of neurons are called nerves. A tract is a group of nerves with a similar location and function, and groups of tracts with related functions are called nerve pathways[36].

2.1.2 The Spine

The Vertebral Column

The vertebral column is a long, central structure that extends from the base of the skull to the tailbone. Its trabecular bony structure provides support and stability to the body, protection to the inner spinal cord, and allows for body movement[35,37,38]. The vertebral column is composed of 33 vertebrae stacked in a curved, vertical structure[37,38]. Typically, each vertebra consists of a rounded vertebral body, facing anteriorly, with a vertebral arch, facing posteriorly[37–39]. The vertebral body enables weight-bearing, and the vertebral arch provides attachment sites for muscles and ligaments[37]. A space in the centre of each vertebra, known as the vertebral foramen, contains the spinal cord[39]. The size and shape of each vertebra varies, with larger vertebrae located more inferiorly and smaller vertebrae more superiorly[38]. Most vertebrae are separated by intervertebral discs (i.e., layers of fibrocartilage) and held together by a series of ligaments[35,37,38]. This structure prevents excessive movement (i.e., separation or sliding) while enabling flexion and extension, rotation, and some lateral flexion of the upper body[38]. The varying shapes and sizes of adjacent vertebrae contribute to a distinct curvature of the vertebral column in the sagittal plane which allows for absorption of compressive forces[38].

Each vertebra defines one level of the vertebral column, which can be identified using palpation of the prominent vertebral arch on the posterior side[38]. The vertebral column can be divided into five regions according to morphology, location, and function: cervical, thoracic, lumbar, sacral, and coccygeal[37–39]. The cervical region is the most superior region along the vertebral column, containing seven vertebrae (denoted as C1 to C7)[38]. The cervical region connects the more inferior vertebral column to the skull and enables movement of the head and neck. Beneath the cervical region is the thoracic region, consisting of twelve vertebrae (T1 to T12). This region is more rigid than the cervical region due to more viscous intervertebral discs, as well as the connection of the vertebrae to the ribcage (one rib on either side of each vertebra) and sternum[38]. Stiffness of the thoracic region is beneficial for the protection of major organs, such as the heart[38]. The next five vertebrae define the lumbar region (L1 to L5), characterized by stronger and denser ligaments[38]. The most inferior regions are the sacrum consisting of five fused vertebrae (S1 to S5) and the coccygeal with four vertebrae, (Co1 to Co4), three of which are often fused[38,39].

The Spinal Cord

The spinal cord is a cylindrical collection of ascending and descending neurons, located within the vertebral column, that relays information between the brain and the peripheral nervous system[32,36,39]. The spinal cord is composed of two types of nervous tissue called gray matter and white matter[36], as presented in Fig. 1. Grey matter forms the centre of the spinal cord cross-section in the shape of the capital letter 'H', or a butterfly, and is composed of neuronal cell bodies, dendrites, axons, supporting cells, and blood vessels[36]. The two dorsal and ventral 'arms' of the 'H' are called the dorsal and ventral horns, respectively[36]. White matter surrounds the grey matter and is mainly composed of longitudinal columns of myelinated neuron axons[32], often grouped into tracts and nerve pathways by function[36]. White matter also contains supporting cells and blood vessels[36]. Grey matter divides the white matter into dorsal, lateral, and ventral regions. The spinal cord is surrounded in protective outer layers of tissue known as the meninges, composed of the pia mater, arachnoid mater, and dura mater[32]. The space between the arachnoid and pia, i.e., the subarachnoid space, is filled with cerebrospinal fluid. The purpose of cerebrospinal fluid is to add protection and provide a pathway for nutrient delivery[39]. The epidural space describes an added layer of space between the spinal cord and vertebral column[32], containing fat, lymphatic tissue, and blood vessels.

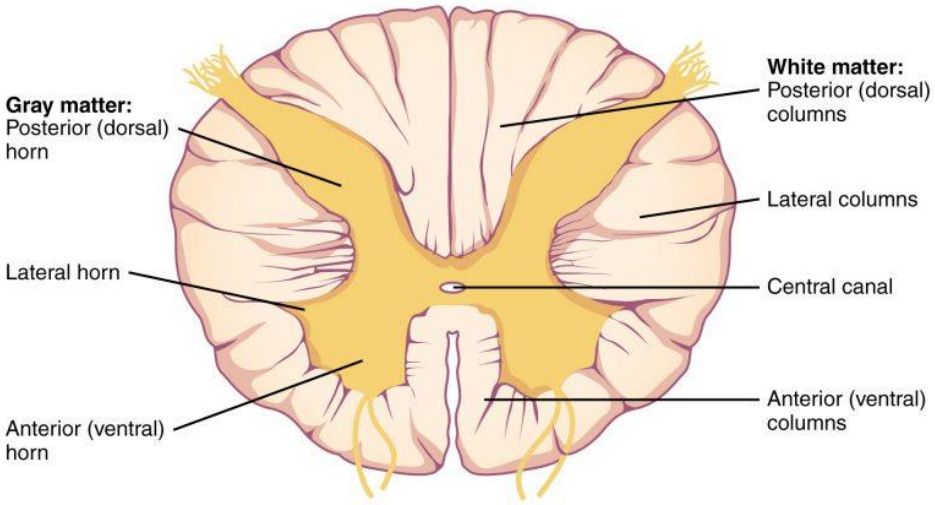

Figure 1. Transverse cross-section of the spinal cord. Gray matter forms an 'H'-shape surrounded by white matter. The anterior and posterior 'arms' of the 'H' are known as the ventral and dorsal horns, respectively. Retrieved from (Bega et al., 2019), licensed under Creative Commons Attribution-ShareAlike 4.0 International (CC BY-SA)[40].

The average transverse and anteroposterior diameter of the spinal cord varies along its length in the range of 4.7 to 13.3 mm and 3.9 to 8.3 mm, respectively[41]. With an average length of 42 to 45 cm[36], the spinal cord is shorter than the vertebral column and typically aligns with the C1 to L1/L2 vertebrae levels[32,36,39,41,42]. However, the length of the spinal cord may vary according to body posture (e.g., supine versus erect, neck flexion versus extension)[43]. Similarly, body position can change the position of the spinal cord within the vertebral column. For example, lying in a prone position can cause an anterior shift of the lower thoracic spinal cord, likely due to gravity[44]. Lastly, commonly observed variability across non-disabled adults can also affect positioning of the spinal cord within the vertebral column. The midline of the spinal cord is generally assumed to align with the midline of the vertebral column; however, the midlines have been found to vary up to 2 mm[44]. This observation may be the result of asymmetrical left/right spinal root lengths, asymmetrical vertebrae, or scoliosis[44].

Spinal Innervation and Organization

Sensory and motor information is relayed between the peripheral and central nervous systems through 31 pairs of grouped afferent and efferent nerves, called spinal nerves[42,45]. Spinal nerves enter or exit the spine through gaps between the vertebrae, called the intervertebral foramen[36]. Prior to reaching the spinal cord, each spinal nerve divides and connects to the spinal cord on the anterior and posterior sides[42,45]. The locations where the spinal nerve connects to the anterior and posterior spinal cord are called the ventral and dorsal root, respectively[42]. Dorsal roots carry sensory fibres, whereas ventral roots carry motor and some sensory fibres[32,42,45].

The human spinal cord can be divided along the rostro-caudal axis into 31 segments: eight cervical (denoted as C1 to C8), twelve thoracic (T1 to T12), five lumbar (L1 to L5), five sacral (S1 to S5), and one coccygeal (Co1)[32,36,42]. Unlike the vertebral column, which is composed of individual vertebra, the spinal cord is one continuous structure. The spinal cord is segmented according to spinal nerve or dorsal root innervation. As mentioned previously, prior to spinal innervation, a spinal nerve passes through the intervertebral foramen between two vertebrae. In the cervical region, spinal segments are named according to the vertebra located just below where the innervated spinal nerves enter the spinal cord through the intervertebral foramen. For example, the spinal segment that corresponds to the spinal nerve entering just above the C1 vertebra is labelled as the C1 segment[36]. This naming convention changes at the C7 vertebra. At this vertebra, one

spinal nerve innervates above C7, labelled as C7, and one innervates below the C7 vertebra, labelled as C8. This gives the cervical spinal cord 8 segments despite the cervical vertebral column only having 7 segments. Caudal to the C8 spinal level, the spinal segments are named based on the vertebra below which the nerve enters the spinal cord. A visual representation of the alignment between the levels of the vertebral column and the segments of the spinal cord is presented in Fig. 2. Note, however, that significant variation across individuals in the rostrocaudal location of the spinal cord segments in relation to vertebral levels exists, which decreases the accuracy of this model[46].

A spinal segment can be further categorized according to the role of the sensory and motor neurons that innervate the segment. A dermatome describes the region of skin connected to one spinal segment by sensory neurons in one spinal nerve[47]. Similarly, a myotome describes a voluntary skeletal muscle group connected to one spinal segment by motor neurons in one spinal nerve. Fibres within a muscle may be innervated by motor neurons from different spinal segment levels[47]. Kendall et al.[30] identified the spinal segments which correspond to various muscle groups. The results for trunk muscles relevant to this thesis are presented below in Fig. 2.

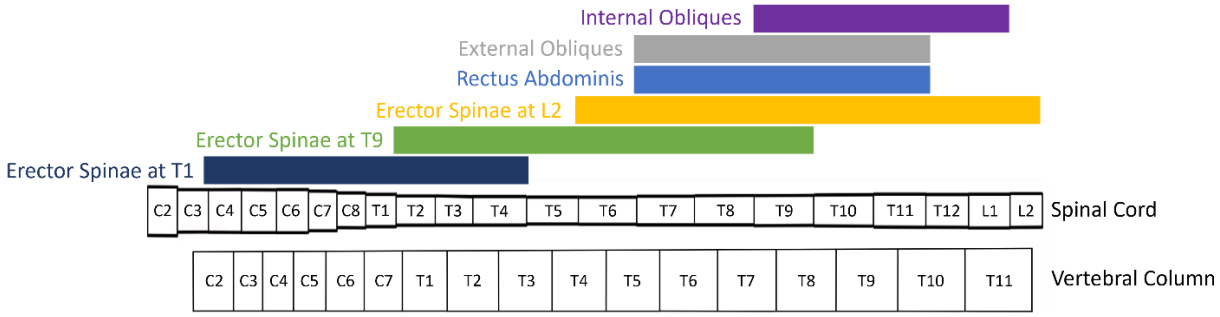

Figure 2. Alignment of the vertebral column (C2 to T11) and spinal segments (C2 to L2) according to Mendez et al., 2021[31]. Muscle innervation zones of the spinal cord according to Kendall et al., 1993[30]. Zones agreed upon by five or more sources are shown; however, some sources (3 to 4) agree that certain muscles may have a wider spinal innervation range. Specifically, the rectus abdominis may range from T5 to T12, external obliques from T7 to L1 and internal obliques from T7 to L1.

Along the longitudinal axis, ascending sensory nerves form columns transmitting signals toward the brain and are grouped into tracts based on function[39]. For example, white matter on the dorsal side of the spinal cord predominantly contains sensory tracts of the dorsal column medial lemniscus system (often called 'dorsal columns') responsible for sensory information including discriminative touch, vibration sensation, and awareness of joint positioning[39]. Similarly, motor fibres form columns descending the spinal cord, carrying information away from the brain. For example, white matter on the lateral side of the spinal cord contains descending corticospinal tracts responsible for voluntary muscle movement[39]. Intersegmental neurons are shorter than sensory and motor neurons and begin and end within the spinal cord. Their purpose is to relay information between neurons within the spinal cord.

Generally, signals are relayed to and from the brain using these ascending and descending pathways. However, reflex pathways allow signal transmission within the grey matter of the spinal cord without input from the brain (i.e., involuntary)[39]. In a reflex pathway, the afferent neuron may directly (i.e., monosynaptic) or indirectly through interneurons (i.e., polysynaptic), synapse with the efferent neuron within the spinal cord[39]. This allows signals from sensory fibres to initiate a motor response without receiving input from the brain. One such reflex pathway is a 'stretch reflex'. When a muscle is stretched, sensory receptors in the muscle detect changes in the length and stiffness of the muscle. As a result, signals are transmitted through a reflex pathway in the spinal cord, which synapses with a motor neuron to trigger a contraction of the muscle[39]. This pathway is important for preventing the muscle from over-stretching, for maintaining balance, posture, and muscle tone[39], and for keeping the muscle at its optimal length.

2.2 Anatomy and Physiology of Skeletal Muscle and its Activation Pathway

2.2.1 Anatomy of Skeletal Muscle

Skeletal Muscle

The muscular system contains three types of muscle tissue: (1) cardiac, (2) smooth, and (3) skeletal[48,49]. All muscle tissue is composed of muscle cells or fibres which, unlike other cells, have the ability to contract (i.e., shorten) and subsequently relax (i.e., lengthen)[50]. Cardiac muscle is located within the walls of the heart and is unique for its ability to produce action potentials spontaneously without input from the nervous system[49]. Smooth muscle produces slow,

involuntary contraction and is found in internal organs such as blood vessels[49]. Skeletal muscle is the most common muscle tissue found within over 600 skeletal muscles in the human body[50]. Skeletal muscle is most commonly attached to bones of the skeleton to produce movement of the human body when triggered by the connected nervous system[49]. It also acts to provide structure and support to the body and to produce heat[48].

Skeletal muscle can be decomposed into a hierarchical structure, as presented in Fig. 3. The smallest units of skeletal muscle are two myofilaments called myosin and actin[48,50]. Myosin is a thick protein filament and actin is a thin protein filament[49,50]. Myosin and actin units lie adjacently to form a sarcomere and provide the mechanism by which muscle fibres can shorten and lengthen[50]. Repeating sarcomeres form a myofibril and many myofibrils form a specialized cell known as a muscle fibre. Muscle fibres are surrounded by a membrane called a sarcolemma[50]. Within the muscle fibres exist storage units of calcium ions, called sarcoplasmic reticulum, which will be discussed further in Section 2.2.2[50]. Multiple muscle fibres form a fascicle and bunches of adjacent fascicles form a muscle[48,50]. Once combined, a muscle can be composed of thousands of muscle fibres[48].

Fibrous connective tissue surrounds the units within skeletal muscle to provide protection and house blood vessels for supplying nutrients to the muscle. There are three types of connective tissues present within skeletal muscle: (1) endomysium, (2) perimysium, and (3) epimysium[48]. Tendon, a strong connective tissue, attaches skeletal muscle to bone to transfer the force produced by means of a muscle contraction to pull the bone[48,50]. Muscles are often attached to two or more bones/tendons, allowing for multiple functions[50]. Fascia surrounds muscle to add support and provide a smooth surface to minimize friction caused by movement[49].

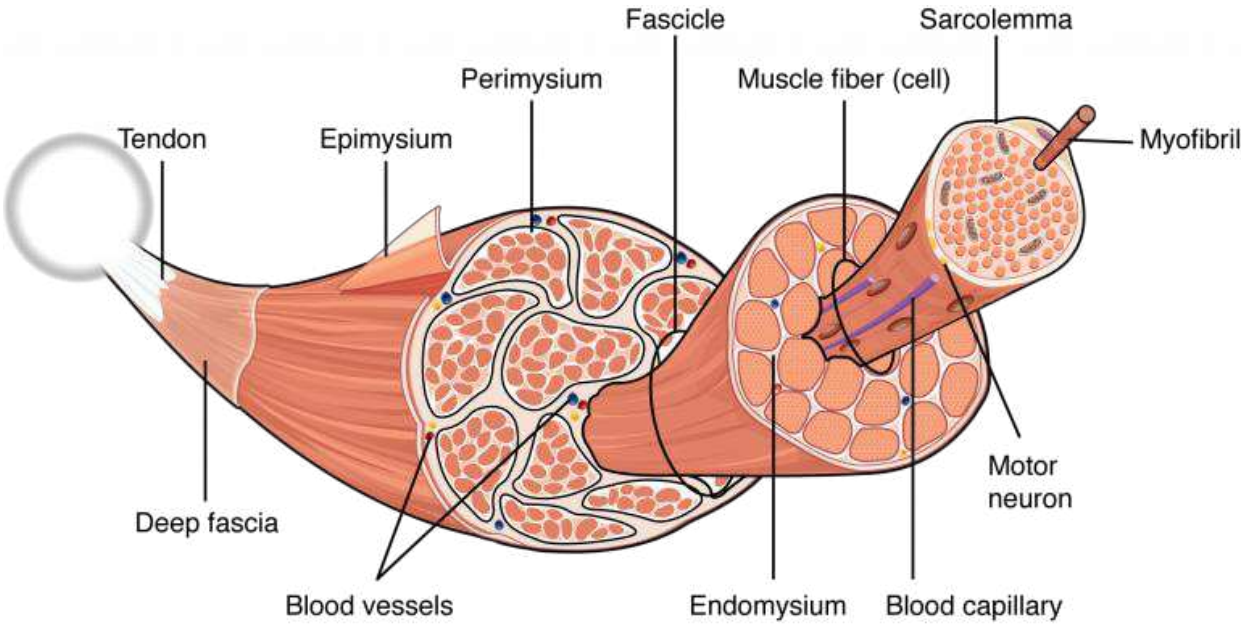

Figure 3. Hierarchical structure of skeletal muscle. Many myofibrils form a muscle fibre surrounded by sarcolemma. Multiple muscle fibres form a fascicle, and multiple fascicles form a muscle. Endomysium, perimysium, and epimysium make up the connective tissue found within skeletal muscle. Retrieved from (Bega et al., 2019), licensed under Creative Commons Attribution-ShareAlike 4.0 International (CC BY-SA)[40].

The Motor Neuron

Motor or efferent neurons are responsible for transmitting information from the central nervous system to the peripheral nervous system. Motor neurons within the nervous system can be categorized into upper and lower motor neurons. Upper motor neurons are located within the brain with relatively shorter axons transmitting signals to the spinal cord. Lower motor neurons are located within the spinal cord and are responsible for transmitting signals longer distances to tissue in the peripheral nervous system, such as muscles. Lower motor neurons that extend to skeletal muscle are known as somatic motor neurons[51]. The cell body of a somatic motor neuron is commonly found within the ventral horn of the spinal cord[51] and the axon extends through the ventral spinal root toward the skeletal muscles it innervates. A motor neuron and the innervated muscle fibres (ranging from two to hundreds) form a motor unit[50]. The point of connection between a motor neuron and a muscle fibre is called a neuromuscular junction or motor endplate[50,51].

2.2.2 Physiology of Skeletal Muscle Contraction

To evoke a voluntary movement, signals must be initiated in the brain and transmitted to relevant muscles. This is enabled through signal propagation and transmission within and between neurons in the nervous system.

Signal Transmission

Potassium, sodium, and chloride ions exist inside and outside a neuron, across the cell membrane, and in the intracellular fluid and extracellular fluid, respectively[52]. The cell membrane of the cell body and dendrites enables *passive* and *active* diffusion of the ions[52,53]. Ions *passively* diffuse according to a balance of concentration and electrical gradients (i.e., electrochemical gradients) using protein channels embedded in the membrane[52]. At rest, potassium flows through a potassium channel along its concentration gradient into the cell, while some ions return along the electrical gradient. Simultaneously, a sodium-potassium pump *actively* (i.e., using energy) pumps sodium out of the cell and potassium into the cell against the electrochemical gradient[52,53]. This ion movement results in a greater concentration of potassium ions in the cell and a greater concentration of sodium and chloride ions outside the cell, creating a voltage difference across the membrane of approximately -70 mV[52,53]. This potential difference or cell polarization enables the excitable nature of a neuron at resting state[52].

An action potential describes a series of three events: (1) depolarization, (2) hyperpolarization, and (3) repolarization[53]. An action potential is initiated when a stimulant at the synapse shifts the cell membrane to a threshold voltage of -55 mV[52]. Once this threshold is reached, an action potential will occur in an 'all-or-nothing' nature, such that greater activation beyond -55 mV does not produce a greater action potential[52,53]. Once initiated, the membrane rapidly increases permeability to sodium ions into the cell, shifting the membrane potential away from resting potential, in a process known as depolarization[52,53]. This is followed by an increase in permeability to potassium ion movement out of the cell, acting to restore the potential back to its resting state[52,53]. Subsequently, permeability to the sodium and potassium ions returns to normal[53]. However, potassium channels return at a slower rate than sodium ones, causing the membrane potential to become more negative than resting potential, in a state known as hyperpolarization[52,53]. Finally, passive and active diffusion then restore the cell membrane to resting potential (repolarization).

Action potentials are initiated at the synapse of a neuron when a stimulant, such as a neurotransmitter, causes a rapid change in membrane potential. When a neurotransmitter connects with dendrites, they can cause the opening or closing of voltage-gated ion-specific protein channels within the membrane[33,53]. Increased or decreased ion permeability can result in excitatory or inhibitory responses[33]. An inhibitory response is triggered when the result of binding of the neurotransmitter hyperpolarizes the neuron[54]. One such example is gamma-aminobutyric acid (GABA) which, when bonded to the postsynaptic membrane, causes chloride channels to open[53]. When this occurs, the voltage-gated sodium channels are not opened, and an action potential does not occur. Conversely, an excitatory response is initiated when the result of binding of the neurotransmitter depolarizes the neuron and initiates an action potential[33]. One example of such an excitatory neurotransmitter is acetylcholine which, when bonded to the neuron, initiates the opening of sodium channels and subsequent depolarization of the cell[50,51,53]. An action potential is transmitted within a neuron with successive local depolarization of the membrane along the axon toward the axon terminal[52]. The speed at which an action potential propagates, known as conduction velocity, is affected by the diameter of the fibre and the presence of a myelin sheath surrounding the axon[52]. Larger fibres have quicker conduction velocities due to larger membrane surface areas and decreased resistance to current flow[52,53]. Myelin sheath describes an insulating layer around a neuron axon produced by Schwann cells. A gap between each Schwann cell, known as the node of Ranvier, allows an action potential to 'jump' from node to node, accelerating the conduction velocity along an axon[52]. Once an impulse reaches the nerve ending or axon terminal, it is transmitted through the release of neurotransmitters to the end target, such as another neuron or a skeletal muscle to initiate a muscle contraction[53].

Skeletal Muscle Contraction

When a nerve impulse from the spine reaches a neuromuscular junction, the muscle begins to contract[50]. The sliding filament mechanism describes the process by which a muscle can shorten or contract[49,50]. As discussed in Section 2.2.1, muscle fibres contain myosin and actin filaments lying adjacently in a sarcomere[49]. At rest, inhibiting proteins (troponin and tropomyosin) block binding sites along the actin filament to prevent myosin from binding, and the sarcolemma remains at resting potential[50]. When an electrical impulse reaches a neuromuscular junction, an excitatory neurotransmitter, acetylcholine, is released from the efferent neuron[50]. Acetylcholine binds to the

sarcolemma (i.e., outer membrane) of the muscle fibre, triggering an excitatory response of the membrane. A depolarization of the membrane occurs (i.e., sodium channels open and sodium flows in), which travels in both directions from the site of the neuromuscular junction, as well as toward inner muscle fibres along inward folds called transverse tubules[49]. Membrane depolarization triggers the release of calcium ions from the sarcoplasmic reticulum[50]. Calcium ions bind to the troponin and tropomyosin proteins, which removes them from their binding site. As a result, myosin can bind to the actin filaments, which initiates fibre shortening. Using energy in the form of adenosine triphosphate molecules (ATP), the myosin filament pulls the actin filament toward the centre of the sarcomere. As a result, all sarcomeres in a fibre shorten and the muscle fibre contracts[49,50]. This process is known as muscle twitch, which will last approximately 100 milliseconds[49]. When calcium ions become depleted, troponin and tropomyosin bind to myosin and block the myosin-binding sites once again[50]. The myosin and actin filaments then return to their original, lengthened state, and the sarcolemma repolarizes[50].

Muscle contraction induces a tensile force on a bone or joint; however, muscle relaxation cannot induce a compressive force. Therefore, movement requires coordinated contraction and/or relaxation of various muscles[50]. An agonist is the primary muscle responsible for inducing a movement. An antagonist is a muscle that, when contracted, has an opposing action to the desired movement, and relaxation may be required to enable certain movements. For example, contraction of the biceps brachii produces forearm flexion, whereas contraction of the triceps brachii located on the opposite side of the arm produces forearm extension. As a result, when performing a bicep curl (i.e., forearm flexion), the biceps brachii must contract (agonist muscle) while the triceps brachii relaxes (antagonist muscle) to induce the intended movement. Co-contraction of synergistic and antagonistic muscles can also exist to enable joints to achieve voluntary movements[50]. Co-contraction of synergistic muscles to an agonist can increase the force or control of a movement. For example, the brachialis, an upper arm muscle that flexes the forearm when contracted, works synergistically with the biceps brachii during forearm flexion of heavy weight[50]. Co-contraction of agonist-antagonist muscles is common in instances where increased stiffness or stability is required about a joint[55,56]. For example, the body may co-activate antagonist trunk and back muscles to maintain a stable, controlled posture during static or dynamic tasks[55,56].

The duration and strength of a muscle contraction must be adjusted for various movements. For example, holding a pencil requires a sustained muscle contraction, often described as tonic activation. Conversely, sprinting requires stronger, shorter muscle contractions often described as phasic activation. The duration of a muscle response can be controlled through the frequency of nerve signals delivered to the muscle. One nerve impulse produces a single muscle twitch, as described previously. However, trains of nerve impulses can produce a sustained contraction called tetanus[49,50]. For example, sustained contractions (i.e., tonic activations) are seen in trunk muscles when maintaining a stable upright posture while sitting, discussed further in Section 2.4.2. The frequency of nerve impulses delivered to a muscle can also affect the strength of a muscle contraction[49]. When muscle twitches overlap each other, the resulting muscle tension is a summation of the individual twitches and increases the muscle strength[49]. The strength of a muscle contraction can also be controlled by the number of motor units that are simultaneously activated, such that increasing the number of contracted muscle fibres increases the strength of the muscle contraction. During sustained muscle contraction of multiple motor units, the activated muscle fibres within a muscle may alternate to prevent fatiguing[49].

2.3 Electromyography

EMG is a technique that measures muscle activity through the detection of changes in electrical potential around a muscle fiber[57].

2.3.1 Data Collection

EMG data can be collected using an intramuscular electrode, either needle or wire, placed invasively into a muscle fiber[58]. Intramuscular electrodes are beneficial for their proximity to the fiber, reducing noise, signal contamination[59], and spatial low-pass filtering effects[58], discussed further in Section 2.3.3. Furthermore, intramuscular electrodes can reach deep, small, and/or occluded muscles[59]. However, intramuscular electrodes may cause discomfort to the patient due to their invasive nature[60]. Surface electrodes are a more common technique for EMG data collection which involve placing an electrode on the surface of the skin above the muscle of interest, typically between the innervation zone and end of the fiber[61]. The electrode is often placed parallel to the muscle fiber orientation to detect the profile of the electric potential distribution as it propagates beneath the surface electrode[61]. Surface electrodes are preferred for their less-invasive

nature; however, they face challenges resulting from the larger distance between the signal source and the electrode, such as spatial filtering effects and/or difficulty detecting the activity of deep, occluded muscles[59]. Moreover, surface electrodes can be affected by changes in skin resistance (i.e., dead cells, dirt, perspiration, etc.)[59] and unwanted signal contamination or noise[59], discussed further in Section 2.3.3. Unlike intramuscular electrodes, which detect electrical activity from individual muscle fibers, surface electrodes detect a summation of electrical signals from multiple muscle fibers beneath the electrode[62]. When electrical stimulation is used to evoke muscle responses (i.e., electrical activity), this signal summation is referred to as a compound muscle action potential or M-wave[61,62]. An electric potential distribution is detectable on the surface of the skin through a metal component in the surface electrode which converts the ionic current in the tissue to electron flow in the metal. This propagating electrical potential is sampled at a certain frequency[63] and then used as an analysis tool for muscle activity. EMG signals are measured with respect to a reference electrode, placed distant from the signal source, usually in an area without muscles, where the electrical signal is assumed to be neutral[59]. It is common to collect data from bipolar[59] or multipolar electrodes, rather than monopolar, to reduce noise and increase the selectivity of signals through differential amplification[59], discussed further in Section 2.3.2.

2.3.2 Data Processing and Analysis

Differential amplification is commonly used to pre-process EMG data collected from bipolar or multipolar electrodes[21,22,26,64]. Signals common among two or more electrodes are removed, and the remaining signal is amplified to reduce unwanted noise (i.e., crosstalk or artifacts). EMG data is also filtered to reduce noise (often at both high and low frequencies) using, for example, a band-pass filter[21,22,26,64] and/or notch-filter[21]. The amplified EMG signal is demeaned, to ensure the baseline signal is zero[22,26,64]. Noise contamination and baseline shifts must be removed to ensure further analyses, such as amplitude-based calculations, are accurate.

The quantitative analysis of EMG signal amplitude and timing can provide insight into relative muscle excitation and the timing of muscle activation[57]. In electrical stimulation studies, it is common to perform a post-stimulus analysis up to 50 and 100 milliseconds following stimulation onset for upper and lower limb muscles, respectively[65]. Amplitude, as a measure of muscle excitation, relates to relative muscle activation and force production[57]. Various techniques have been employed in the literature to quantify the amplitude of an EMG signal. Amplitude can be

measured by finding the average value of the rectified EMG signal, known as the average rectified value (ARV), mean rectified value (MRV), or mean absolute value (MAV)[61,66]. The root mean square (RMS) of the EMG signal is another common measure of amplitude[61,66,67]. RMS is calculated by squaring EMG data within a defined time window, calculating the average, and then calculating the square root of this value[61,66–68]. Amplitude is also often measured as the peak-to-peak value of the muscle activity[67,69]. Lastly, electrical stimulation studies often quantify EMG amplitude as the magnitude of the evoked potential or integrated EMG[21,22,26,64,70], which is calculated as the area under the full-wave rectified M-wave[67]. Integrated EMG can provide valuable insights into muscle force or strength[70]. Latency of evoked muscle responses is another common technique for quantifying EMG data used for the analysis of the timing of muscle activation[67]. In electrical stimulation studies, latency of evoked muscle responses can be measured as the time between the onset of electrical stimulation and the time when the detected electrical potential exceeds a percentage above baseline[67]. Stimulation studies have typically used three times the standard deviation of the baseline for onset detection[26]. The epoch, or time duration, of muscle activity following an electrical stimulation can also be quantified and used for analysis[10,26].

When datasets are compared across participants, muscles, or experimental variations, EMG data is often normalized to facilitate such comparisons[61,71]. Normalization techniques can vary based on the context of the experiment and the intended comparisons[71]. The most common and recommended normalization technique normalizes EMG data to the maximum voluntary contraction (MVC), either in the same task/context or in a standardized form[61,71]. A participant will contract the muscle at a maximum voluntary amount and all other activity is reported relative to this maximum value. This normalization technique is ideal for its physiological meaning and ease of interpretation[71]. Normalization to sub-maximal voluntary contractions, or muscle activation during a task that requires submaximal activation[71,72] can also be used. These methods are not recommended when observing an evoked muscle response, such as from electrical stimulation[71]. When observing evoked muscle responses, EMG data is normalized to the maximal M-wave amplitude[71]. This maximum value may be measured as a peak-to-peak amplitude, the area under the M-wave[22,26], or the average rectified amplitude of the M-wave[71] and occurs during stimulation at a supramaximal intensity. Supramaximal intensity may be determined from a recruitment curve[61] or input-output curve[73]. The intensity of an electrical stimulus can affect the number of recruited motor units[62]. The amplitude or integral of an evoked muscle response plotted

against increasing stimulus intensity produces a M-wave recruitment curve with a sigmoid-like shape, characterized by an initial exponential increase, a linear phase, followed by a plateau or stationary phase[61,67]. The exponential and/or linear phase describes the increasing recruitment of motor units in relation to increasing stimulation intensity[67]. A recruitment curve has two significant features: (1) motor threshold (MT); and (2) maximal compound muscle action potential which occurs at the maximal intensity[61]. MT is the minimum stimulation intensity which allows for the recruitment of motor units. This value can be determined from the start of the region of exponential increase on a recruitment curve. In transcranial magnetic stimulation applications, resting MT can be determined directly from EMG signals using the relative frequency method[65]. Using this approach, the motor threshold is the stimulation intensity which initiates a peak-to-peak amplitude greater than 50 μV in 5 of 10 trials[74] or, more recently, 10 of 20 trials to improve accuracy[75]. This range has been identified as a common noise range in EMG signals, and EMG signals exceeding this range are likely the result of muscle activity[65,74]. A recent study has challenged this threshold value and reliably evoked muscle responses distinguishable from noise with peak-to-peak amplitudes smaller than the traditional 50 uV threshold[76]. This is also seen in electrical stimulation studies using a MT of 20 μV[21]. In ESS studies, MT has also been defined as the stimulation intensity that produces a muscle response with an integrated EMG greater than the average plus three times the standard deviation of baseline in 2 of 3 trials[22]. Maximal intensity is the stimulation intensity at which the number of recruited motor units becomes saturated and does not increase further[61,73]. The maximal intensity can be determined from a recruitment curve as the intensity at the beginning of the plateau or stationary phase[61]. Using this technique, EMG signals can be normalized to the M-wave amplitude measured at a supramaximal stimulus (i.e., stimulation intensity 20% above maximal intensity)[61]. When this is not possible, due to limitations on stimulation intensity, for example, electrical stimulation studies have normalized to the maximum evoked response observed in a muscle[21]. Following normalization, comparisons between experimental variations are often performed using normalized amplitudes at a stimulation intensity above motor threshold but below maximal intensity.

2.3.3 Data Interpretation and Limitations

EMG amplitude and timing are affected by physiological and anatomical factors as well as variations in the data acquisition equipment which can present challenges and limitations to interpretation of surface EMG signals[57,71].

Surface electrodes experience impedance resulting from contact between the electrode and skin. This impedance can increase noise within the data as the ionic current travels through the skin. Various techniques aimed at reducing electrode-skin impedance include preparing the skin with ethyl prior to attachment or the use of gels or abrasive conductive pastes[68,72]. In addition to electrode-skin impedance, electrical signals must travel from the muscle source through biological tissue, which acts as a volume conductor, prior to reaching the electrode on the surface of the skin[58]. Tissue can have a spatial low-pass filtering effect which alters or deforms the data[58].

Surface electrodes can resolve electrical signals from unintentional sources, causing signal contamination or noise. The electrode may detect electrical signals from the heart, brain, nearby electronic equipment[59], or may experience powerline interference. Powerline interference is noise created from the equipment or cables involved in EMG data collection. Similarly, surface electrodes may detect signals from nearby muscles[58]. This phenomenon, known as "crosstalk", is one of the most common issues with interpretation of surface EMG data[58,59]. Various spatial filters can be used to reduce crosstalk including single-differential, double-differential, two-dimensional, or bulls-eye filtering techniques[77]. Signal artifacts can also contaminate EMG data and cause inaccurate interpretations of results. One example is a stimulation artifact common in electrical stimulation applications[59]. A stimulation artifact occurs when the surface electrode detects the electrical signal from the electrical stimulation source[59,62]. A stimulation artifact appears as muscle activity if not properly interpreted and may even overlap with the M-wave, thereby affecting amplitude and timing[62]. An additional electrode is often used to identify the stimulation artifact for offline data analysis[70,78]. Similarly, surface electrodes may detect movement or mechanical artifacts in which movement at the electrode interface or movement of the electrode data acquisition system creates unwanted noise[59].

Electrode size and shape, location and orientation along the muscle fiber, as well as the length, depth, inclination, and orientation of the muscle fiber with respect to the surface electrode may

affect the amplitude or frequency content of the EMG signal[58]. Environmental factors, including skin temperature or room temperature, and humidity can also affect EMG amplitude[71].

2.4 Postural Control and Stability of the Trunk

The trunk is the region of the body composed of the thorax, abdomen, and pelvis. As the trunk is the body segment with the greatest mass, its postural control is crucial for maintaining balance during static and dynamic tasks, such as reaching, sitting, or walking. Postural control is achieved through coordination between the sensory systems, central nervous system, and the musculoskeletal system[79].

2.4.1 Muscles of the Trunk

The musculoskeletal system enables movement of body segments. Through contraction of various muscles located within the trunk, trunk movement strategies may be produced that enable postural control and stability. The external and internal oblique muscle groups are located bilaterally on the anterolateral regions of the trunk, characterized by their angled fibre orientation[80]. The external obliques are located closest to the surface (i.e., more superficial), and under these muscles are the internal obliques[80]. These muscle groups enable trunk movement through synergistic contraction and relaxation, such that the oblique on one body side will contract while the contralateral oblique relaxes, producing lateral flexion or trunk rotation. Bilateral contraction of the obliques can enable trunk flexion and increased abdominal pressure[80]. Located under the internal obliques are the transverse abdominis muscles, extending from the spine to the middle of the anterior abdomen. Contraction of the transverse abdominis increases abdominal pressure[80]. The rectus abdominis muscles are located anteriorly on the abdomen. Contraction of the rectus abdominis generates trunk flexion and increased abdominal pressure[80]. The erector spinae muscles are located on the posterior side of the trunk, spanning its vertical length from the neck to the sacrum. The erector spinae muscles can be divided further into three columns, grouped by lateral to medial location: the iliocostalis, longissimus, and spinalis muscles. Each column can be further divided into three muscles, varying by origin and insertion location. Contraction of this muscle group moves the vertebral column to enable trunk extension, trunk rotation, and lateral flexion[80]. Also located on the posterior side of the trunk is the quadratus lumborum. Similar to the obliques, unilateral

contraction can produce ipsilateral lateral flexion[80]. The mechanisms by which trunk muscles enable postural control and stability will be discussed further in Section 2.4.2.

Trunk muscles also aid in additional functions, including movement of the upper and lower limbs as well as respiration. Muscles located superiorly on the trunk, including the pectoralis major and minor muscles, the deltoid muscles, and the latissimus dorsi muscles, are responsible for movement of the shoulders and arms[80]. Movement of the scapula is enabled by the serratus anterior muscles[80]. Conversely, trunk muscles located inferiorly on the trunk, including the gluteus maximus, gluteus medius, gluteus minimus, and piriformis muscles, support the movement of the hips and thighs[80]. Lastly, the diaphragm, and intercostal muscles located between the rib bones, produce movement to enable inhalation and exhalation[80].

2.4.2 Musculoskeletal Involvement in Trunk Control and Stability

The alignment of body segments, known as body posture[81], is an important consideration for balance and stability in an environment characterized by gravitational forces and perturbations[2]. Body posture is considered balanced when the vertical projection of both the centre of mass and the centre of gravity lies within the base of support[2,81]. Postural control mechanisms maintain this balanced and stable posture through coordination of the sensory systems – the visual[1,2,82], vestibular[1,2,82,83], and somatosensory systems[1,2,82] – as well as the central nervous system and the musculoskeletal system[79]. There are two main goals discussed in the context of postural control: (1) Postural orientation, for example during upright sitting[1,82] and (2) postural equilibrium, for example during forward reaching[1,82].

The body maintains a postural orientation that minimizes efforts against gravity[84], such as the vertically extended posture of the trunk, through passive and active mechanisms[1]. Passive stability of the trunk arises from rigid bone-on-bone contact, viscoelastic properties of muscles[1,84], intra-abdominal pressure[85], and the presence of soft tissue. Active stability results from increased trunk stiffness via continuous, involuntary, low-level activation of tonic trunk muscles, such as the erector spinae and transverse abdominis muscles[1,83,86]. Tonic co-activation of trunk flexors and extensors increases trunk stiffness to maintain an extended, upright posture and augment the stability of the trunk and spine[1,55,87–89]. Continuous, tonic activation is believed to result from the recruitment of slow muscle fibres which are fatigue-resistant[1].

Postural equilibrium describes coordinated sensorimotor strategies that maintain a balanced, stable posture when subjected to self-initiated or external perturbations[82]. When a perturbation is perceived, postural equilibrium may be maintained through reactionary or anticipatory postural adjustments[2,79,90] that are reflected in phasic muscle activity. Reactionary adjustments result when the individual was unaware that the perturbation would occur, such as when seated on a bus that abruptly stops[79]. Reactionary postural adjustments occur after a perturbation to return the body to postural equilibrium as in feedback control[91]. Such adjustments are often compensatory movements to alter the geometry of the body and keep the centre of mass within the base of support via movement at the hip or lower lumbar spine[2,82,92] or via rotation of the trunk and pelvis during unstable sitting[93]. Co-contraction of back (e.g., latissimus dorsi, erector spinae) and abdominal muscles (e.g., rectus abdominis, external/internal obliques) following a trunk perturbation may also occur to oppose the perturbation[88,94] and increase intraabdominal pressure which reduces compressive loading on the spine[94–96]. More commonly, in daily tasks, an individual is aware of the perturbation that will occur, such as the offset of trunk balance during forward reaching. This may result in anticipatory postural adjustments to minimize the impact of the foreseen perturbation on postural equilibrium. Milosevic et al. demonstrated that an anticipated external perturbation results in quicker trunk stabilization[97]. This, in part, may be explained by postural adjustments *prior* to an anticipated perturbation activated in a feed-forward manner[2,90,91]. An individual may pre-activate flexor and extensor muscles to increase intra-abdominal pressure and, hence, stiffness of the trunk and spine[86] or activate muscles which oppose the dominant moment for increased trunk stability[98]. An individual may also employ movement strategies to maintain balance, such as simultaneously moving the hips and knees in the opposite direction of forward or backward trunk motion[99].

2.4.3 Impairment of Trunk Control and Stability Following SCI

SCI can lead to impaired sensorimotor function. Individuals affected by cervical[100] and thoracic SCI[101] often experience impaired trunk muscle function, resulting in reduced postural control and stability of the trunk[100]. Depending on injury level and severity, affected individuals may adopt varying compensatory strategies to restore stability during common upper limb tasks, such as forward reaching. Individuals affected by thoracic SCI with residual control of trunk muscle function may reduce the range of motion of their trunk when reaching forward to avoid losing

balance[102], or use upper extremities for added support, such as bracing against the back of the wheelchair[103]. However, in high-thoracic or cervical injuries, trunk muscle impairment is often more severe. As a consequence, affected individuals often develop new muscle activation strategies to increase trunk stability. Individuals with SCI commonly rely on non-postural muscles, such as the latissimus dorsi or trapezius ascendens, for enabling trunk stability and control[3,102–104]. Individuals with cervical SCI may also delay muscle activation during reaching tasks, to reduce internal perturbations and increase stability[102].

Impaired trunk stability and control can lead to physical limitations such as limited reaching distances[103] or difficulty remaining upright following external perturbations. Such impairment can also lead to serious secondary health complications. Shoulder pain, for example, is often experienced due to increased reliance on the upper limbs for stability[101]. Moreover, difficulty sustaining an upright posture can lead to long-term kyphotic positions, which can compromise lung function, increase pressure sore formation, and increase neck pain[105]. Therefore, it is not surprising that restoring trunk control is a top priority among individuals affected by spinal cord injury[106].

2.5 Epidural Spinal Stimulation

Spinal stimulation is the delivery of electrical current to the spinal cord for the purpose of therapy or rehabilitation. It has most commonly been utilized as a treatment for chronic neuropathic pain (e.g., chronic lower back pain) as early as 1967[107]. More recently, spinal stimulation has been utilized as a methodology for restoring or improving voluntary and involuntary muscle function following neuromuscular impairment, such as SCI, as well as in other applications, which are discussed in Section 2.5.2.

There are three methods of spinal stimulation: (1) transcutaneous, (2) intraspinal, and (3) epidural spinal stimulation. TSS uses electrodes placed on the surface of the skin to electrically stimulate the spinal cord. As a noninvasive technique, TSS allows for relatively simple placement and the ability for temporary use[108]. As a result, TSS may be advantageous as it avoids risks associated with invasive surgery and allows for use without hospitalization. However, due to its external application, TSS is less accurate than invasive approaches at targeting specific spinal networks and often requires large stimulation intensities which can cause discomfort and skin irritation[108].

As a result, invasive approaches to spinal stimulation are used in many applications. Intraspinal stimulation involves placing fine needle electrodes directly into the spinal cord. This technique allows for increased accuracy and specificity at smaller stimulation intensities[108,109]. As such, intraspinal electrodes are preferred in cases when high accuracy or single muscle activation is required[109]**.** However, due to the proximity of the electrodes to the spinal cord, damage to the spinal cord can occur[110]. ESS is an invasive method of spinal stimulation more commonly seen in human studies and long term applications[108]. ESS involves implantation of electrodes within the epidural space on the dorsal side of the spine and is advantageous for its high accuracy/selectivity and reliable invasive approach (i.e., fewer risks/complications)[108,110].

2.5.1 Hardware and Implantation

ESS involves the implantation of an electrode into the epidural space on the dorsal side of the spine to deliver electrical current to the structures within the spinal cord. The primary hardware in an ESS system includes the electrode leads and the pulse generator.

There are two common types of electrode leads used in spinal stimulation applications: (1) cylindrical-leads[111–120] and (2) electrode arrays or paddles[26,70,70,78,121–127]. Cylindrical leads describe a cylindrical wire commonly containing one to eight contact points in a linear arrangement which can produce an electric field 360 degrees around the lead. Cylindrical leads are beneficial for their less-invasive percutaneous implantation procedure which reduces the risk of infection. However, cylindrical leads often experience lead migration or dislodgement following implantation and are limited in the number of contact points[125]. Electrode arrays describe a paddle, often containing 16 to 32 contact points arranged in a two-dimensional array, where the electric field is only created on the contact side. Electrode arrays are beneficial for their numerous contact points which allow for a variety of stimulation sites and configurations[125]. Moreover, the array arrangement results in a lower occurrence of lead migration[125]. However, due to their size, electrode arrays require implantation using an invasive laminectomy approach which can lead to infection or surgical complications[125].

Once implanted and positioned, electrode lead wires are connected to a stimulator or implantable pulse generator placed subcutaneously within the abdomen[78,117,120,121,128]. The implantable pulse generator is responsible for delivering current to the electrodes[108], using either a voltage-controlled

or current-controlled power source. A current-controlled power source is often preferred by participants undergoing ESS for chronic lower back pain treatment[129]. Once implanted, the stimulator controls stimulation parameters, including pulse width, frequency, and amplitude, as well as stimulation paradigms or sequences[108] which may then be manipulated for intended outcome or dependent on the participant. Stimulation parameters will be discussed further in Section 2.5.2.

2.5.2 Improved Muscle Function Following SCI

ESS is most commonly used for treatment of chronic neuropathic pain, such as lower back pain[107,130–132]. More recently, ESS has been considered for other applications, including advancements in prosthetic limb design[133], treatment of heart failure[134] and, most notably, as a therapeutic approach or assistive technology following SCI. Studies performed on varying severity (i.e., complete versus incomplete) and injury level (i.e., cervical versus thoracic) have investigated electrophysiological and functional outcomes of ESS following SCI. One such outcome being the use of ESS for improving or restoring muscle function following SCI.

Electrophysiological Studies

Electrophysiological studies, summarized in Table 1, collect EMG data from individuals with SCI to investigate the effects of systematic ESS parameter manipulation on evoked muscle responses.

Table 1. Summary of parameter manipulation in electrophysiological studies. ESS = epidural spinal stimulation.

Study	SCI Injury, Injury Level	Level of ESS	ESS Frequency (Hz)	ESS Pulse Width (μs)	ESS Amplitude (V)	Electrode Configuration
Murg 2000	Complete/incomplete, Cervical/thoracic	T11-L1	2.1-5	210	0 – 10 V	– Rostrocaudal cathode location (i.e., -0/+3 vs -3/+0)
Minassian 2004	Motor complete, Cervical/thoracic	T10-L1	2.2-50	210	1 – 10 V	– Rostrocaudal cathode location
Sayenko 2014	Motor complete, Thoracic/cervical	T11-L1	2	210	0.5 – 10 V	– Rostrocaudal cathode location – Localized versus widefield stimulation (i.e., stimulating electrodes close together vs far apart)
Calvert 2019	Complete, Thoracic	T11-L1	0.5-1.0	210	0 – 10 V	– Rostrocaudal cathode location – Localized versus widefield stimulation (i.e., stimulating electrodes close together vs far apart)
Luna 2021	Motor complete, Thoracic/cervical	T11-L1	2-100	210	1 – 10 V	– Rostrocaudal cathode location (i.e., -0/+3 vs -3/+0)
Hoglund 2022	Motor complete, Thoracic	T11-L1	2	300	0 – 10 mA	– Rostrocaudal cathode location – Vertical, horizontal, and diagonal anode/cathode configurations

Metrics are calculated to analyze the effect of parameter manipulation on evoked muscle responses. For example, peak-to-peak amplitude[118–120], magnitude (i.e., area under the curve)[26,128], and RMS[118,128] of the evoked response within a 50 ms post-stimulus window may be calculated[111,119]. Recruitment curves or input-output curves are created using a plot of muscle amplitude/magnitude versus stimulation amplitude[26,118]. Recruitment curves show, schematically, the relationship between evoked amplitude/magnitude and stimulation amplitude, often at a sampling frequency of 2 Hz[26,118]. Such curves can be used to determine MT and investigate recruitment patterns (i.e., the shape of the recruitment curve)[26]. Recruitment order/sequence is determined by comparing the MT of each muscle[119]. The latency of the evoked response can be quantified to provide insight into relative muscle activation timing[26,119,120,128]. The latency of the muscle response can be defined as the time between stimulation onset and initiation of an evoked muscle response[26,118,120,128], quantified as the first time the EMG signal deviates by baseline ± three times its standard deviation[26,128]. The response timing can be further characterized into early (ER) and medium response (MR) to provide insight into activation pathways[26]. The MR describes activation of afferent, polysynaptic pathways whereas the ER, characterized by an earlier onset latency at higher stimulation amplitudes, describes direct activation of efferent structures[26]. The amplitude or magnitude of each component may then be quantified for analysis[26,118]. Similarly, response duration can be quantified as the time between response onset and offset (e.g., last deflection from baseline peak-to-peak amplitude ± 5%)[10].

Effect of stimulation amplitude manipulation: The amplitude or magnitude of an evoked response is dependent on stimulation amplitude. The amplitude increases as stimulation amplitude increases until a plateau is reached[118–120]. This plateau is related to saturation of all recruited motor units. The latency of an evoked muscle response is not affected by stimulation amplitude[118–120] and is often consistent across trials[118] and similar between muscle groups[120]. However, this may only be the case during localized stimulation, as Sayenko et al. (2014) found that, when a wide-field stimulation configuration is utilized, the onset and magnitude of ER can vary with increasing stimulation amplitude[26].

Effect of stimulation frequency manipulation: At frequencies less than 15 Hz, successive pulses will not impact the amplitude or shape of evoked muscle responses[118,119]. However, increasing the frequency beyond 15 Hz can reduce the amplitude of successive responses if sufficient time for

repolarization is not allowed[118,119]. Trains, or repetitively applied stimulation, can lead to patterned or rhythmic muscle activity in the lower limbs, including sustained extension at lower frequencies and step-like EMG activity at higher frequencies[119]. Higher frequencies can increase response latency[119] and evoked responses can reach a plateau earlier[118].

Effect of stimulation location manipulation: Recruitment sequence, MT, and response amplitude depend on rostrocaudal and mediolateral position of stimulation along the spine[26,119,120]. Localized stimulation varying along the rostrocaudal axis of the spine can more selectively activate muscles (i.e., greater magnitudes) according to expected location of myotomes[26,120,128]. The location of the stimulating cathode determines the "segmental-selective" activation[119,120,135,136]. For stimulation at T11 to L1 vertebral levels, rostral stimulation preferentially activates proximal leg muscles (i.e., greater response amplitudes, lower MT) while caudal activates distal[26,128]. The location of stimulation can also impact the latency of the muscle response with stimulation further from the muscle requiring greater latency for the signal to travel a larger distance[118]. This has been observed with greater latencies in calf compared to thigh muscles[118].

Effect of stimulation configuration manipulation: Manipulating the polarity can affect the amplitude of muscle responses as well as MT[118]. This is linked to the idea that spinal structures near the cathode are targeted[118]. Recruitment patterns are affected by local versus wide-field stimulation configurations[26]. Localized stimulation near expected muscle innervation zones results in greater magnitudes of corresponding evoked muscle responses, whereas wide-field stimulation can result in more general activation of many muscles[26]. Diagonal stimulation configurations result in increased muscle activity compared to horizontal configurations, likely resulting from the broader electric current reaching more regions of the spinal cord[136].

Functional Outcome Studies

Optimal stimulation location and parameter selection can enable functional outcomes via ESS, as listed in Table 2. In general, a frequency within 2 to 100 Hz, a pulse width within 150 to 1000 μs, and stimulation amplitudes within 0.1 to 10 V (voltage-controlled) or 0.1 to 10 mA (current-controlled) can achieve functional outcomes. However, spinal mapping methods provide a systematic approach to adjusting stimulation parameters to enable a desired functional outcome[26,119,135]. Sayenko et al. (2014), outlined one such mapping method for a paddle

electrode[26,135]. Sayenko's mapping method involves testing five electrode configurations which differ in rostrocaudal location of the cathode and localized versus wide-field stimulation. For each configuration, stimulation is delivered at 2 Hz and constant pulse width while stimulation amplitude is increased from 0.5 to 10 V in 0.5 V increments[26]. Through analysis of evoked muscle responses through EMG or visible muscle contractions, 'optimal' parameters are defined for the intended function[135]. Studies may define their own mapping techniques, manipulating frequency pulse width, location, and amplitude.

Table 2. Summary of functional outcome studies regarding the restoration of muscle function following spinal cord injury (SCI). Stimulation parameters which enabled the functional outcome are listed, however, a greater range of parameters may have been tested for the purpose of spinal mapping. ESS = epidural spinal stimulation, PWBT = Partial Weight Bearing Therapy.

Study	SCI Injury, Injury Level	Level of ESS	ESS Frequency (Hz)	ESS Pulse Width (μs)	ESS Amplitude	Functional Outcome(s)
Lower Limb Function						
Herman 2002	Incomplete, Cervical	Upper lumbar enlargement	20-60	800	Above sensory, below motor threshold	– Improved stepping over-treadmill and over-ground – Enhanced PWBT
Carhart 2004	Incomplete, Cervical	T10-T12	40-60	>500 (800 = optimal)	Above sensory, below motor threshold	– Improved gait over-treadmill and over-ground – Enhanced PWBT
Minassian 2004	Complete, Thoracic/cervical	T10-L1	5-15 (tonic) 25-50 (rhythmic)	210	>6 V	– Modulated tonic EMG activity for extension of lower extremities – Burst-style EMG activity in flexors and extensors (step-like activity)
Harkema 2011	Motor complete, Thoracic/cervical	T11-L1	15 (standing) 30-40 (stepping)	210 or 450	>4 V	– Weight bearing standing – Sit-to-stand transition – Step-like activity – Volitional toe, ankle, and leg movement

Angeli 2014	Motor complete, Thoracic/cervical	T11-T12	25-30	210 or 450	0.5-9 V	– Volitional, coordinated leg, ankle, and toe movement – Over-treadmill stepping – Standing
Grahn 2017	Complete, Thoracic	T11-L1	15 (standing) 25 and 40 (volitional control and stepping)	210	>1.5 V	– Volitional leg movement – Volitional step-like activity – Independent standing
Angeli 2018	Motor complete, Thoracic/cervical	T11-L1	20-50	450	>1 V	– Over-ground stepping with assistance – Independent stepping over-treadmill
Gill 2018	Complete, Thoracic	T11-L1	15-40	210	2.5-6 V	– Independent stepping over-treadmill – Over-ground stepping with assistance – Standing
Rowald 2022	Complete, Thoracic	T11-L1 or T12-L2	20-100	300	1-10 mA	– Immediate independent stepping over-treadmill with support – Modulation of step length – Swimming, pedaling, squatting movements – Independent ascent of staircase

Gorgey 2022	Complete, Thoracic	T11-T12	20	240	5-6 V	– Improved standing
Gorgey 2023	Motor complete. Thoracic/cervical	T10-L2	15-30	250-750	>1 mA	– Over-ground standing – Stepping in parallel bars – Over-ground stepping with assistance (i.e., walker, exoskeleton)
Upper Limb Function						
Lu 2016	Incomplete, Cervical	C5-T1	10-20	210	0.7 – 6 mA	– Improved grip force – Improved hand control
Trunk Function						
Angeli 2018	Motor complete, Thoracic/cervical	T11-L1	30	450	3.2 V	– Improved trunk extension and upright sitting posture
Gill 2020	Complete, Thoracic	T11-L1	20 - 25	200 - 450	2.0 – 7.8 V	– Improved forward and lateral reaching
Rowald 2022	Complete, Thoracic	T11-L1 or T12-L2	120	300	0-10 mA	– Normalized trunk postures – Improved control of trunk movement (i.e., trunk extension)
Gorgey 2022	Complete, Thoracic	T11-T12	20	240	5.5-6	– Improved trunk control with perturbations (i.e., raising hands above head)
Gorgey 2023	Motor complete. Thoracic/cervical	T10-L2	20	700-750	>8.5 mA	– Improved trunk control

In addition to the muscle function studies provided in Table 2, ESS has been shown to improve autonomic function, including cardiovascular[124,127], respiratory[112,113], sexual, and bladder/bowel[78,126] function following SCI.

2.5.3 Mechanisms of Epidural Spinal Stimulation

Studies have proposed the potential targeted structures within the spinal cord as well as the mechanisms by which ESS is able to modulate muscle activity and restore muscle function following SCI.

Targeted Neural Structures

Many afferent (i.e., sensory) pathways are located on the dorsal side of the spine[137]; as a result, ESS is believed to primarily target large primary afferents of dorsal roots[11,78,111,118–120,138] and, at higher stimulation intensities, afferent fibers in the dorsal columns[11,78,117] near the site of stimulation. Structures near the cathode site are often most impacted by ESS[118,120,136]. However, structures farther from the site of ESS may also be affected, especially when wide-field stimulation configurations are utilized[26]. This may be the result of the broad coverage of the electric field produced by ESS and augmented by the presence of a conductive fluid that surrounds the spinal cord and vertebral canal, known as cerebrospinal fluid[11,26,139]. Electric current may be transferred through this fluid to surrounding structures or spinal segments leading to effects from ESS in more distant structures[11,26,119]. Additional structures believed to be modulated, either directly or indirectly, during ESS are motor neurons[78,112,117,119,120], propriospinal networks[11,70], interneuronal networks[70,78,118,119,138,140], and/or glial cells[11].

Mechanisms for Improved Muscle Function

There are three proposed mechanisms by which ESS restores muscle function following SCI: (1) activation of spinal pathways, (2) modulation of excitability, and (3) manipulation of the chemical environment within the spinal cord.

As previously described, spinal stimulation is believed to activate dorsal roots which carry afferent neurons towards the spinal cord[28,135,141,142]. Activation of proprioceptive afferent neurons can result in activation of interneurons and/or motor neurons and thus muscle activation in a reflex nature (i.e., stretch reflex)[28,142,143]. Direct stimulation of nearby interneurons or motor neurons muscles

may also occur; however, this would not explain rhythmic activation. While modulating neural structures, ESS may activate intrinsic pattern generators within the spinal cord. Most discussed in lower-limb studies is the central pattern generator (CPG) for locomotion. A CPG is an intrinsic circuit within the spinal cord that allows an organism to move in rhythmic locomotion patterns, such as walking or flying. A CPG differs from typical, voluntary locomotion, as it operates as a reflex mechanism without the need for descending supraspinal control (i.e., control from the brain) or external feedback. The application of an electrical stimuli to the lumbar spinal cord is believed to modulate neural structures, such as interneuronal networks, and activate the CPG for locomotion in humans leading to lower limb movement[11,114,119]. The existence of a CPG in humans was studied by Dimitrijevic et al. (1998)[114] who utilized ESS at the L2 vertebra level to trigger rhythmic, step-like movements following complete SCI. As a complete SCI, there is no supraspinal control below the site of injury, hence ESS is believed to have modulated neural structures (i.e., afferent inputs) and triggered CPG networks to restore muscle function. However, in addition to rhythmic locomotion, more recent studies have restored voluntary or task-specific muscle function that required intent (i.e., leg movements following cues, task-specific motor function). Intentional movement resulting from ESS cannot be entirely explained by direct activation of motoneurons through CPG networks, therefore, additional mechanisms must be explored.

ESS can modulate or increase the excitability of targeted neuronal structures. This mechanism improves muscle function by: (1) enabling or reactivating supraspinal-spinal connections and (2) encouraging use-dependent plasticity[11]. Trauma to the spinal cord can lead to partial or complete damage to supraspinal-spinal connections across the site of injury. Partial damage may result in an "incomplete SCI" clinical diagnosis, where remaining supraspinal-spinal connections exist across the site of injury allowing for limited sensory or motor function. When the connections across the lesion are completely damaged and no sensory or motor signals are clinically observed, the result is a "complete SCI" clinical diagnosis. More commonly discussed in ESS applications is the possibility of a "discomplete SCI"[70,78,123,144]. A discomplete injury occurs when there is no clinical evidence of spared sensory/motor function below the site of injury (i.e., clinically complete), however, further neurophysiological tests reveal spared supraspinal-spinal connections across the site of injury[144]. These spared, anatomical connections may be sub-functional or "silent" and unable to activate motor function below the lesion[70,144] due to physical damage (i.e., damaged myelin or ionic channels in neurons) or lowered excitability[70]. The electric field created by ESS

can increase the excitability or resting membrane potential of nearby sublesional structures, shifting them closer to MT[70,127,135,140]. Consequently, this enables the spared supraspinal-spinal connections to sufficiently transmit signals across the site of injury to initiate muscle function below the site of injury[70,78,123,126,140,141]. Secondly, through modulation of excitability, ESS can augment use-dependent neural plasticity within the spinal cord[111]. Neural plasticity describes the ability of networks within the spinal cord to grow (i.e., sprouting) or reorganize for improved function[145]. This phenomenon can occur spontaneously after SCI, which explains some functional improvement directly following injury[145]. Physical rehabilitation is often implemented following SCI to provide additional sensory input, which can encourage regrowth and reorganization of the spinal networks[145]. Electrical stimulation, such as ESS, can also augment neuronal growth/sprouting and/or strengthen (i.e., remyelination) spared connections across the site of injury, presented in Fig. 4[11,70,78,145]. ESS also encourages reorganization of nerve fibers, which can allow signals to "bypass" the lesion which once blocked signal transmission[70,121]. ESS, in combination with task training, can enhance the benefits of neural plasticity[70,78,116,121], which may result in long-term, remaining function after ESS is removed following SCI.

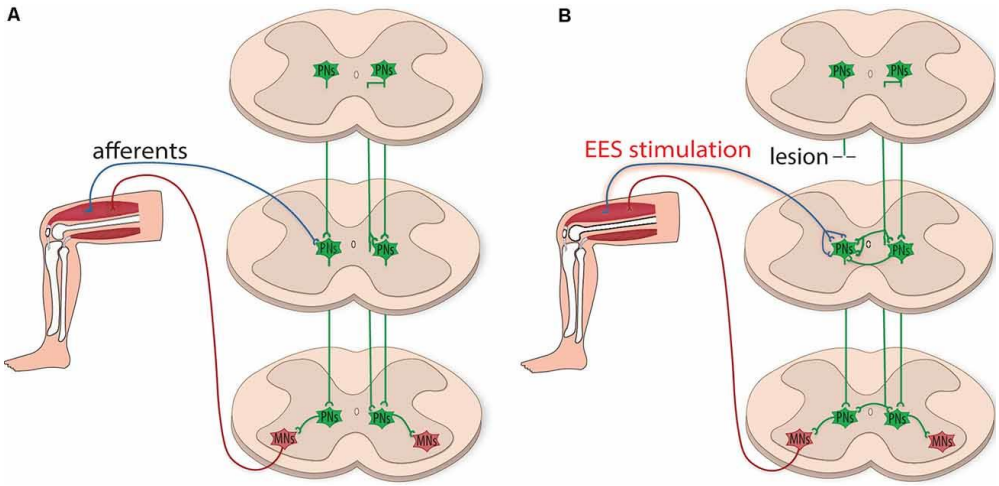

Figure 4. (A) In a healthy spinal cord, connections between afferent neurons, propriospinal interneurons (PNs), and motoneurons (MNs) enable effective signal transmission between the peripheral nervous system and central nervous system. (B) Following a SCI, there may be damage to pathways within the spinal cord at the lesion site. Delivery of epidural electrical stimulation (EES) can promote neuronal regrowth and reorganization of spinal networks, leading to new connections and pathways. Retrieved from (Eisdorfer et al., 2020), licensed under the Creative Commons Attribution License (CC BY)[146].

In chronic pain applications, spinal stimulation on the dorsal side of the spine has demonstrated effects on the chemical environment within the spinal cord, including increasing concentrations of gamma-aminobutyric acid (GABA)[147], serotonin[148,149], and Substance P[11,139,148] within the dorsal horn. These neurotransmitters/neuromodulators modulated by ESS contribute to the pain-relief outcome from ESS. Similarly, ESS is believed to cause a release of a variety of neurotransmitters in the spinal cord, which may act to facilitate or improve motor function[11]. Animal studies have found that injection of neurotransmitters, including clonidine, tizanidine, serotonin, and NMDA, can induce or modulate locomotion in animals following spinal cord injury[150]. It is possible that ESS releases similar chemicals and follows a similar mechanism to encourage or improve muscle movement following SCI[11].

3 Methods

3.1 Participants

Experimental data were collected in thirteen individuals undergoing clinically indicated surgery for the implantation of an epidural spinal stimulator as part of their chronic pain syndrome treatment. All participants provided informed consent to the experimental procedures. These procedures were performed in accordance with standard of care protocols in the operating room and were conducted under research protocol Pro00023336, approved by the Institutional Review Board of the Houston Methodist Research Institute. Data from two participants were excluded from the analysis due to inconsistencies in stimulation frequency or amplitude range. As such, data from eleven participants (10 female and 1 male; age: 59 ± 11 years, weight: 75.1 ± 11.7 kg, height: 163 ± 10 cm) were analyzed. A summary of participant characteristics is presented in Table 3.

Table 3. Summary of participant characteristics.

Participant ID	Age (years)	Sex	Height (cm)	Weight (kg)	Reason for Implant
P9	78	F	160	95.0	– Chronic pain syndrome; failed back syndrome – Persistent lumbar radiculopathy, radiculitis – Intervertebral disc disorder with radiculopathy, lumbosacral
P10	69	M	185	73.9	– Chronic pain syndrome; post laminectomy syndrome – Intervertebral disc disorder with radiculopathy, lumbosacral
P11	68	F	168	90.7	– Chronic pain syndrome; failed back syndrome – Intervertebral disc disorder with radiculopathy, lumbosacral
P12	60	F	152	62.5	– Chronic pain syndrome; post laminectomy syndrome – Intervertebral disc disorder with radiculopathy, lumbosacral – Malfunction and migration of spinal cord stimulator
P13	68	F	172	79.7	– Failed back syndrome – Intervertebral disc disorder with radiculopathy, lumbosacral
P14	44	F	172	82.1	– Chronic pain syndrome; failed back syndrome – Intervertebral disc disorder with radiculopathy, lumbosacral
P15	66	F	157	69.9	– Chronic pain syndrome; failed back syndrome – Persistent lumbar radiculopathy, radiculitis
P16	51	F	155	64.2	– Chronic pain syndrome; failed back syndrome – Persistent lumbar radiculopathy, radiculitis – Intervertebral disc disorder with radiculopathy, lumbosacral
P21	49	F	160	79.3	– Chronic pain syndrome
P22	51	F	157	70.8	– Chronic pain syndrome
P26	46	F	157	57.6	– Revision surgery to replace stimulator to treat pain

3.2 Delivery of Epidural Spinal Stimulation

A Spectra WaveWriter Spinal Cord Stimulator (Boston Scientific, Marlborough, MA, USA) or Senza Trial Stimulator TSM1000 (Nevro, Redwood City, CA, USA) were used to generate the electrical stimulation pulses. ESS was delivered via implanted, current-controlled, 16-channel (Artisan MRI Surgical Lead, SC-8216-50, Boston Scientific, Marlborough, MA, USA, or Nevro Surpass Surgical Lead, LEAD3005-50B, Nevro, Redwood City, CA, USA) or 32-channel (CoverEdge 32 Surgical Lead, SC-8336-50, Boston Scientific, Marlborough, MA, USA) electrode arrays. All electrodes were placed on the dorsal dura approximately on the midline within the T4 to T10 vertebrae level range, employing a laminectomy approach. X-ray images of the electrode array placement for each participant are provided in Fig. 5.

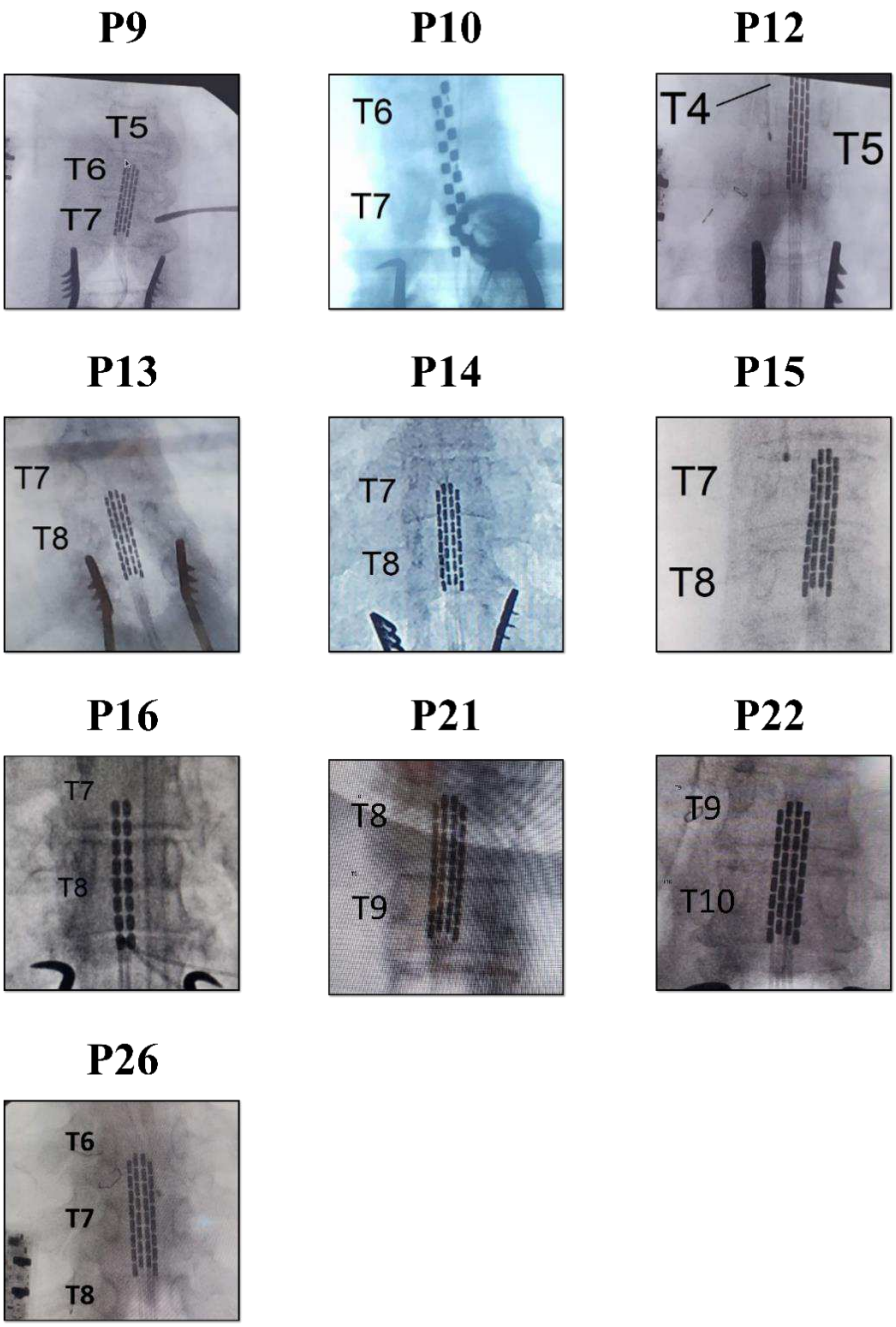

Figure 5. X-ray images of the electrode paddle placements for each participant. An x-ray image for P11's electrode paddle placement at T7 to T8 was not available.

The stimulator and electrode array type were tailored to patient preferences, whereas the placement and stimulation pulse width were aligned with the surgeon's specifications for chronic pain treatment, as summarized in Tables 4 and 5.

Table 4. Electrode array specifications.

Electrode Type	Model	Lead Shape	Number of Electrode Contacts	Array Length (Rostro-caudal)	Array Width (Mediolateral)	Electrode Size (Width x Length)	Electrode Spacing (longitudinal)	Electrode Spacing (latitudinal)
CoverEdge 32 Surgical Lead[1]	SC-8336-50	4 x 8 array	32	50 mm	9 mm	1 mm x 3.4 mm	1 mm	*Information not provided in data sheets*
Artisan MRI Surgical Lead[1]	SC-8216-50	2 x 8 array	16	45 mm	8 mm	2 mm x 3 mm	1 mm	*Information not provided in data sheets*
Nevro Surpass Surgical Lead[2]	LEAD3005-50B	2 x 8 array	16	64 mm	10 mm	1.25 mm x 3.0 mm	4.25 mm	1.0 mm

[1] Boston Scientific, Marlborough, MA, USA.
[2] Nevro, Redwood City, CA, USA.

Table 5. Participant summary of ESS electrode placement and ESS stimulation parameters.

Participant ID	External Stimulator	Electrode Array	Electrode Contacts	Array Placement (Vertebral Levels)	Pulse Width (μs)	Stimulation Amplitude Range (mA)
P9	Spectra WaveWriter Spinal Cord Stimulator[1]	CoverEdge 32 Surgical Lead[1]	32	T6 to T7	300	4.0 to 6.0
P10	Senza Trial Stimulator TSM1000[2]	Nevro Surpass Surgical Lead[2]	16	T6 to T7	350	1.0 to 9.0
P11	Spectra WaveWriter Spinal Cord Stimulator[1]	CoverEdge 32 Surgical Lead[1]	32	T7 to T8	350	1.0 to 6.0
P12	Spectra WaveWriter Spinal Cord Stimulator[1]	CoverEdge 32 Surgical Lead[1]	32	T4 to T5	350	1.0 to 9.0
P13	Spectra WaveWriter Spinal Cord Stimulator[1]	CoverEdge 32 Surgical Lead[1]	32	T7 to T8	350	1.0 to 8.0 *Left caudal only: 1.0 to 9.0
P14	Spectra WaveWriter Spinal Cord Stimulator[1]	CoverEdge 32 Surgical Lead[1]	32	T7 to T8	350	1.0 to 10.0
P15	Spectra WaveWriter Spinal Cord Stimulator[1]	CoverEdge 32 Surgical Lead[1]	32	T7 to T8	300	1.0 to 7.0
P16	Spectra WaveWriter Spinal Cord Stimulator[1]	Artisan MRI Surgical Lead[1]	16	T7 to T8	350	1.0 to 10.0
P21	Spectra WaveWriter Spinal Cord Stimulator[1]	CoverEdge 32 Surgical Lead[1]	32	T8 to T9	300	1.0 to 6.0
P22	Spectra WaveWriter Spinal Cord Stimulator[1]	CoverEdge 32 Surgical Lead[1]	32	T9 to T10	350	1.0 to 5.0
P26	Spectra WaveWriter Spinal Cord Stimulator[1]	CoverEdge 32 Surgical Lead[1]	32	T6 to T7	350	1.0 to 7.0

[1] Boston Scientific, Marlborough, MA, USA.
[2] Nevro, Redwood City, CA, USA.

The participant was placed in prone position, supported at the head, shoulders and hips. Monophasic ESS was applied at 2 Hz while two parameters were systematically explored: (1) anode and cathode location; and (2) stimulation amplitude. The electrode configurations shown in Fig. 6 were used while stimulation amplitude was continuously increased in 1.0 mA increments from 1.0 mA up to 10.0 mA (or until the ESS evoked response plateaued). Between 3 and 65 stimuli were delivered for each stimulation amplitude. Once all trials for the maximum stimulation amplitude were completed, the next electrode configuration was tested after a no-stimulation period of 20 seconds or more. In total, stimulation was delivered for approximately five minutes, after which the experimental session was completed. For each participant, the pulse width was either 300 or 350 μs, according to the requirements for treatment of chronic pain, as listed in Table 5. Applied charge, calculated as stimulation amplitude multiplied by stimulation pulse width, in units of microcoulombs (μC), was used for further analysis to account for differences in pulse width across participants. Spinal structures near the cathode are most targeted by ESS[118–120]; therefore, the location of the cathode was considered the stimulation location.

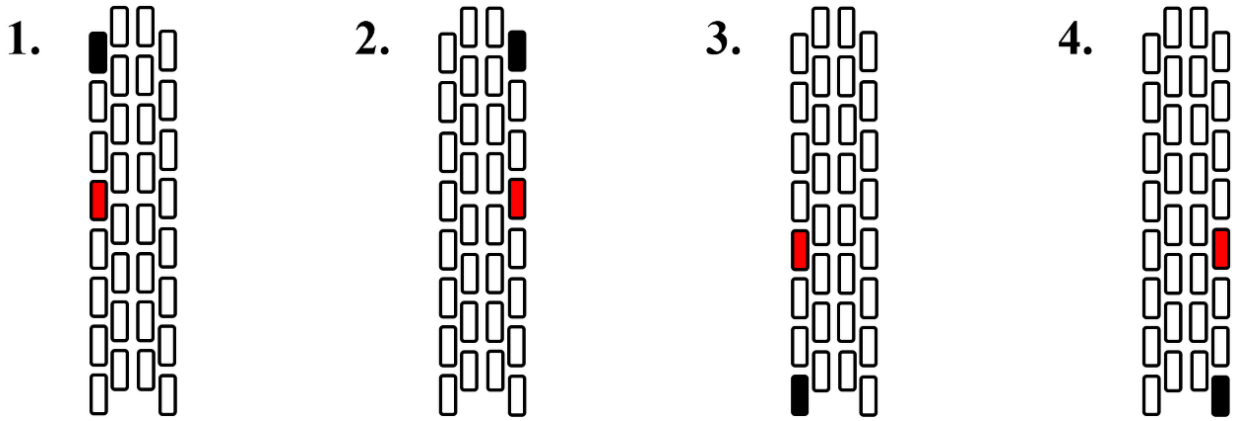

Figure 6. Electrode configurations: (1) Left rostral, (2) right rostral, (3) left caudal, and (4) right caudal. The cathode is depicted in black, and the anode is depicted in red. The cathode was assumed to be the stimulation location as spinal structures near the cathode are most targeted by ESS[118–120]. The image shows a 32-channel array; however, the same configurations were tested for a 16-channel array.

3.3 Experimental Data Acquisition

Trigno Avanti wireless surface EMG electrodes (Delsys Inc., Natick, Massachusetts, USA) were placed on muscles relevant to trunk stability and control. EMG electrodes were placed bilaterally on the external obliques (EO)[18,88,151,152] , internal obliques (IO)[88,151], and rectus abdominus (RA)[18,88,151,152] muscles. Two surface EMG electrodes were placed unilaterally on the body side opposite to the surgeon on the erector spinae muscles at the levels corresponding to the sixth and seventh thoracic vertebrae (EST7)[18], and the second and third lumbar vertebrae (ESL3)[18,88,152]. This corresponded to placement on the left side for 8 participants and the right side for 3 participants. Two pairs of subdermal needle EMG electrodes of 20 mm length (Rhythmlink Columbia, SC, USA) were placed by an intraoperative electrophysiologist on the midline between the second and third thoracic vertebrae levels (T2/T3), and on the midline between the fifth and sixth thoracic vertebrae levels (T5/T6), with an interelectrode distance of 4 cm. The T2/T3 needle electrode was used for identification of the ESS stimulation artifact. If the T2/T3 needle electrode data was obstructed with signal noise, the T5/T6 surface electrode was used for stimulus artifact identification. For two participants only (P16 and P26), the EST6T7 channel was used for identification of the stimulation artifact due to an experimental error with the T2/T3 and T5/T6 needle electrodes. Details on electrode placement are presented in Table 6.

Table 6. Guidelines for placing the EMG surface electrodes.

Muscle	Electrode Placement	Electrode Orientation
Rectus abdominis	3 cm lateral of the umbilicus[88,151,152]	Aligned vertically
External obliques	15 cm lateral of the umbilicus[88,151,152]	Aligned at 45 degrees off the vertical
Erector spinae above the T6/T7 vertebral level	5 cm lateral of T6/T7 vertebral level[88,151,152]	Aligned vertically
Erector spinae above the L2/L3 vertebral level	3 cm lateral of L2/L3 vertebral level[88,151,152]	Aligned vertically
Internal obliques	At the midpoint between the anterior superior iliac spine and the symphysis pubis, above the inguinal ligament[88,151]	Aligned at 45 degrees off the vertical

Data from the EMG electrodes were sampled at 2 kHz and reconstructed by the EMG system as an analog signal. A 16-channel analog adapter streamed the EMG data into the PowerLab data acquisition system (Model 16/35, AD Instruments, Sydney, NSW, Australia) using BNC connections where EMG data were sampled at 10 kHz. For a single participant (P26), data were sampled at 2 kHz. The data were upsampled to 10 kHz prior to further analysis. An image of the data acquisition system is presented in Fig. 7.

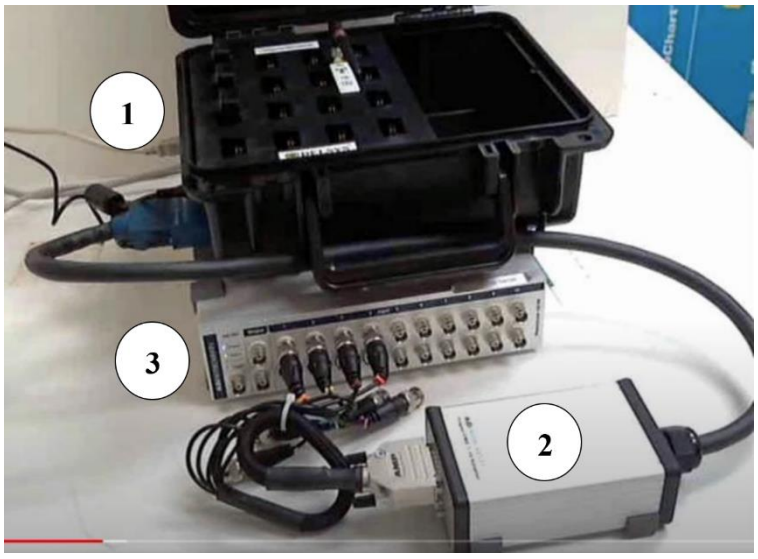

Figure 7. The Delsys Trigno Avanti wireless EMG sensors (1) sample the data at 2 kHz and reconstruct an analog signal. A 16-channel analog adapter (2) allowed us to input the EMG data into PowerLab using BNC connections. The PowerLab data acquisition system (3) samples the data at 10 kHz.

3.4 Experimental Data Processing and Analysis

3.4.1 Data Extraction and Processing

Using LabChart (version 8.1.19, AD Instruments, Otago, New Zealand), EMG time series data from three trials (i.e., stimuli) were exported for each electrode configuration and stimulation amplitude, capturing approximately 300 ms before and 300 ms after the stimulus. Three trials were selected, as this was the minimum number of trials delivered at each stimulation amplitude, and for which the stimulation artifact was unobstructed in the recording from one of the two needle electrodes. Note that a temporal offset of 61.1 ms between the signal recorded via surface electrodes and the actual stimulation event existed, resulting from analog signal reconstruction (according to manufacturer's specifications[153] and confirmed within the dataset), which was corrected in LabChart prior to data export. All data analysis was performed in MATLAB (ver 2021b, MathWorks, Natick, MA, USA) using a custom-made algorithm. As described previously, one dataset (P26) was first upsampled to 10 kHz to accommodate a difference in sampling frequency during data acquisition. The time series data from all participants were demeaned using an average of the baseline activity calculated from the first 100 ms of exported data, starting

approximately 300 ms prior to the stimulus. Peaks in the artifact recording were used to identify the time of stimulation onset and this time was set to zero. Once demeaned and zeroed, the time series data from all participants were processed for a time period from 100 ms before stimulation onset to 200 ms after stimulation onset to encompass the response.

3.4.2 Characterization of Evoked Muscle Responses

Muscle responses were characterized by the metrics peak-to-peak amplitude, MT, onset latency, and response duration using the collected EMG data, as portrayed in Fig. 8 below. All metrics were averaged across three trials. Muscles and associated EMG data excluded from further analysis are presented in Appendix A.

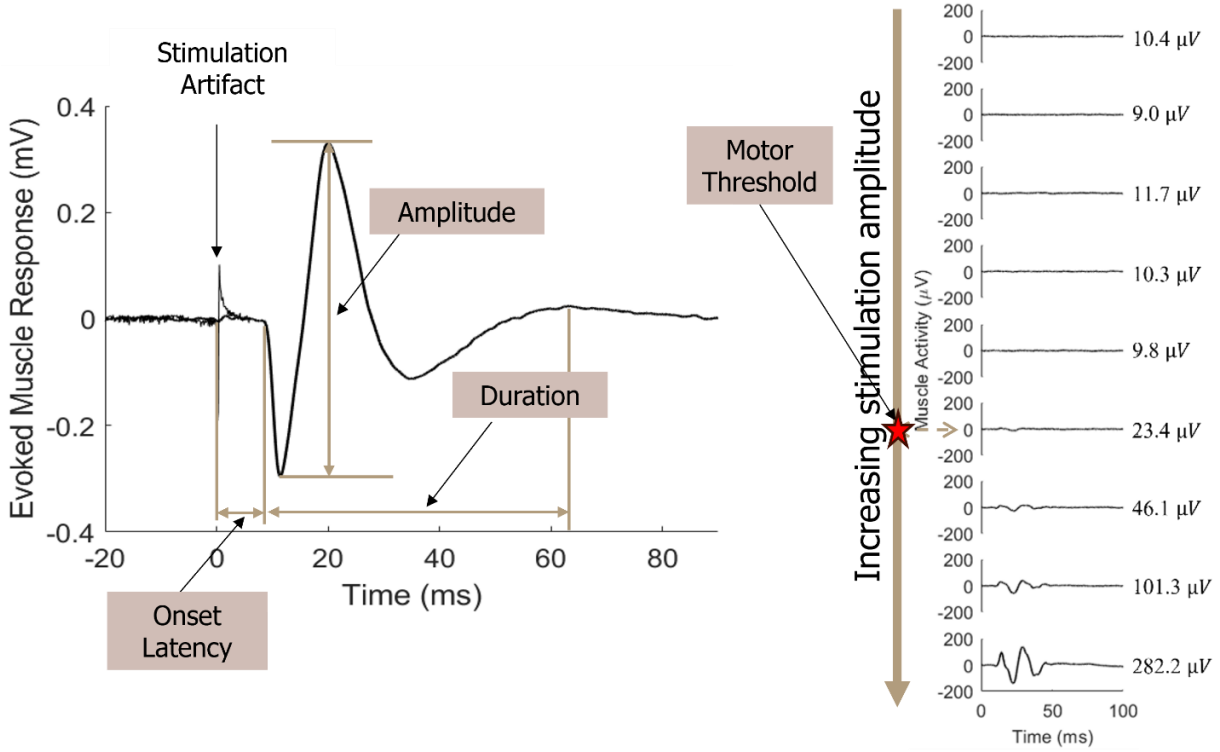

Figure 8. A representative evoked muscle response from one stimulation location and amplitude is presented on the left. Muscle responses were characterized by the metrics response peak-to-peak amplitude, onset latency, and duration. Representative evoked muscle responses with increasing stimulation amplitude are presented on the right. The peak-to-peak amplitude value of each response is listed. Once a response with a peak-to-peak amplitude greater than 20 μV is evoked, the corresponding stimulation amplitude is considered the motor threshold, as identified by a red star.

Peak-to-peak amplitude of the evoked responses was calculated within a 50 ms post-stimulus window without considering the stimulus artifact. For one participant (P15), a 30 ms post-stimulus window was used for the left internal oblique muscle only, as movement artifacts were present after 30 ms. Recruitment curves of muscle responses were created for each participant, identifying the relationship between applied charge and average peak-to-peak EMG response amplitude. Using visual inspections, MT intensity was defined as the smallest applied charge that resulted in a motor evoked response with a peak-to-peak amplitude greater than 20 µV in all three trials[21]. The representative waveforms and recruitment curves of muscle responses, presented in Fig. 9, demonstrate that 20 µV was an appropriate choice. Muscle responses that did not reach 20 µV within the tested range of applied charge were deemed 'non-responsive'.

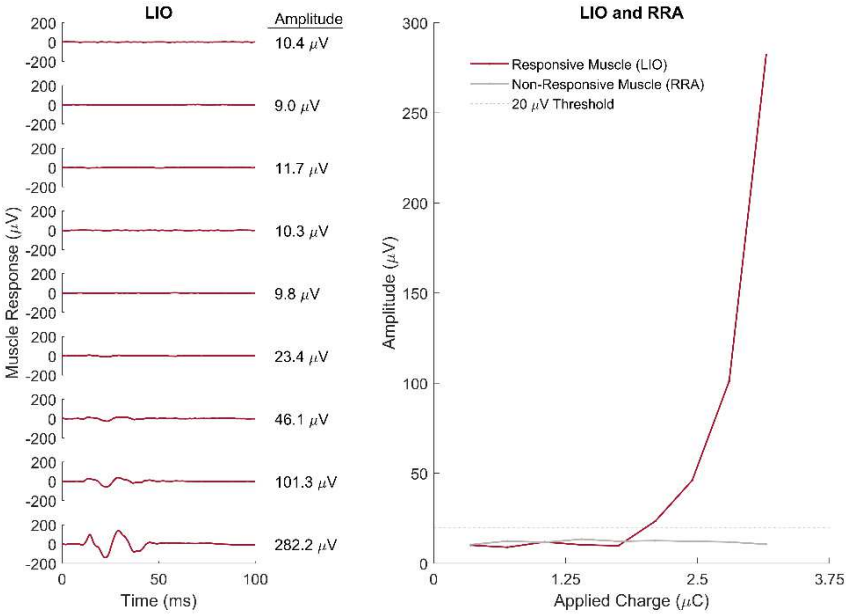

Figure 9. Sample recruitment curves of muscle responses from P10 (stimulation location: top left of T6 vertebra). The left internal oblique (LIO; left panel and red trace in the right panel) demonstrates a responsive muscle. The right rectus abdominis (RRA; grey trace in the right panel) demonstrates a non-responsive muscle. The dotted line represents the 20 µV threshold such that amplitudes greater than 20 µV suggest the presence of a muscle response. A responsive muscle will experience amplitudes greater than 20 µV when the applied charge surpasses a threshold (i.e., motor threshold, MT). A non-responsive muscle will not experience amplitudes greater than 20 µV for the applied charges tested, indicating that the measured amplitudes are more likely due to noise in the signal than due to a muscle response.

The timing of evoked muscle responses was characterized by onset latency and duration using a custom-made algorithm in MATLAB. The algorithm identified the onset and end of the main response waveform using a baseline band (baseline ± three times the standard deviation[26]), while eliminating noise or residual tissue signals. Response duration is the time difference between the end and onset of the response. Non-responsive muscles were omitted from onset latency and duration analysis. Activation of the erector spinae muscle at the T7 vertebral level occurred at the same time as the stimulation artifact; therefore, onset and duration could not be calculated. Further details on the MATLAB algorithm for calculating response onset and duration are presented in Appendix B. For comparison, onset latency was also calculated using a simpler, more traditional approach, as the first time the response exceeded the baseline band (baseline ± three times the standard deviation[26]), hereby referred to as the baseline band approach.

Based on previous studies, evoked muscle responses may be divided into ER and MR components. ER and MR components correspond to the activation of efferent and afferent pathways, respectively[9]. At lower stimulation intensities, ESS is believed to produce an MR component through activation of afferent pathways in the spinal cord. The onset latency of the MR will remain constant with increasing stimulation intensity. At higher stimulation intensities, a response with a shorter onset latency may occur, which suggests additional activation of efferent pathways in the spinal cord and, therefore, an ER component[9]. If ER responses were detected in the data, an analysis of growth in ER and MR was performed. For a given muscle, the start of ER was defined as the response onset at the highest applied charge for a given electrode configuration[26]. The end of ER and the start of MR were defined as the response onset at the lowest applied charged that evoked a response in one electrode configuration. Once the ER and MR intervals were defined, the peak-to-peak amplitude of the response within each interval was calculated[26].

4 Results

4.1 Effect of Stimulation Location on Trunk Muscle Amplitude and Selectivity

Figure 10 presents the distribution of stimulation locations tested. For each participant, two stimulation locations were used within the T4 to T10 vertebral level range. The manipulation of stimulation location and stimulation amplitude produced observable differences in the waveforms of the ESS evoked responses.

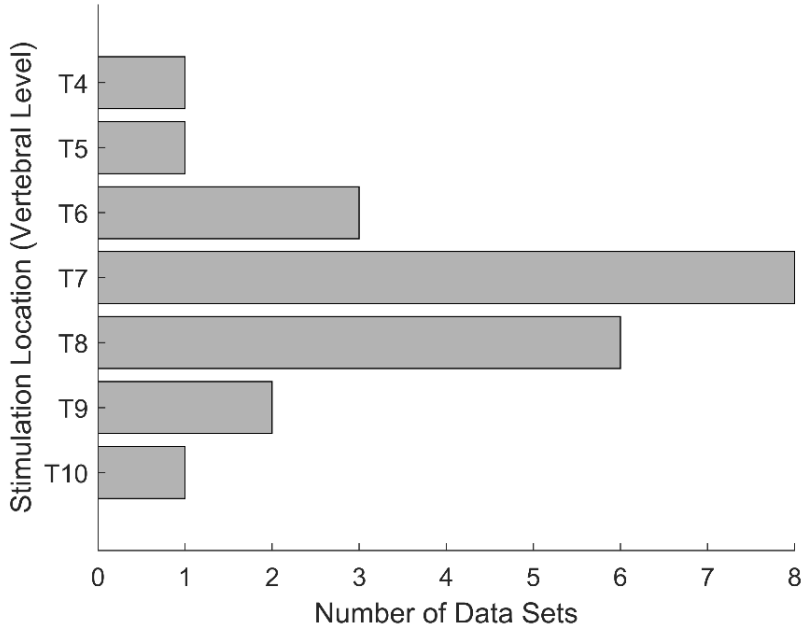

Figure 10. Distribution of the tested stimulation locations. Stimulation locations ranged from the T4 to T10 vertebral levels, with the greatest number of data sets occurring for the T7 and T8 vertebral levels.

In Fig. 11, representative average muscle responses from one participant in response to varying the stimulation location and amplitude are presented for the left and right external obliques (LEO and REO). At stimulation amplitudes greater than MT, single-pulse ESS evoked muscle responses that occurred within a 50-millisecond window. The evoked potentials from the abdominal (i.e., EO, IO, and RA) and ESL3 muscles were distinguishable from the stimulation artifact. Conversely, the evoked potentials from the EST7 muscle often appeared occluded by the stimulation artifact (see Appendix C, Fig. C-3). Based on a visual inspection, waveform timing (i.e., onset and duration)

appeared consistent across trials and stimulation amplitudes for all abdominal muscles. The same trend was seen in all other participants. Note that representative evoked responses from the muscles not presented in Fig. 11 can be found in Appendix C.

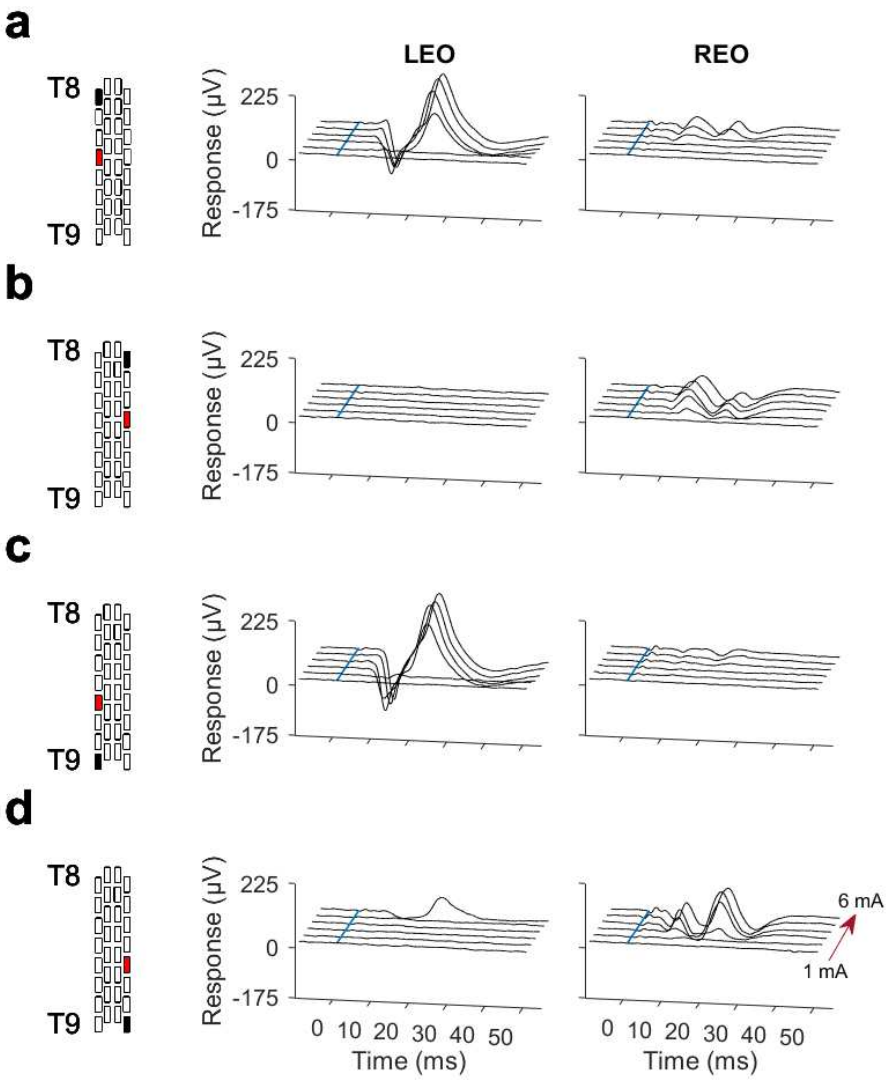

Figure 11. Representative evoked responses from one participant (P21) for the left and right external obliques (LEO and REO), with electrode placement above the T8 and T9 vertebrae. The stimulating cathode is represented in black, and the anode in red. Waveforms, averaged across three trials, are depicted for increasing stimulation amplitudes (1 to 6 mA in 1 mA increments, represented by the red arrow) and when delivering stimulation above: (a) the left T8 vertebra, (b) the right T8 vertebra, (c) the left T9 vertebra, and (d) the right T9 vertebra. Stimulation occurs at zero milliseconds, represented by the blue line. Representative responses for the same participant from all other recorded trunk muscles can be found in Appendix C.

Figure 12 presents the recruitment curves of muscle responses, demonstrating the relationship between applied charge and peak-to-peak amplitude of the evoked muscle responses during ESS delivered at different locations over the thoracic spine. Based on a visual inspection, ESS evoked responses in trunk muscles may be characterized by increasing peak-to-peak amplitude beyond MT. At greater applied charge a subset of recruitment curves plateaued, likely representing saturation of motor unit recruitment. Within the range of applied charge tested, the responses recorded in the abdominal muscles (EO, IO, and RA) and the ESL3 muscle increased the most toward a plateau when stimulating caudal to the T7 vertebra level. The responses recorded in the EST7 muscle experienced growth at all stimulation levels tested. Individual MT values varied depending on the muscle and stimulation location, which motivated further analysis of the MT data.

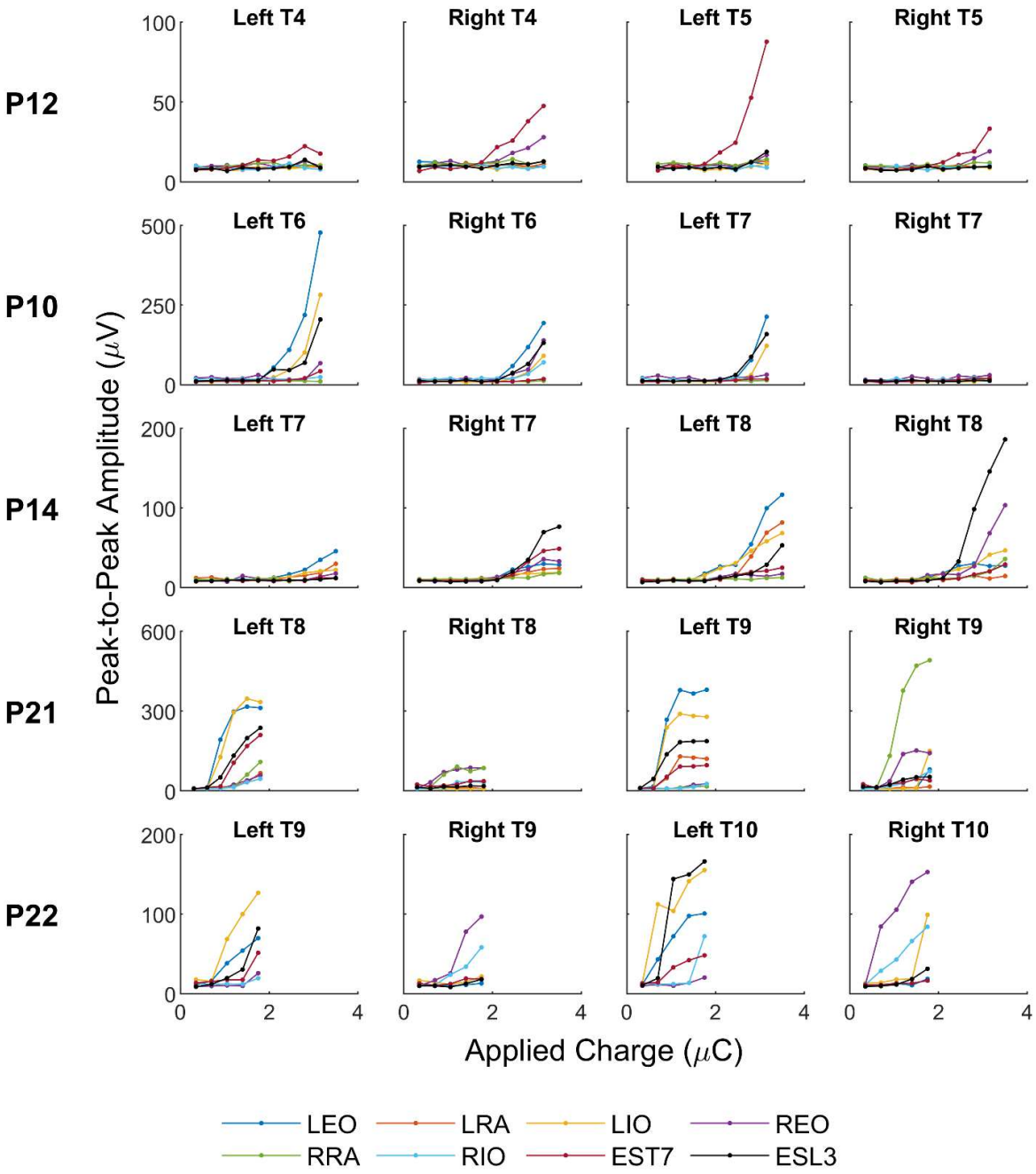

Figure 12. Representative recruitment curves of muscle responses during stimulation above the T4 and T5 (P12), T6 and T7 (P10), T7 and T8 (P14), T8 and T9 (P21), and T9 and T10 (P22) vertebrae. Peak-to-peak amplitude of the left and right external obliques (LEO and REO), internal obliques (LIO and RIO), rectus abdominis (LRA and RRA), and erector spinae above the T7 and L3 vertebral levels (EST7 and ESL3), are shown in dependence of applied charge. Peak-to-peak amplitude values were averaged across three trials. Recruitment curves of muscle responses from the remaining six participants can be found in Appendix D.

Figure 13 demonstrates the relationship between MT and stimulation location along the rostrocaudal and mediolateral axes. Muscle responses were evoked from single-pulse stimulation caudal to the T5 vertebral level in the EO, IO, RA, and ESL3 muscles. Responses in the EST7 muscle were observed for stimulation at all locations. Individual MT values varied by stimulation location and muscle, with recorded responses demonstrating lower motor thresholds for ipsilateral stimulation (EO: 1.5 ± 0.8, IO: 1.7 ± 0.9, RA: 2.0 ± 0.9, EST7: 1.7 ± 0.9, ESL3: 1.5 ± 0.7 μC) compared to contralateral stimulation (EO: 1.9 ± 0.6, IO: 2.1 ± 0.7, RA: 2.1 ± 0.8, EST7: 1.9 ± 0.9, ESL3: 1.8 ± 0.8 μC). On average, a 30% lower motor threshold was identified for ipsilateral compared to contralateral stimulation. Based on a visual inspection of Fig. 13, all muscles experienced the lowest MT for ipsilateral stimulation, with the cathode located caudal to the T8 vertebral level. For the T9 and T10 vertebral levels, contralateral stimulation did not evoke a response in the RA (T9), EO (T10), and EST7 (T10) muscles.

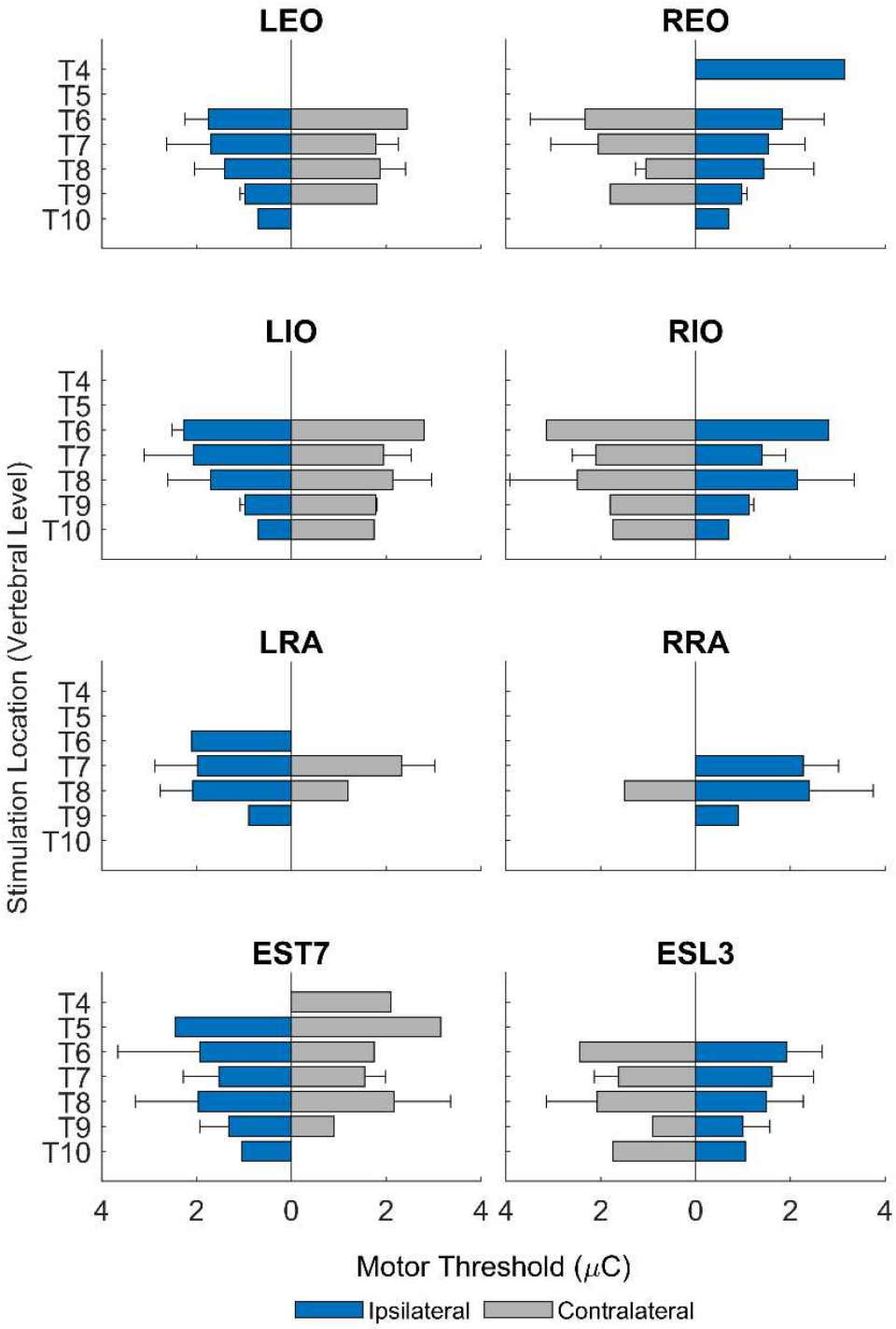

Figure 13. Effect of stimulation location on the MT of evoked trunk muscle responses. Stimulation was delivered at different locations along the rostrocaudal axis of the spine (vertebral levels T4 to T10) and on the mediolateral axis of the spine (left and right side of the electrode array, represented accordingly as ipsilateral and contralateral). Values across participants (mean + one standard deviation) at each stimulation location are shown. Non-responsive muscles were omitted.

Figure 14 presents the dependency of the maximum amplitude of the evoked trunk muscle responses (across all stimulation amplitudes) on ipsilateral versus contralateral stimulation location. For each stimulation location along the rostrocaudal axis of the spine, peak-to-peak amplitudes were normalized to the maximum response for each participant and muscle. Ipsilateral stimulation evoked approximately 2.4 times greater maximum response amplitudes compared to contralateral stimulation in all muscles and stimulation locations. At some stimulation locations, contralateral stimulation did not evoke a response which may, in part, be the result of the larger distance to contralateral dorsal roots and/or limitations associated with the size of the electric field produced for the tested range of applied charge.

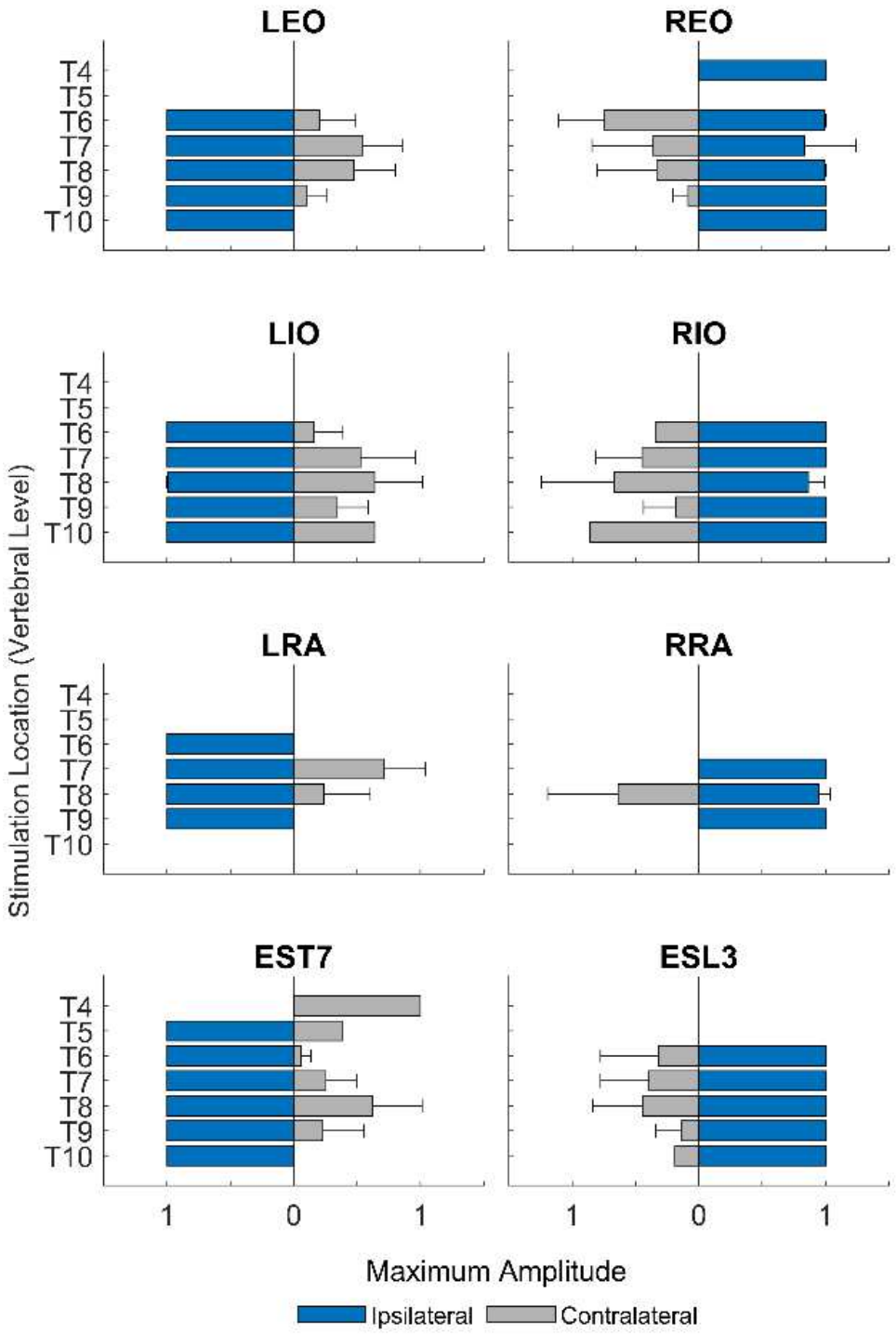

Figure 14. Maximum evoked response at each stimulation location in dependence of ipsilateral versus contralateral stimulation. For each stimulation location along the rostrocaudal axis of the spine, peak-to-peak amplitudes were normalized to the maximum response for each participant and muscle. Values across participants (mean + one standard deviation) at each stimulation location are shown. Non-responsive muscles were omitted.

Figure 15 presents the relationship between the maximum evoked amplitude of trunk muscle responses and stimulation location along the rostrocaudal axis. Muscle response amplitude values are limited in their ability to be compared across participants, therefore, amplitude comparisons were made *within* the electrode array for each a participant. A comparison of amplitude between stimulation on the ipsilateral rostral region and ipsilateral caudal region of the array was performed. For each muscle, maximum response values for each electrode configuration were normalized to the maximum response for each participant on the ipsilateral stimulation side. The difference in normalized response amplitude resulting from caudal and rostral stimulation was calculated. A positive difference suggests a greater maximum response was achieved through the ipsilateral caudal cathode location. On the other hand, a negative difference suggests a greater maximum response was achieved through the ipsilateral rostral cathode location. There was no clear trend in maximum amplitude with respect to cathode location along the rostrocaudal axis, likely due to the close proximity of the dorsal roots neighboring the rostral and caudal region of each electrode paddle, which will be discussed further in Section 5.2.

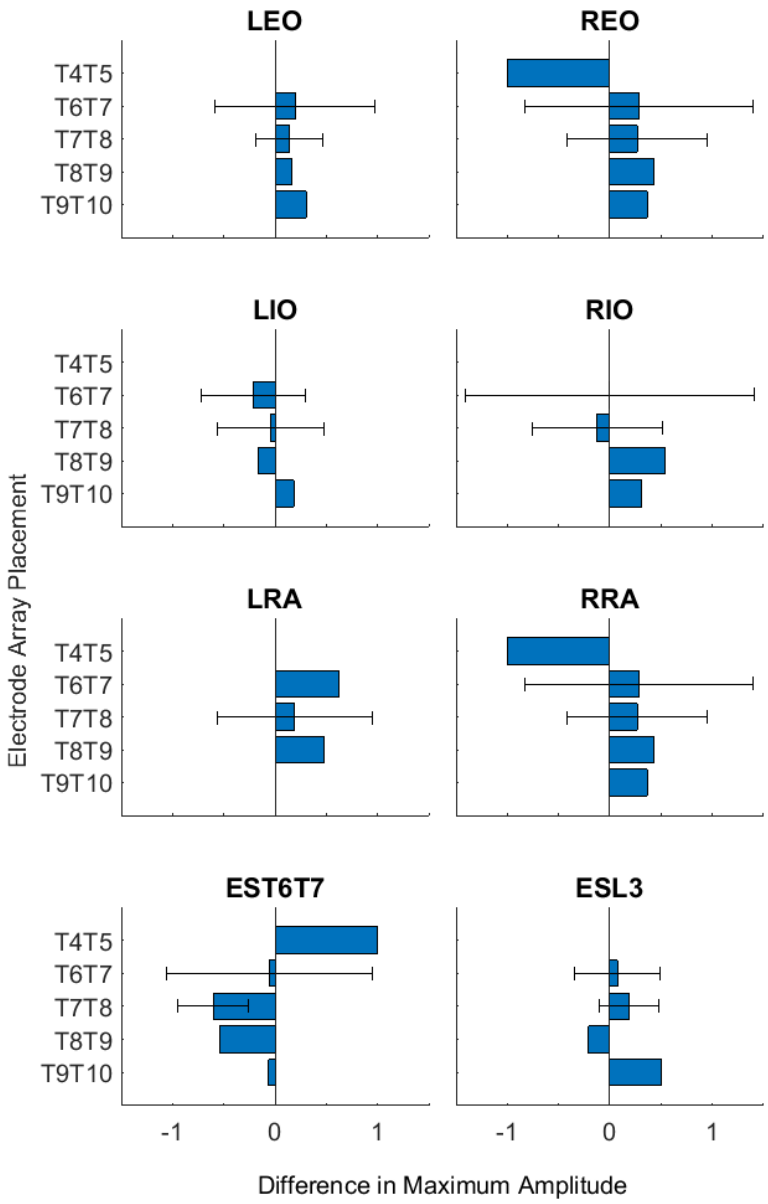

Figure 15. The mean difference (± one standard deviation) in maximum ipsilateral peak-to-peak amplitude evoked from stimulation on the caudal region and rostral region of the electrode array. For each muscle, maximum response values for each electrode configuration were normalized to the maximum response for each participant on the ipsilateral stimulation side. The difference in normalized response amplitude resulting from caudal and rostral stimulation was calculated. A positive difference suggests a greater maximum response was achieved through the caudal cathode location. On the other hand, a negative difference suggests a greater maximum response was achieved through the rostral cathode location. Values at each stimulation location were averaged across participants. Non-responsive muscles were omitted.

4.2 Effect of Stimulation Location on Trunk Muscle Activity Timing

Onset latency was calculated using a custom-made script in MATLAB and a baseline band approach. The results from the latter provided more repeatable and consistent results across three trials therefore were used for further analyses. Figure 16 presents, for the maximum stimulation amplitude, the relationship between the latency of evoked trunk muscle responses and stimulation location along the mediolateral and rostrocaudal axes using the baseline band approach. The onset latency values calculated with the custom-made script in MATLAB may be found in Appendix B for comparison. The onset latency values varied along the rostrocaudal axis, and exhibited a general trend toward shorter onset latencies from ipsilateral (EO: 7.4 ± 2.6, IO: 8.5 ± 2.6, RA: 9.2 ± 2.4, ESL3: 4.2 ± 1.6 ms) compared to contralateral stimulation (EO: 8.2 ± 2.8, IO: 9.5 ± 2.1, RA: 11.2 ± 4.1, ESL3: 4.8 ± 1.8 ms). We identified an average difference of 0.9 ms between ipsilateral and contralateral stimulation (EO: 0.6, IO: 1.2, RA: 1.1, ESL3: 0.6 ms). Visually, there was a trend toward shorter onset latencies from stimulation more caudal on the spine. Based on a visual inspection of Fig. 16, responses recorded in the ESL3 muscle experienced shorter onset latencies at maximum stimulation compared to the abdominal muscles.

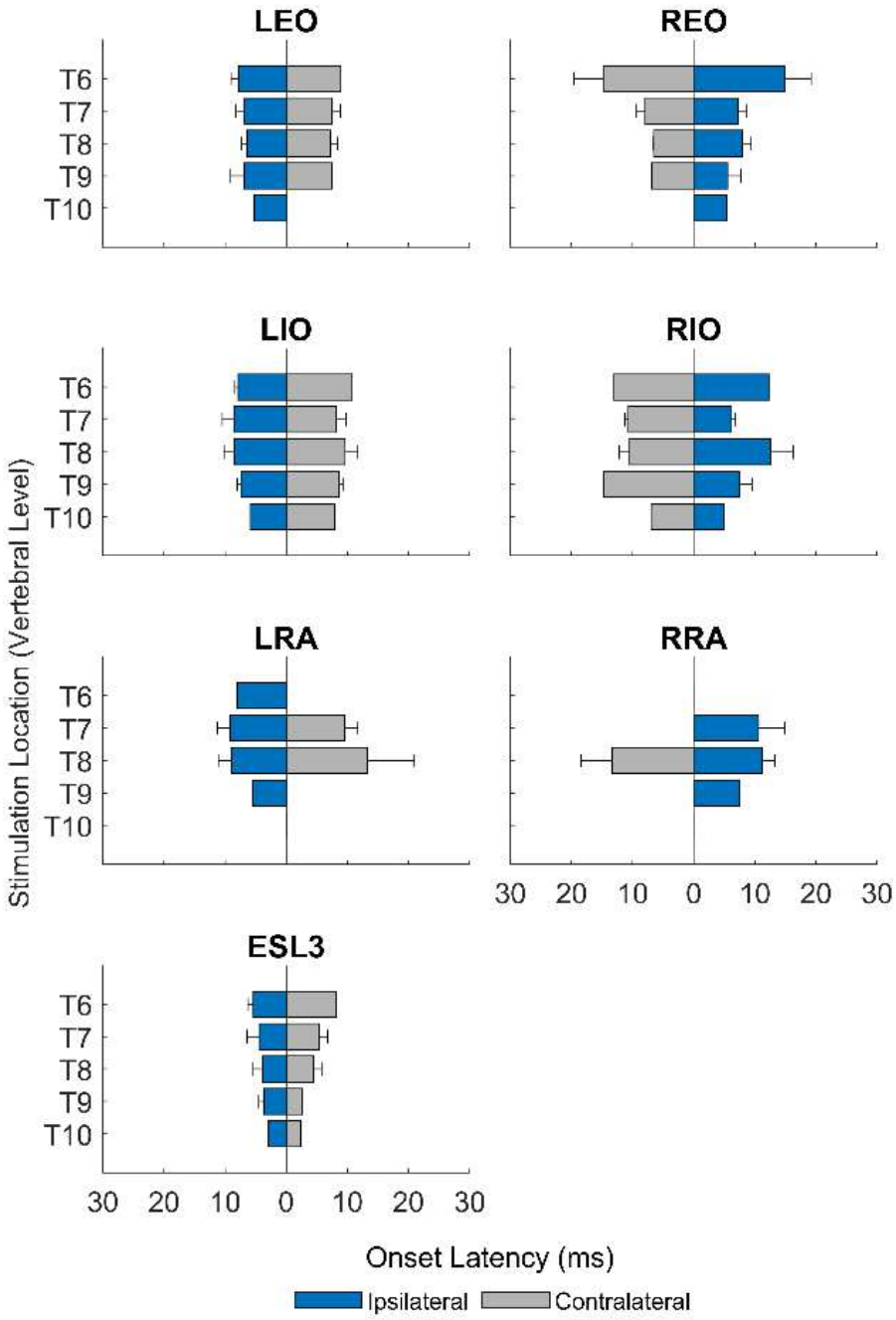

Figure 16. Onset latency at maximum stimulation amplitude for each stimulation location along the rostrocaudal axis of the spine (vertebral levels T6 to T10) and along the mediolateral axis of the spine (left and right side of the electrode array, represented accordingly as ipsilateral and contralateral). Onset latency was calculated as the first time the signal deviated from a baseline band (baseline ± three times the standard deviation[26]). Onset latency values at each stimulation location were averaged across participants (mean + one standard deviation). Non-responsive muscles were omitted.

In Fig. 17, the presence of ER and MR responses in the ESL3 muscle are presented for P21. An MR was detected at lower stimulation amplitudes. At greater stimulation amplitudes, a decrease in onset latency was observed, which suggests the presence of an ER component. ER and MR responses were also seen in the ESL3 muscle for P22 (Appendix E).

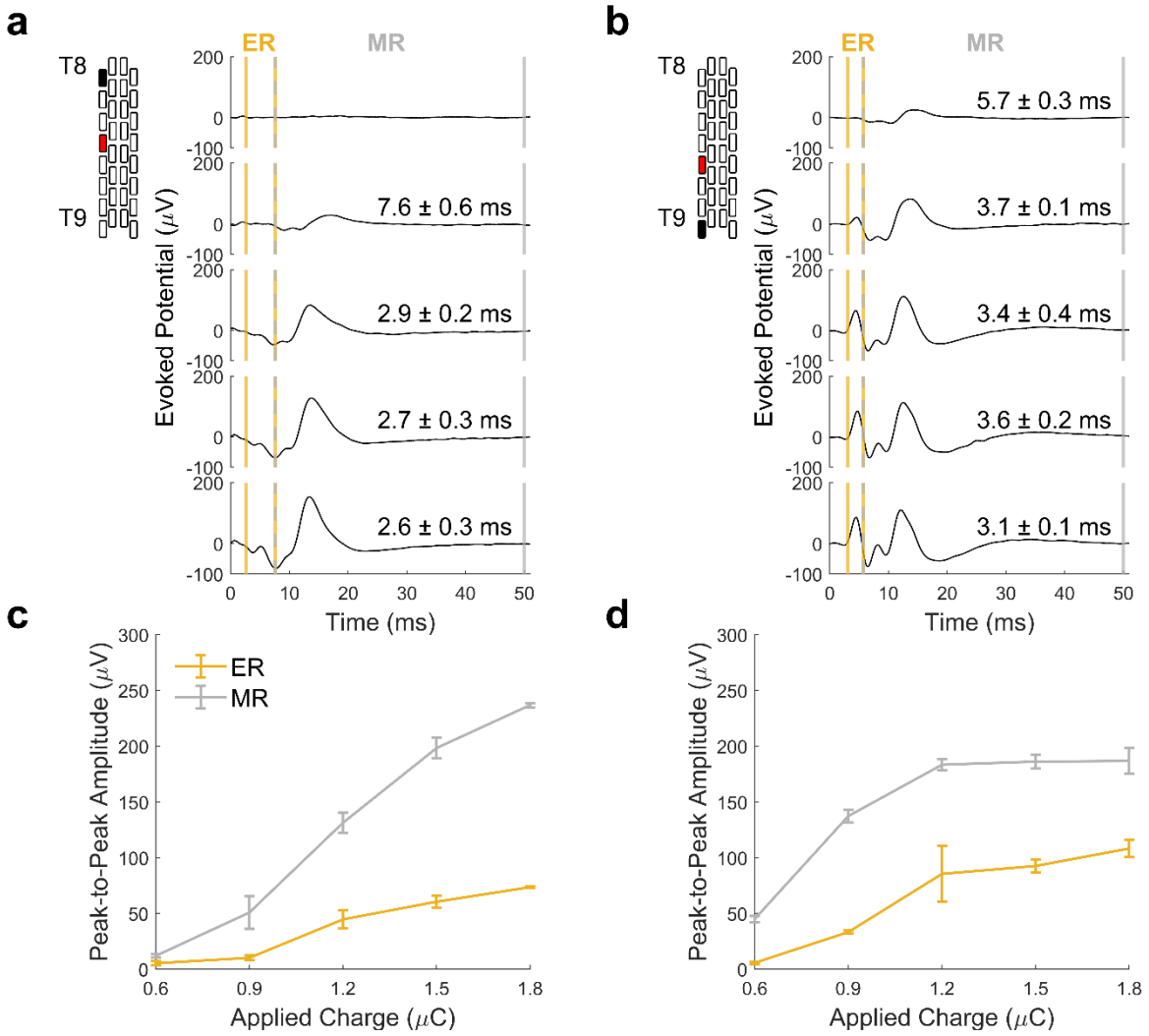

Figure 17. Onset latency analysis for responses recorded in the ESL3 muscle for P21. Evoked responses with increasing applied charge are shown for ipsilateral stimulation above: (a) the left T8 vertebra, and (b) the left T9 vertebra. Onset latency averaged across three trials (mean ± one standard deviation stated on each waveform) decreased at higher applied charge. The start of the early latency response (ER; solid yellow, vertical line) is identified as the onset latency at the highest applied charge for a given electrode configuration. The start of the medium response (MR; vertical dotted yellow and grey line) is identified as the onset latency at the lowest applied charge that evoked a response. The end of the MR (vertical solid grey line) is 50 ms. In (c) and (d), the peak-to-peak amplitudes of the ER and MR components are compared when increasing applied charge. All waveforms and outputted metrics were averaged across three trials. The onset latency analysis for P22 can be found in Appendix E.

Figure 18 presents, for the maximum stimulation amplitude, the relationship between the duration of evoked trunk muscle responses and stimulation location along the mediolateral and rostrocaudal axes using the custom-made MATLAB algorithm. Residual signals in the surface EMG data resulting from variability in tissue thickness between the muscle and the EMG electrode presented a challenge when identifying an accurate end of the muscle response. Therefore, the response offset identified with the custom-made MATLAB algorithm was not repeatable and consistent across trials. There was no clear trend in evoked response duration in relation to stimulation location.

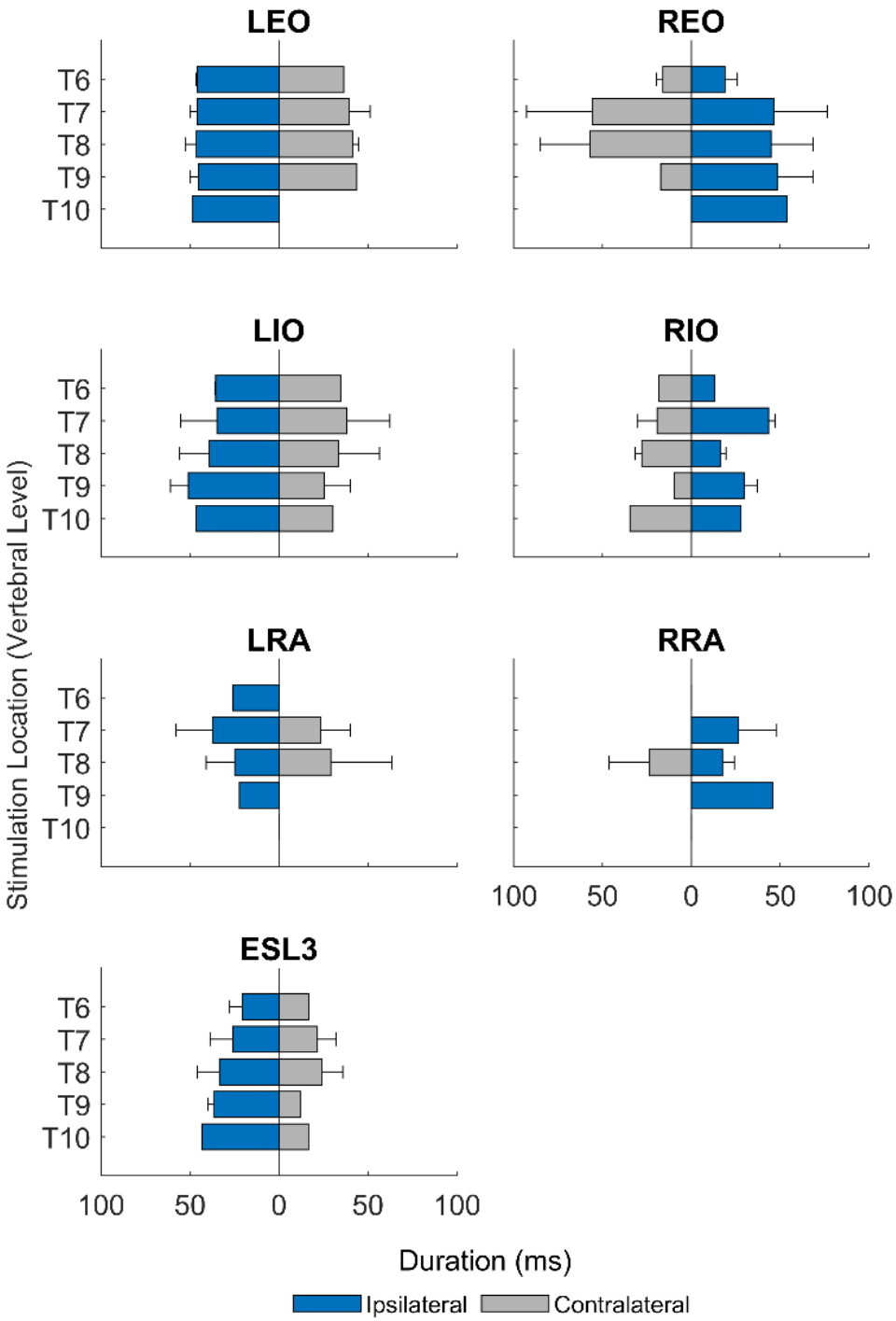

Figure 18. Duration at maximum stimulation amplitude for each stimulation location along the rostrocaudal axis of the spine (vertebral levels T6 to T10) and along the mediolateral axis of the spine (left and right side of the electrode array, represented accordingly as ipsilateral and contralateral). Duration values at each stimulation location were averaged across participants (mean + one standard deviation). Non-responsive muscles were omitted.

5 Discussion

The purpose of this study was to investigate the effect of ESS delivered to the thoracic spinal cord on the activity of trunk muscles involved in postural control and stability. The results demonstrate that the amplitude, MT, and timing of evoked trunk muscle responses depend on the location of ESS. Furthermore, the results provide evidence for activation of both afferent and efferent spinal pathways when applying thoracic ESS.

5.1 Side-Selectivity of Trunk Muscles Enabled by Thoracic ESS

Lateral ESS evoked ipsilateral and contralateral muscle responses; however, lower MTs, greater response amplitudes, and shorter onset latencies occurred during ipsilateral stimulation. Similarly, recruitment curves of muscle responses were more likely to reach a plateau from ipsilateral stimulation. It is important to note that this side-selectivity was seen in trunk muscles during stimulation at all thoracic vertebral levels, ranging from T6 to T10. In addition, it is consistent with findings from previous studies investigating the location-specific effects of lumbar ESS that demonstrated greater muscle responses amplitudes in ipsilateral trunk and lower limb muscles[21,28]. Stimulation caudal to the T8 vertebral level did not produce a response in the contralateral RA muscle, and stimulation caudal to the T9 vertebra did not produce a response in the contralateral EO and EST7 muscles. However, at these two levels, stimulation was only increased to 6 mA (P21; equivalent applied charge: 1.8 μC) and 5 mA (P22; equivalent applied charge: 1.75 μC), respectively; therefore, contralateral responses may still be achieved at higher stimulation amplitudes, as seen at other levels.

Side-selectivity is beneficial for applications that require side-specific muscle activity, such as during ESS-assisted stepping following SCI[121,154,155]. This need for side-specific activity may also be valuable in trunk control applications, for example enabling unilateral trunk excursion during lateral reaching[28]. Using lower frequency stimulation (0.5 Hz), Rowald et al. delivered ESS at the T12 to L2 vertebral levels to assess side-selectivity of trunk muscles[28]. Lateral stimulation above the T12 vertebra induced responses in ipsilateral upper RA, obliques, and the quadratus lumborum, which, when translated to a higher frequency stimulation, resulted in ipsilateral trunk excursion[28]. For future applications, the present work suggests lateral thoracic ESS at lower stimulation intensities to be able to target ipsilateral trunk muscles while preventing contralateral activation.

Irrespective of the important findings discussed above, this study is limited in its ability to assess side-selectivity in dependence of stimulation distance from the midline. Some participants presented asymmetrical evoked responses and, at times, greater responses from contralateral stimulation. This, in part, may be the result of the electrode array placement (i.e., deviations from the midline) or variations in the placement of EMG electrodes across participants. Previous studies also reported an asymmetry between the left and right responses[21,22], attributing that to anatomical variability, including uneven muscle innervation[156], asymmetric musculature[157], or asymmetric dorsal root ganglia position and morphology[158]. Some participants in the present study were also diagnosed with lumbar radiculopathy, which may be linked to asymmetric atrophy of paraspinal muscles[159]. Based on the geometry of the electrode array, and assuming central placement, lateral stimulation occurred approximately 2 mm from the midline. However, simulation results suggest placing the electrodes 4.7 mm from the midline to allow for the greatest side-selectivity while accounting for mediolateral variations in electrode array positioning[28].

5.2 Rostrocaudal Manipulation Modulates Trunk Muscle Amplitude and Selectivity

Previous work has shown that manipulation of stimulation location along the rostrocaudal axis modulates the amplitude and selective activation of lower limb, abdominal, and trunk muscles[26,28]. For example, upper abdominal muscles exhibited a greater response amplitude from ESS targeting the T12 vertebral level compared to the L1/L2 vertebral level[28]. In the context of trunk control and stability, the same modulation can be harnessed in studies aimed to improve functional outcomes. ESS targeting the T12 to L1/L2 vertebral levels induced lateral trunk excursion, however, selective activation of trunk muscles without unintentional leg muscle activation was better achieved with stimulation in the more rostral region of the electrode array, corresponding to the T12 vertebral level[28]. ESS electrode placement within T11 to L1 vertebral levels improved forward reaching following complete, thoracic SCI, with stimulation from the caudal region of the electrode array enabling the greatest improvement[122]. Interestingly, the same electrode placement did not improve lateral reach distance[122]. These findings demonstrate that localized stimulation along the rostrocaudal axis targets specific motor pools projecting to trunk muscles, resulting in varying

functional outcomes. However, these findings also highlight the need for further testing of ESS at additional vertebral levels within the thoracic spine, as addressed in the present work.

The results from this study demonstrated that ESS along the rostrocaudal axis within the thoracic region of the spine, and particularly between the T4 and T10 vertebral levels, can activate trunk muscles. The anterior abdominal (EO, IO, and RA) and ESL3 muscles were activated from stimulation at and more caudal to the T6 vertebral level. Stimulation rostral to the T6 vertebral level did not evoke muscle responses in the abdominal muscles within the range of applied charge tested. This was expected as current anatomical knowledge suggests innervation of each muscle to lie within the T7 to L1 spinal segment range, which approximately aligns with the vertebral segment range between the caudal region of the T5 vertebra and the rostral region of the T11 vertebra[30,31]. The erector spinae muscle recorded at the T7 vertebrae level was activated at all stimulation locations tested. In addition, multiple muscles were activated during ESS delivered at multiple locations between the T6 to T10 vertebral levels, demonstrating the ability to target an ensemble of trunk muscles with one stimulation location.

Despite differences in expected innervation zones, all trunk muscle responses demonstrated a general trend towards a lower MT and shorter onset latency from stimulation in the lower thoracic region compared to the midthoracic region. This trend was even seen in the EST7 muscle; however, results may be impacted by response occlusion from stimulation artifacts more rostral on the spine. In this context, it is important to note that activation thresholds of dorsal roots are affected by the location, orientation, and curvature of the dorsal root with respect to the electric field[160–163]. Lower thresholds resulting from lower thoracic stimulation may also result from the spread of the electric field reaching a greater number of dorsal roots projecting to trunk muscles. This idea is feasible considering stimulation projecting laterally likely targets nearby ascending dorsal roots, in addition to the dorsal root entry zone at the level near the cathode[143]. Contrary to the results for MT and onset latency, there was no clear trend when investigating the effect of rostrocaudal manipulation on maximum response amplitude. In fact, comparing EMG amplitudes across individuals has limited value; therefore, amplitudes can only be compared between rostral and caudal stimulation *within* the electrode array (i.e., across two vertebral levels) for each participant. Due to the close proximity between the rostral and caudal electrode within the electrode array, the electric field

from rostral stimulation may have excited dorsal roots neighboring the caudal electrode, and vice versa, reducing the impact of rostrocaudal manipulation.

Our findings may enable objectively guided electrode placement in future applications which require targeting of specific motor pools. However, methodological considerations may limit accurate comparisons of stimulation location along the rostrocaudal axis; hence, generalizations must be viewed with caution. Anatomic variability of the alignment of the spinal segments and vertebral levels[164] as well as varied placement of electrode arrays, even across participants tested at the same stimulation location, impact the accuracy of rostrocaudal comparisons. Minute variation in rostrocaudal array placement can impact the location of the cathode relative to the dorsal root entry zone, which has been shown to influence the amplitude of an evoked muscle response even more than manipulation of vertebral level[165]. Signal transmission speed and distance are variable across participants, e.g., due to differences in height and age, limiting onset latency comparisons[166,167]. MT as a metric for inter-participant comparison is limited due to variability in dorsal root anatomy (i.e., fibre diameter, innervation angle), which affects excitability[160,161], and/or variability in tissue layer thickness, which affects the measured amplitude through surface EMG[58]. Lastly, our results are based on a different number of data sets at each stimulation location, which limits generalizability of results.

5.3 Trunk Muscle Activation Pathways from Thoracic ESS

In the present work, preferential activation of ipsilateral trunk muscles supports the idea that lateral ESS off the midline mainly targets dorsal roots as they ascend prior to or at the junction with the spinal cord. Contralateral responses at higher intensities and longer onset latencies suggest additional activation of nearby inter-neuronal structures, dorsal columns, or contralateral dorsal roots due to the spread of the electrical field[21]. The present work showed a difference between ipsilateral and contralateral onset latencies of approximately 1 ms, varying by muscle and stimulation location. This agrees with previous findings reporting an approximately 2 ms difference, which could be explained by contralateral activation through crossed reflex pathways in abdominal muscles in these studies[168,169].

Spinal stimulation studies differentiate between ER and MR responses[26,165]. ER and MR responses have been evoked in lower limb muscles resulting from lumbosacral ESS, with ER responses only

appearing at higher stimulation intensities[26,170,171]. ER responses, at higher stimulation intensities are attributed to direct motor neuron activation[26,170–172], whereas MR responses are believed to result from activation via transsynaptic pathways[9,26,170–173]. These components are often overlapping and produce a combined waveform[26,172]. In the present work, for stimulation at and caudal to the T8 vertebra, the ESL3 muscle experienced shorter onset latencies and overlapping waveforms at higher stimulation amplitudes. This was not seen in the abdominal muscles or EST7 muscle, however, the EST7 response was often occluded by the stimulation artifact preventing further analysis. Due to the proximity of the ESL3 muscle to the electrode array, one would expect motor neurons projecting to this muscle to be closer to the electrode array when compared to abdominal muscles. These findings suggest that thoracic ESS can target both afferent and efferent reflex pathways projecting to back muscles. However, the presumed activation of efferent pathways was only seen in two participants (P21 and P22), therefore generalizations about the response of this muscle at this stimulation location should be viewed with caution.

5.4 Limitations and Future Directions

In addition to the anatomic variability mentioned previously, the present work is limited by the relatively small sample size. Future efforts require a larger pool of data, especially above the most rostral (T4 to T5) and most caudal (T9 to T10) vertebral levels. Differences in the size and type of implanted electrode array also pose limitations; however, the interelectrode distances remained relatively constant, allowing for inter-participant comparisons. Future work must determine if TSS produces comparable results in the context of trunk muscle activation. Finally, translation of these findings to functional outcomes, both with ESS and TSS, is a future direction. Since the presented results are for individuals with no known neurological deficits, it is unknown if comparable result patterns will be obtained in individuals with SCI.

6 Conclusions

In a dynamic world such as ours, trunk stability can be maintained through postural control mechanisms. Such mechanisms require relaying information between the nervous system and skeletal muscles to ensure coordinated activation of various trunk muscles. Impaired trunk stability, e.g., as a consequence of SCI, can significantly impact one's quality of life; therefore, spinal stimulation techniques, such as ESS, have shown to be a highly valuable tool for activating trunk muscles in a systematic and coordinated manner, with the goal of improving trunk control and stability following SCI. In such applications, stimulation location along the rostrocaudal and mediolateral axes of the spine plays an important role in facilitating selective muscle activation due to the relative positioning of ESS delivery to motor pools projecting to specific muscles. Due to this fact, identifying the location-dependent effect of ESS on selective trunk muscle activation is a critical next step towards the development of clinical ESS applications for enhancing trunk stability and control.

In the present work, motor pools within the thoracic spinal cord were modulated through a systematic rostrocaudal and mediolateral manipulation of ESS, with the goal of selectively activating trunk muscles. Previous work employing ESS for targeted activation of trunk muscles has been limited to ESS delivered within the lower thoracic to upper lumbosacral regions. The first significant contribution of this thesis research stems from the reported quantitative evidence that ESS delivered within higher thoracic regions, specifically between the T6 and T10 vertebral levels, can evoke trunk muscle responses, with lower motor thresholds and shorter onset latencies resulting from stimulation between the T8 and T10 vertebral levels. As the second significant contribution, this thesis research demonstrates that ipsilateral trunk muscles are preferentially activated by ESS relative to contralateral trunk muscles. As a consequence of the first two contributions, this thesis research establishes, for the first time, a spatial map of trunk muscle activation in response to ESS delivered within the upper to lower thoracic regions. These contributions expand our knowledge of how manipulation of the location of ESS delivery in the thoracic region can modulate trunk muscle activation. This knowledge can guide electrode placement in future therapeutic and rehabilitative ESS applications and can lead the way for further optimization of ESS stimulation parameters for improving trunk stability and postural control following SCI. The results may also guide electrode placement for non-invasive stimulation

techniques such as TSS; however, further work utilizing TSS with a larger sample is required to confirm transferability of ESS results to TSS approaches.

References

1. Ivanenko, Y. & Gurfinkel, V. S. Human postural control. *Front. Neurosci.* **12**, 171 (2018).
2. Massion, J. Postural control system. *Curr. Opin. Neurobiol.* **4**, 877–887 (1994).
3. Seelen, H. A. M., Potten, Y. J. M., Drukker, J., Reulen, J. P. H. & Pons, C. Development of new muscle synergies in postural control in spinal cord injured subjects. *J. Electromyogr. Kinesiol.* **8**, 23–34 (1998).
4. Anson, C. A. & Shepherd, C. Incidence of secondary complications in spinal cord injury. *Int. J. Rehabil. Res.* **19**, 55–66 (1996).
5. Anderson, K. D. Targeting recovery: Priorities of the spinal cord-injured population. *J. Neurotrauma* **21**, 1371–1383 (2004).
6. Gerasimenko, Y., Gorodnichev, R., Moshonkina, T., Sayenko, D., Gad, P. & Reggie Edgerton, V. Transcutaneous electrical spinal-cord stimulation in humans. *Ann. Phys. Rehabil. Med.* **58**, 225–231 (2015).
7. Sayenko, D. G., Rath, M., Ferguson, A. R., Burdick, J. W., Havton, L. A., Edgerton, V. R. & Gerasimenko, Y. P. Self-assisted standing enabled by non-invasive spinal stimulation after spinal cord injury. *J. Neurotrauma* **36**, 1435–1450 (2019).
8. Roy, F. D., Bosgra, D. & Stein, R. B. Interaction of transcutaneous spinal stimulation and transcranial magnetic stimulation in human leg muscles. *Exp. Brain Res.* **232**, 1717–1728 (2014).
9. Minassian, K., Persy, I., Rattay, F., Dimitrijevic, M. R., Hofer, C. & Kern, H. Posterior root-muscle reflexes elicited by transcutaneous stimulation of the human lumbosacral cord. *Muscle Nerve* **35**, 327–336 (2007).

10. Hofstoetter, U. S., Freundl, B., Binder, H. & Minassian, K. Common neural structures activated by epidural and transcutaneous lumbar spinal cord stimulation: Elicitation of posterior root-muscle reflexes. *PLoS ONE* **13**, e0192013 (2018).

11. Taccola, G., Sayenko, D. G., Gad, P., Gerasimenko, Y. & Edgerton, V. R. And yet it moves: Recovery of volitional control after spinal cord injury. *Prog. Neurobiol.* **160**, 64–81 (2018).

12. Burnside, E. R. & Bradbury, E. J. Manipulating the extracellular matrix and its role in brain and spinal cord plasticity and repair. *Neuropathol. Appl. Neurobiol.* **40**, 26–59 (2014).

13. Kitano, K. & Koceja, D. M. Spinal reflex in human lower leg muscles evoked by transcutaneous spinal cord stimulation. *J. Neurosci. Methods* **180**, 111–115 (2009).

14. Hofstoetter, U. S. & Minassian, K. Transcutaneous spinal cord stimulation: Advances in an emerging non-invasive strategy for neuromodulation. *J. Clin. Med.* **11**, 3836 (2022).

15. Oh, J., Steele, A. G., Varghese, B., Martin, C. A., Scheffler, M. S., Markley, R. L., Lo, Y.-K. & Sayenko, D. G. Cervical transcutaneous spinal stimulation for spinal motor mapping. *iScience* **25**, 105037 (2022).

16. de Freitas, R. M., Sasaki, A., Sayenko, D. G., Masugi, Y., Nomura, T., Nakazawa, K. & Milosevic, M. Selectivity and excitability of upper-limb muscle activation during cervical transcutaneous spinal cord stimulation in humans. *J. Appl. Physiol.* **131**, 746–759 (2021).

17. Keller, A., Singh, G., Sommerfeld, J. H., King, M., Parikh, P., Ugiliweneza, B., D'Amico, J., Gerasimenko, Y. & Behrman, A. L. Noninvasive spinal stimulation safely enables upright posture in children with spinal cord injury. *Nat. Commun.* **12**, 5850 (2021).

18. Rath, M., Vette, A. H., Ramasubramaniam, S., Li, K., Burdick, J., Edgerton, V. R., Gerasimenko, Y. P. & Sayenko, D. G. Trunk Stability Enabled by Noninvasive Spinal Electrical Stimulation after Spinal Cord Injury. *J. Neurotrauma* **35**, 2540–2553 (2018).

19. Inanici, F., Samejima, S., Gad, P., Edgerton, V. R., Hofstetter, C. P. & Moritz, C. T. Transcutaneous Electrical Spinal Stimulation Promotes Long-Term Recovery of Upper Extremity Function in Chronic Tetraplegia. *IEEE Trans. Neural Syst. Rehabil. Eng. Publ. IEEE Eng. Med. Biol. Soc.* **26**, 1272–1278 (2018).

20. Zhang, F., Momeni, K., Ramanujam, A., Ravi, M., Carnahan, J., Kirshblum, S. & Forrest, G. F. Cervical Spinal Cord Transcutaneous Stimulation Improves Upper Extremity and Hand Function in People With Complete Tetraplegia: A Case Study. *IEEE Trans. Neural Syst. Rehabil. Eng.* **28**, 3167–3174 (2020).

21. Calvert, J. S., Manson, G. A., Grahn, P. J. & Sayenko, D. G. Preferential activation of spinal sensorimotor networks via lateralized transcutaneous spinal stimulation in neurologically intact humans. *J. Neurophysiol.* **122**, 2111–2118 (2019).

22. Sayenko, D. G., Atkinson, D. A., Dy, C. J., Gurley, K. M., Smith, V. L., Angeli, C., Harkema, S. J., Edgerton, V. R. & Gerasimenko, Y. P. Spinal segment-specific transcutaneous stimulation differentially shapes activation pattern among motor pools in humans. *J. Appl. Physiol.* **118**, 1364–1374 (2015).

23. Bryson, N., Lombardi, L., Hawthorn, R., Fei, J., Keesey, R., Peiffer, J. D. & Seáñez, I. Enhanced selectivity of transcutaneous spinal cord stimulation by multielectrode configuration. *J. Neural Eng.* **20**, 046015 (2023).

24. Lorach, H., Galvez, A., Spagnolo, V., Martel, F., Karakas, S., Intering, N., Vat, M., Faivre, O., Harte, C., Komi, S., Ravier, J., Collin, T., Coquoz, L., Sakr, I., Baaklini, E., Hernandez-Charpak, S. D., Dumont, G., Buschman, R., Buse, N., Denison, T., van Nes, I., Asboth, L., Watrin, A., Struber, L., Sauter-Starace, F., Langar, L., Auboiroux, V., Carda, S., Chabardes,

S., Aksenova, T., Demesmaeker, R., Charvet, G., Bloch, J. & Courtine, G. Walking naturally after spinal cord injury using a brain–spine interface. *Nature* **618**, 126–133 (2023).

25. Ladenbauer, J., Minassian, K., Hofstoetter, U. S., Dimitrijevic, M. R. & Rattay, F. Stimulation of the human lumbar spinal cord with implanted and surface electrodes: A computer simulation study. *IEEE Trans. Neural Syst. Rehabil. Eng.* **18**, 637–645 (2010).
26. Sayenko, D. G., Angeli, C., Harkema, S. J., Reggie Edgerton, V. & Gerasimenko, Y. P. Neuromodulation of evoked muscle potentials induced by epidural spinal-cord stimulation in paralyzed individuals. *J. Neurophysiol.* **111**, 1088–1099 (2014).
27. Gorgey, A. S. & Gouda, J. J. Single lead epidural spinal cord stimulation targeted trunk control and standing in complete paraplegia. *J. Clin. Med.* **11**, 5120 (2022).
28. Rowald, A., Komi, S., Demmesmaeker, R., Baaklini, E., Hernandez-Charpak, S. D., Paoles, E. & Montanaro, H. Activity-dependent spinal cord neuromodulation rapidly restores trunk and leg motor functions after complete paralysis. *Nat. Med.* **28**, 260–271 (2022).
29. Chen, C.-L., Yeung, K.-T., Bih, L.-I., Wang, C.-H., Chen, M.-I. & Chien, J.-C. The relationship between sitting stability and functional performance in patients with paraplegia. *Arch. Phys. Med. Rehabil.* **84**, 1276–1281 (2003).
30. Kendall, F. P., McCreary, E. K. & Provance, P. Plexuses, and spinal nerve and muscle charts. in *Muscles, Testing and Function: with Posture and Pain* 375–410 (Williams & Wilkins, Baltimore, Md, 1993).
31. Mendez, A., Islam, R., Latypov, T., Basa, P., Joseph, O. J., Knudsen, B., Siddiqui, A. M., Summer, P., Staehnke, L. J., Grahn, P. J., Lachman, N., Windebank, A. J. & Lavrov, I. A. Segment-specific orientation of the dorsal and ventral roots for precise therapeutic targeting of human spinal cord. *Mayo Clin. Proc.* **96**, 1426–1437 (2021).

32. Drake, R. L., Vogl, W. & Mitchell, A. Neuroanatomy. in *Grey's Anatomy for Students* 1–72 (Elsevier, 2023).

33. Newman, P. P. Neurophysiological concepts and methods. in *Neurophysiology* 3–25 (Springer, Dordrecht, 1980).

34. Splittgerber, R. Neurons and neuroglia. in *Snell's Clinical Neuroanatomy* 33–70 (Lippincott Williams & Wilkins, 2019).

35. Splittgerber, R. Introduction and organization of the nervous system. in *Snell's Clinical Neuroanatomy* 1–32 (Lippincott Williams & Wilkins, 2019).

36. Watson, C. & Kayalioglu, G. The organization of the spinal cord. in *The Spinal Cord* (eds. Watson, C., Praxinos, G. & Kayalioglu, G.) 1–7 (Academic Press, Boston, 2009).

37. Drake, R. L., Vogl, W. & Mitchell, A. Back. in *Grey's Anatomy for Students* 51–122 (Elsevier, 2023).

38. Oliver, J. & Middleditch, A. Structure of the vertebral column. in *Functional Anatomy of the Spine* 1–58 (Butterworth-Heinemann, Oxford, 1991).

39. Splittgerber, R. Spinal cord and ascending, descending, and intersegmental tracts. in *Snell's Clinical Neuroanatomy* 131–184 (Lippincott Williams & Wilkins, 2019).

40. Biga, L. M., Bronson, S., Dawson, S., Harwell, A., Hopkins, R., Kaufmann, J., LeMaster, M., Matern, P., Morrison-Graham, K., Oja, K., Quick, D., Runyeon, J., OERU, O. & OpenStax. *Anatomy & Physiology*. (OpenStax/Oregon State University, 2019).

41. Frostell, A., Hakim, R., Thelin, E. P., Mattsson, P. & Svensson, M. A review of the segmental diameter of the healthy human spinal cord. *Front. Neurol.* **7**, (2016).

42. Oliver, J. & Middleditch, A. Innervation of the vertebral column. in *Functional Anatomy of the Spine* 206–241 (Butterworth-Heinemann, Oxford, 1991).

43. Kuwazawa, Y., Pope, M., Bashir, W., Takahashi, K. & Smith, F. W. The length of the cervical cord: Effects of postural changes in healthy volunteers using positional magnetic resonance imaging. *Spine* **31**, E579–E583 (2006).

44. Holsheimer, J., den Boer, J. A., Struijk, J. J. & Rozeboom, A. R. MR assessment of the normal position of the spinal cord in the spinal canal. *Am. J. Neuroradiol.* **15**, 951–959 (1994).

45. Kayalioglu, G. The spinal nerves. in *The Spinal Cord* (eds. Watson, C., Praxinos, G. & Kayalioglu, G.) 37–56 (Academic Press, Boston, 2009).

46. Cadotte, D. W., Cadotte, A., Cohen-Adad, J., Fleet, D., Livne, M., Wilson, J. R., Mikulis, D., Nugaeva, N. & Fehlings, M. G. Characterizing the location of spinal and vertebral levels in the human cervical spinal cord. *Am. J. Neuroradiol.* **36**, 803–810 (2015).

47. Splittgerber, R. Nerve fibers and peripheral innervation. in *Snell's Clinical Neuroanatomy* 71–130 (Lippincott Williams & Wilkins, 2019).

48. Dave, H. D., Shook, M. & Varacallo, M. Anatomy, skeletal muscle. *Anatomy, skeletal muscle* (2022).

49. Hill, J. A. & Olson, E. N. An introduction to muscle. in *Muscle* (eds. Hill, J. A. & Olson, E. N.) vol. 1 3–9 (Academic Press, Boston, 2012).

50. Scanlon, V. & Sanders, T. The muscular system. in *Essentials of Anatomy and Physiology* 138–165 (F. A. Davis Company, 2018).

51. Bradley, P. B. The somatic motor system. in *Introduction to Neuropharmacology* 35–42 (Butterworth-Heinemann, 1989).

52. Newman, P. P. Nerve impulses. in *Neurophysiology* 27–57 (Springer, Dordrecht, 1980).

53. Carpenter, R. & Reddi, B. Neural mechanisms. in *Neurophysiology: A Conceptual Approach* 1–74 (Taylor & Francis Group, 2012).

54. Newman, P. P. Synaptic transmission. in *Neurophysiology* 59–80 (Springer, Dordrecht, 1980).

55. Cholewicki, J., Panjabi, M. M. & Khachatryan, A. Stabilizing function of trunk flexor-extensor muscles around a neutral spine posture. *Spine* **22**, 2207–2212 (1997).

56. van Dieën, J. H., Kingma, I. & van der Bug, J. C. E. Evidence for a role of antagonistic cocontraction in controlling trunk stiffness during lifting. *J. Biomech.* **36**, 1829–1836 (2003).

57. Vigotsky, A. D., Halperin, I., Lehman, G. J., Trajano, G. S. & Vieira, T. M. Interpreting signal amplitudes in surface electromyography studies in sport and rehabilitation sciences. *Front. Physiol.* **8**, 985 (2017).

58. Farina, D., Stegeman, D. F. & Merletti, R. Biophysics of the generation of EMG signals. in *Surface Electromyography: Physiology, Engineering, and Applications* (eds. Merletti, R. & Farina, D.) 30–53 (IEEE Press, Piscataway, New Jersey, 2016).

59. Türker, K. S. Electromyography: some methodological problems and issues. *Phys. Ther.* **73**, 698–710 (1993).

60. Subasi, A. Chapter 2 - Biomedical Signals. in *Practical Guide for Biomedical Signals Analysis Using Machine Learning Techniques* (ed. Subasi, A.) 27–87 (Academic Press, 2019).

61. Baudry, S., Minetto, M. A. & Duchateau, J. Surface EMG applications in neurophysiology. in *Surface Electromyography: Physiology, Engineering, and Applications* (eds. Merletti, R. & Farina, D.) 333–360 (IEEE Press, Piscataway, New Jersey, 2016).

62. Botter, A. & Merletti, R. EMG of electrically stimulated muscles. in *Surface Electromyography: Physiology, Engineering, and Applications* (eds. Merletti, R. & Farina, D.) 311–332 (IEEE Press, Piscataway, New Jersey, 2016).

63. Barbero, M., Merletti, R. & Rainoldi, A. EMG imaging: geometry and anatomy of the electrode-muscle system. in *Atlas of Muscle Innervation Zones: Understanding Surface Electromyography and Its Applications* 39–47 (Springer, New York, 2012).

64. Sayenko, D. G., Atkinson, D. A., Floyd, T. C., Gorodnichev, R. M., Moshonkina, T. R., Harkema, S. J., Reggie Edgerton, V. & Gerasimenko, Y. P. Effects of paired transcutaneous electrical stimulation delivered at single and dual sites over lumbosacral spinal cord. *Neurosci. Lett.* **609**, 229–234 (2015).

65. Rossini, P. M., Barker, A. T., Berardelli, A., Caramia, M. D., Caruso, G., Cracco, R. Q., Dimitrijevic, M. R., Hallett, M., Katayama, Y., Lücking, C. H., Maertens de Noordhout, A. L., Marsden, C. D., Murray, N. M. F., Rothwell, J. C., Swash, M. & Tomberg, C. Non-invasive electrical and magnetic stimulation of the brain, spinal cord and roots: basic principles and procedures for routine clinical application. Report of an IFCN committee. *Electroencephalogr. Clin. Neurophysiol.* **91**, 79–92 (1994).

66. Barbero, M., Merletti, R. & Rainoldi, A. Features of the single-channel sEMG signal. in *Atlas of Muscle Innervation Zones: Understanding Surface Electromyography and Its Applications* 49–59 (Springer, New York, 2012).

67. Giridharan, S. R., Gupta, D., Pal, A., Mishra, A. M., Hill, N. J. & Carmel, J. B. Motometrics: A toolbox for annotation and efficient analysis of motor evoked potentials. *Front. Neuroinformatics* **13**, (2019).

68. Hofstoetter, U. S., Krenn, M., Danner, S. M., Hofer, C., Kern, H., McKay, W. B., Mayr, W. & Minassian, K. Augmentation of voluntary locomotor activity by transcutaneous spinal cord stimulation in motor-incomplete spinal cord-injured individuals. *Artif. Organs* **39**, E176–E186 (2015).

69. Andrews, J. C., Stein, R. B. & Roy, F. D. Post-activation depression in the human soleus muscle using peripheral nerve and transcutaneous spinal stimulation. *Neurosci. Lett.* **589**, 144–149 (2015).

70. Angeli, C. A., Reggie Edgerton, V., Gerasimenko, Y. P. & Harkema, S. J. Altering spinal cord excitability enables voluntary movements after chronic complete paralysis in humans. *Brain* **137**, 1394–1409 (2014).

71. Besomi, M., Hodges, P. W., Clancy, E. A., van Dieën, J. H., Hug, F., Lowery, M., Merletti, R., Søgaard, Wrigley, T., Besier, T., Carson, R. G., Disselhorst-Klug, C., Enoka, R. M., Falla, D., Farina, D., Gandevia, S., Holobar, A., Kiernan, M. C., McGill, K., Perreault, E., Rothwell, J. C. & Tucker, K. Consensus for experimental design in electromyography (CEDE) project: amplitude normalization matrix. *J. Electromyogr. Kinesiol.* **53**, 102438 (2020).

72. Cavazzuti, L., Merlo, A., Orlandi, F. & Campanini, I. Delayed onset of electromyographic activity of vastus medialis obliquus relative to vastus lateralis in subjects with patellofemoral pain syndrome. *Gait Posture* **32**, 290–295 (2010).

73. Devanne, H., Lavoie, B. A. & Capaday, C. Input-output properties and gain changes in the human corticospinal pathway. *Exp. Brain Res.* **114**, 329–338 (1997).

74. Groppa, S., Oliviero, A., Eisen, A., Quartarone, A., Cohen, L. G., Mall, V., Kaelin-Lang, A., Mima, T., Rossi, S., Thickbroom, G. W., Rossini, P. M., Ziemann, U., Valls-Solé, J. &

Siebner, H. R. A practical guide to diagnostic transcranial magnetic stimulation: report of an IFCN committee. *Clin. Neurophysiol.* **123**, 858–882 (2012).

75. Rossini, P. M., Burke, D., Chen, R., Cohen, L. G., Daskalakis, Z., Di Iorio, R., Di Lazzaro, V., Ferreri, F., Fitzgerald, P. B., George, M. S., Hallett, M., Lefaucheur, J. P., Langguth, B., Matsumoto, H., Miniussi, C., Nitsche, M. A., Pascual-Leone, A., Paulus, W., Rossi, S., Rothwell, J. C., Siebner, H. R., Ugawa, Y., Walsh, V. & Ziemann, U. Non-invasive electrical and magnetic stimulation of the brain, spinal cord and roots: Basic principles and procedures for routine clinical application. An updated report from an IFCN committee. *Clin. Neurophysiol.* **126**, 1071–1107 (2015).

76. Zhongxi, L., Peterchev, A. V., Rothwell, J. C. & Goetz, S. M. Detection of motor-evoked potentials below the noise floor: rethinking the motor stimulation threshold. *J. Neural Eng.* **19**, 056040 (2022).

77. van Vugt, J. P. & van Dijk, J. G. A convenient method to reduce crosstalk in surface EMG. *Clin. Neurophysiol.* **112**, 583–592 (2001).

78. Harkema, S. J., Gerasimenko, Y. P., Hodes, J., Burdick, J., Angeli, C., Chen, Y., Ferreira, C., Willhite, A., Rejc, E., Grossman, R. G. & Edgerton, V. R. Effect of epidural stimulation of the lumbosacral spinal cord on voluntary movement, standing, and assisted stepping after motor complete paraplegia: a case study. *The Lancet* **377**, 1938–1947 (2011).

79. Winter, D. A., Patla, A. E. & Frank, J. S. Assessment of balance control in humans. *Med. Prog. Technol.* **16**, 31–51 (1990).

80. McGuinness, H. The muscular system. in *Anatomy & Physiology* 128–172 (Hodder Education Group, London, 2018).

81. Winter, D. A. Human balance and posture control during standing and walking. *Gait Posture* **3**, 193–214 (1995).

82. Horak, F. B. Postural orientation and equilibrium: what do we need to know about neural control of balance to prevent falls? *Age Ageing* **35 Suppl 2**, ii7–ii11 (2006).

83. Markham, C. H. Vestibular control of muscle tone and posture. *Can. J. Neurol. Sci.* **14**, 493–496 (1987).

84. Masi, A. T. & Hannon, J. C. Human resting muscle tone (HRMT): Narrative introduction and modern concepts. *J. Bodyw. Mov. Ther.* 320–332 (2008).

85. De Keulenaer, B. L., De Waele, J. J., Powell, B. & Malbrain, M. L. N. G. What is normal intra-abdominal pressure and how is it affected by positioning, body mass and positive end-expiratory pressure? *Intensive Care Med.* **35**, 969–976 (2009).

86. Cresswell, A. G., Oddsson, L. & Thorstensson, A. The influence of sudden perturbations on trunk muscle activity and intra-abdominal pressure while standing. *Exp. Brain Res.* **98**, 336–341 (1994).

87. Granata, K. P. & Orishimo, K. F. Response of trunk muscle coactivation to changes in spinal stability. *J. Biomech.* **34**, 1117–1123 (2001).

88. Masani, K., Sin, V. W., Vette, A. H., Adam Thrasher, T., Kawashima, N., Morris, A., Preuss, R. & Popovic, M. R. Postural reactions of the trunk muscles to multi-directional perturbations in sitting. *Clin. Biomech.* **24**, 176–182 (2009).

89. Stokes, I. A. F., Gardner-Morse, M., Henry, S. M. & Badger, G. J. Decrease in trunk muscular response to perturbation with preactivation of lumbar spinal musculature. *Spine* **25**, 1957–1964 (2000).

90. Deliagina, T. G., Orlovsky, G. N., Zelenin, P. V. & Beloozerova, I. N. Neural bases of postural control. *Physiology* **21**, 216–225 (2006).

91. Massion, J. Movement, posture and equilibrium: Interaction and coordination. *Prog. Neurobiol.* **38**, 35–56 (1992).

92. Alshehri, M. A., van den Hoorn, W., Klyne, D. M. & Hodges, P. W. Coordination of hip and spine to maintain equilibrium in unstable sitting revealed by spectral analysis. *J. Neurophysiol.* **125**, 1814–1824 (2021).

93. Van Daele, U., Hagman, F., Truijen, S., Vorlat, P., Van Gheluwe, B. & Vaes, P. Differences in balance strategies between nonspecific chronic low back pain patients and healthy control subjects during unstable sitting. *Spine* **34**, 1233–1238 (2009).

94. Zedka, M., Kumar, S. & Narayan, Y. Electromyographic response of the trunk muscles to postural perturbation in sitting subjects. *J. Electromyogr. Kinesiol.* **8**, 3–10 (1998).

95. Arjmand, N. & Shirazi-Adl, A. Role of intra-abdominal pressure in the unloading and stabilization of the human spine during static lifting tasks. *Eur. Spine J.* **15**, 1265–1275 (2006).

96. Grillner, S., Nilsson, J. & Thorstensson, A. Intra-abdominal pressure changes during natural movements in man. *Acta Physiol. Scand.* **103**, 275–283 (1978).

97. Milosevic, M., Shinya, M., Masani, K., Patel, K., McConville, K. M. V., Nakazawa, K. & Popovic, M. R. Anticipation of direction and time of perturbation modulates the onset latency of trunk muscle responses during sitting perturbations. *J. Electromyogr. Kinesiol.* **26**, 94–101 (2016).

98. Kavcic, N., Grenier, S. & McGill, S. M. Determining the stabilizing role of individual torso muscles during rehabilitation exercises. *Spine* **29**, 1254–1265 (2004).

99. Crenna, P., Frigo, C., Massion, J. & Pedotti, A. Forward and backward axial synergies in man. *Exp. Brain Res.* **65**, 538–548 (1987).

100. Milosevic, M., Masani, K., Kuipers, M. J., Rahouni, H., Verrier, M. C., McConville, K. M. V. & Popovic, M. R. Trunk control impairment is responsible for postural instability during quiet sitting in individuals with cervical spinal cord injury. *Clin. Biomech.* **30**, 507–512 (2015).

101. Sinnott, K. A., Milburn, P. & McNaughton, H. Factors associated with thoracic spinal cord injury, lesion level and rotator cuff disorders. *Spinal Cord* **38**, 748–753 (2000).

102. Castillo-Escario, Y., Kumru, H., Valls-Sole, J., Garcia-Alen, L., Jane, R. & Vidal, J. Quantitative evaluation of trunk function and the StartReact effect during reaching in patients with cervical and thoracic spinal cord injury. *J. Neural Eng.* **18**, (2021).

103. Potten, Y. J. M., Seelen, H. A. M., Drukker, J., Reulen, J. P. H. & Drost, M. R. Postural muscle responses in the spinal cord injured persons during forward reaching. *Ergonomics* **42**, 1200–1215 (1999).

104. Bjerkefors, A., Carpenter, M. G., Cresswell, A. G. & Thorstensson, A. Trunk muscle activation in a person with clinically complete thoracic spinal cord injury. *J. Rehabil. Med.* **41**, 390–392 (2009).

105. Minkel, J. L. Seating and mobility considerations for people with spinal cord injury. *Phys. Ther.* **80**, 701–709 (2000).

106. Anderson, K. D. Targeting Recovery: Priorities of the Spinal Cord-Injured Population. *J. Neurotrauma* **21**, 1371–1383 (2004).

107. Shealy, C. N., Mortimer, J. T. & Reswick, J. B. Electrical inhibition of pain by stimulation of the dorsal columns: preliminary clinical report. *Anesth. Analg.* **46**, 489–491 (1967).

108. Kou, J., Cai, M., Xie, F., Wang, Y., Wang, N. & Xu, M. Complex electrical stimulation systems in motor function rehabilitation after spinal cord injury. *Complexity* **2021**, e2214762 (2021).

109. Mushahwar, V. K. & Horch, K. W. Selective activation of muscle groups in the feline hindlimb through electrical microstimulation of the ventral lumbo-sacral spinal cord. *IEEE Trans. Rehabil. Eng.* **8**, 11–21 (2000).

110. Tao, C., Shen, X., Ma, L., Shen, J., Li, Z., Wang, Z. & Lu, X. Comparative study of intraspinal microstimulation and epidural spinal cord stimulation. *Annu. Int. Conf. IEEE Eng. Med. Biol. Soc.* 3795–3798 (2019).

111. Carhart, M. R., He, J., Herman, R., D'Luzansky, S. & Willis, W. T. Epidural spinal-cord stimulation facilitates recovery of functional walking following incomplete spinal-cord injury. *IEEE Trans. Neural Syst. Rehabil. Eng. Publ. IEEE Eng. Med. Biol. Soc.* **12**, 32–42 (2004).

112. DiMarco, A. F., Kowalski, K. E., Geertman, R. T. & Hromyak, D. R. Spinal cord stimulation: a new method to produce an effective cough in patients with spinal cord injury. *Am. J. Respir. Crit. Care Med.* **173**, 1386–1389 (2006).

113. DiMarco, A. F., Kowalski, K. E., Geertman, R. T. & Hromyak, D. R. Lower thoracic spinal cord stimulation to restore cough in patients with spinal cord injury: results of a National Institutes of Health-sponsored clinical trial. Part I: methodology and effectiveness of expiratory muscle activation. *Arch. Phys. Med. Rehabil.* **90**, 717–725 (2009).

114. Dimitrijevic, M. R., Gerasimenko, Y. & Pinter, M. M. Evidence for a spinal central pattern generator in humans. *Ann. N. Y. Acad. Sci.* **860**, 360–376 (1998).

115. Harandi, S. & Kapural, L. Four-extremity neurostimulation using two cervical octapolar leads and high frequency of 10 kHz. *Pain Pract. Off. J. World Inst. Pain* **18**, 269–272 (2018).

116. Herman, R., He, J., D'Luzansky, S., Willis, W. & Dilli, S. Spinal cord stimulation facilitates functional walking in a chronic, incomplete spinal cord injured. *Spinal Cord* **40**, 65–68 (2002).

117. Hunter, J. P. & Ashby, P. Segmental effects of epidural spinal cord stimulation in humans. *J. Physiol.* **474**, 407–419 (1994).

118. Luna, J. L. V., Brown, J., Krenn, M. J., McKay, B., Mayr, W., Rothwell, J. C. & Dimitrijevic, M. R. Neurophysiology of epidurally evoked spinal cord reflexes in clinically motor-complete posttraumatic spinal cord injury. *Exp. Brain Res.* **239**, 2605–2620 (2021).

119. Minassian, K., Jilge, B., Rattay, F., Pinter, M. M., Binder, H., Gerstenbrand, F. & Dimitrijevic, M. R. Stepping-like movements in humans with complete spinal cord injury induced by epidural stimulation of the lumbar cord: electromyographic study of compound muscle action potentials. *Spinal Cord* **42**, 401–416 (2004).

120. Murg, M., Binder, H. & Dimitrijevic, M. Epidural electric stimulation of posterior structures of the human lumbar spinal cord: 1. muscle twitches - a functional method to define the site of stimulation. *Spinal Cord* **38**, 394–402 (2000).

121. Gill, M., Grahn, P. J., Calvert, J. S., Linde, M. B., Lavrov, I. A., Strommen, J. A., Beck, L. A., Sayenko, D. G., Van Straaten, M. G., Drubach, D. I., Veith, D. D., Thoreson, A. R., Lopez, C., Gerasimenko, Y. P., Edgerton, V. R., Lee, K. H. & Zhao, K. D. Neuromodulation of lumbosacral spinal networks enables independent stepping after complete paraplegia. *Nat. Med.* **24**, 1677–1682 (2018).

122. Gill, M., Linde, M., Fautsch, K., Hale, R., Lopez, C., Veith, D., Calvert, J., Beck, L., Garlanger, K., Edgerton, R., Sayenko, D., Lavrov, I., Thoreson, A., Grahn, P. & Zhao, K. Epidural electrical stimulation of the lumbosacral spinal cord improves trunk stability during seated reaching in two humans with severe thoracic spinal cord injury. *Front. Syst. Neurosci.* **14**, 79 (2020).

123. Grahn, P. J., Lavrov, I. A., Sayenko, D. G., Van Straaten, M. G., Gill, M. L., Strommen, J. A., Calvert, J. S., Drubach, D. I., Beck, L. A., Linde, M. B., Thoreson, A. R., Lopez, C., Mendez, A. A., Gad, P. N., Gerasimenko, Y. P., Edgerton, V. R., Zhao, K. D. & Lee, K. H. Enabling task-specific volitional motor functions via spinal cord neuromodulation in a human with paraplegia. *Mayo Clin. Proc.* **92**, 544–554 (2017).

124. Harkema, S. J., Wang, S., Angeli, C. A., Chen, Y., Boakye, M., Ugiliweneza, B. & Hirsch, G. A. Normalization of blood pressure with spinal cord epidural stimulation after severe spinal cord injury. *Front. Hum. Neurosci.* **12**, 83 (2018).

125. Kinfe, T. M., Schu, S., Quack, F. J., Wille, C. & Vesper, J. Percutaneous implanted paddle lead for spinal cord stimulation: technical considerations and long-term follow-up. *Neuromodulation* **15**, 402–407 (2012).

126. Walter, M., Lee, A. H. X., Kavanagh, A., Phillips, A. A. & Krassioukov, A. V. Epidural spinal cord stimulation acutely modulates lower urinary tract and bowel function following spinal cord injury: a case report. *Front. Physiol.* **9**, 1816 (2018).

127. West, C. R., Phillips, A. A., Squair, J. W., Williams, A. M., Walter, M., Lam, T. & Krassioukov, A. V. Association of epidural stimulation with cardiovascular function in an individual with spinal cord injury. *JAMA Neurol.* **75**, 630–632 (2018).

128. Calvert, J. S., Grahn, P. J., Strommen, J. A., Lavrov, I. A., Beck, L. A., Gill, M. L., Linde, M. B., Brown, D. A., Van Straaten, M. G., Veith, D. D., Lopez, C., Sayenko, D. G., Gerasimenko, Y. P., Edgerton, V. R., Zhao, K. D. & Lee, K. H. Electrophysiological guidance of epidural electrode array implantation over the human lumbosacral spinal cord to enable motor function after chronic paralysis. *J. Neurotrauma* **36**, 1451–1460 (2019).

129. Washburn, S., Catlin, R., Bethel, K. & Canlas, B. Patient-perceived differences between constant current and constant voltage spinal cord stimulation systems. *Neuromodulation* **17**, 28–35; discussion 35-36 (2014).

130. Kumar, K., Nath, R. & Wyant, G. M. Treatment of chronic pain by epidural spinal cord stimulation: a 10-year experience. *J. Neurosurg.* **75**, 402–407 (1991).

131. Stidd, D. A., Rivero, S. & Weinand, M. E. Spinal cord stimulation with implanted epidural paddle lead relieves chronic axial low back pain. *J. Pain Res.* **7**, 465–470 (2014).

132. Stojanovic, M. P. & Abdi, S. Spinal cord stimulation. *Pain Physician* **5**, 156–166 (2002).

133. Chandrasekaran, S., Nanivadekar, A. C., McKernan, G., Helm, E. R., Boninger, M. L., Collinger, J. L., Gaunt, R. A. & Fisher, L. E. Sensory restoration by epidural stimulation of the lateral spinal cord in upper-limb amputees. *eLife* **9**, e54349 (2020).

134. Tse, H.-F., Turner, S., Sanders, P., Okuyama, Y., Fujiu, K., Cheung, C.-W., Russo, M., Green, M. D. S., Yiu, K.-H., Chen, P., Shuto, C., Lau, E. O. Y. & Siu, C.-W. Thoracic spinal cord stimulation for heart failure as a restorative treatment (SCS HEART study): first-in-man experience. *Heart Rhythm* **12**, 588–595 (2015).

135. Gorgey, A. S. & Gouda, J. J. Single lead epidural spinal cord stimulation targeted trunk control and standing in complete paraplegia. *J. Clin. Med.* **11**, 5120 (2022).

136. Hoglund, B. K., Zurn, C. A., Madden, L. R., Hoover, C., Slopsema, J. P., Balser, D., Parr, A., Samadani, U., Johnson, M. D., Netoff, T. I. & Darrow, D. P. Mapping spinal cord stimulation-evoked muscle responses in patients with chronic spinal cord injury. *Neuromodulation* **26**, 1371–1380 (2023).

137. Guertin, P. A. Central pattern generator for locomotion: anatomical, physiological, and pathophysiological considerations. *Front. Neurol.* **3**, 183 (2012).

138. Angeli, C. A., Boakye, M., Morton, R. A., Vogt, J., Benton, K., Chen, Y., Ferreira, C. K. & Harkema, S. J. Recovery of over-ground walking after chronic motor complete spinal cord injury. *N. Engl. J. Med.* **379**, 1244–1250 (2018).

139. Oakley, J. C. & Prager, J. P. Spinal cord stimulation: mechanisms of action. *Spine* **27**, 2574–2583 (2002).

140. Lu, D. C., Edgerton, V. R., Modaber, M., AuYong, N., Morikawa, E., Zdunowski, S., Sarino, M. E., Sarrafzadeh, M., Nuwer, M. R., Roy, R. R. & Gerasimenko, Y. Engaging cervical spinal cord networks to reenable volitional control of hand function in tetraplegic patients. *Neurorehabil. Neural Repair* **30**, 951–962 (2016).

141. Gorgey, A. S., Trainer, R., Sutor, T. W., Goldsmith, J. A., Alazzam, A., Goetz, L. L., Lester, D. & Lavis, T. D. A case study of percutaneous epidural stimulation to enable motor control in two men after spinal cord injury. *Nat. Commun.* **14**, 2064 (2023).

142. Greiner, N., Barra, B., Schiavone, G., Lorach, H., James, N., Conti, S., Kaeser, M., Fallegger, F., Borgognon, S., Lacour, S., Bloch, J., Courtine, G. & Capogrosso, M. Recruitment of upper-limb motoneurons with epidural electrical stimulation of the cervical spinal cord. *Nat. Commun.* **12**, 435 (2021).

143. Hofstoetter, U. S., Perret, I., Bayart, A., Lackner, P., Binder, H., Freundl, B. & Minassian, K. Spinal motor mapping by epidural stimulation of lumbosacral posterior roots in humans. *iScience* **24**, 101930 (2021).

144. Sherwood, A. M., Dimitrijevic, M. R. & McKay, W. B. Evidence of subclinical brain influence in clinically complete spinal cord injury: discomplete SCI. *J. Neurol. Sci.* **110**, 90–98 (1992).

145. Filli, L. & Schwab, M. E. Structural and functional reorganization of propriospinal connections promotes functional recovery after spinal cord injury. *Neural Regen. Res.* **10**, 509–513 (2015).

146. Eisdorfer, J. T., Smit, R. D., Keefe, K. M., Lemay, M. A., Smith, G. M. & Spence, A. J. Epidural Electrical Stimulation: A Review of Plasticity Mechanisms That Are Hypothesized to Underlie Enhanced Recovery From Spinal Cord Injury With Stimulation. *Front. Mol. Neurosci.* **13**, 163 (2020).

147. Linderoth, B., Stiller, C. O., Gunasekera, L., O'Connor, W. T., Ungerstedt, U. & Brodin, E. Gamma-aminobutyric acid is released in the dorsal horn by electrical spinal cord stimulation: an in vivo microdialysis study in the rat. *Neurosurgery* **34**, 484–488; discussion 488-489 (1994).

148. Linderoth, B., Gazelius, B., Franck, J. & Brodin, E. Dorsal column stimulation induces release of serotonin and substance P in the cat dorsal horn. *Neurosurgery* **31**, 289–296; discussion 296-297 (1992).

149. Song, Z., Ultenius, C., Meyerson, B. A. & Linderoth, B. Pain relief by spinal cord stimulation involves serotonergic mechanisms: an experimental study in a rat model of mononeuropathy. *Pain* **147**, 241–248 (2009).

150. Rossignol, S., Giroux, N., Chau, C., Marcoux, J., Brustein, E. & Reader, T. A. Pharmacological aids to locomotor training after spinal injury in the cat. *J. Physiol.* **533**, 65–74 (2001).

151. Bobet, J., Masani, K., Popovic, M. R. & Vette, A. H. Kinematics-based prediction of trunk muscle activity in response to multi-directional perturbations during sitting. *Med. Eng. Phys.* **58**, 56–63 (2018).

152. Roberts, B. W. R., Gholibeigian, F., Lewicke, J. & Vette, A. H. Spatial and temporal relation of kinematics and muscle activity during unstable sitting. *J. Electromyogr. Kinesiol.* **52**, (2020).

153. *Trigno Wireless Biofeedback System User's Guide*. 1–39 (2021).

154. Formento, E., Minassian, K., Wagner, F., Mignardot, J. B., Le Goff-Mignardot, C. G., Rowald, A., Bloch, J., Micera, S., Capogrosso, M. & Courtine, G. Electrical spinal cord stimulation must preserve proprioception to enable locomotion in humans with spinal cord injury. *Nat. Neurosci.* **21**, 1728–1741 (2018).

155. Wagner, F. B., Mignardot, J.-B., Le Goff-Mignardot, C. G., Demesmaeker, R., Komi, S., Capogrosso, M., Rowald, A., Seáñez, I., Caban, M., Pirondini, E., Vat, M., McCracken, L. A., Heimgartner, R., Fodor, I., Watrin, A., Seguin, P., Paoles, E., Van Den Keybus, K., Eberle, G., Schurch, B., Pralong, E., Becce, F., Prior, J., Buse, N., Buschman, R., Neufeld, E., Kuster, N., Carda, S., von Zitzewitz, J., Delattre, V., Denison, T., Lambert, H., Minassian, K., Bloch, J. & Courtine, G. Targeted neurotechnology restores walking in humans with spinal cord injury. *Nature* **563**, 65–71 (2018).

156. Hashimoto, S., Murohashi, T., Yamada, S., Iesato, N., Ogon, I., Chiba, M., Tsukamoto, A., Hitrota, R. & Yoshimoto, M. Broad and asymmetric lower extremity myotomes: Results

from intraoperative direct electrical stimulation of the lumbosacral spinal roots. *Spine* **49**, 805–810 (2024).

157. Fortin, M., Yan Yuan & Battie, M. C. Factors associated with paraspinal muscle asymmetry in size and composition in a general population sample of men. *Phys. Ther.* **93**, 1540–1550 (2013).

158. Shen, J., Wang, H.-Y., Chen, J.-Y. & Liang, B.-L. Morphologic analysis of normal human lumbar dorsal root ganglion by 3D MR imaging. *Am. J. Neuroradiol.* **27**, 2098–2103 (2006).

159. Chon, J., Kim, H.-S., Lee, J. H., Yoo, S. D., Yun, D. H., Kim, D. H., Lee, S. A., Han, Y. J., Lee, H. S., Han, Y. R., Han, S. & Kim, Y. Asymmetric atrophy of paraspinal muscles in patients with chronic unilateral lumbar radiculopathy. *Ann. Rehabil. Med.* **41**, 801–807 (2017).

160. Coburn, B. A theoretical study of epidural electrical stimulation of the spinal cord - Part II: Effects on long myelinated fibers. *IEEE Trans. Biomed. Eng.* **32**, 978–986 (1985).

161. Struijk, J. J., Holsheimer, J. & Boom, H. B. K. Excitation of dorsal root fibers in spinal cord stimulation: a theoretical study. *IEEE Trans. Biomed. Eng.* **40**, 632–639 (1993).

162. Holsheimer, J. Which Neuronal Elements are Activated Directly by Spinal Cord Stimulation. *Neuromodulation Technol. Neural Interface* **5**, 25–31 (2002).

163. Barolat, G. Epidural spinal cord stimulation: anatomical and electrical properties of the intraspinal structures relevant to spinal cord stimulation and clinical correlations. *Neuromodulation Technol. Neural Interface* **1**, 63–71 (1998).

164. Cadotte, D. W., Cadotte, A., Cohen-Adad, J., Fleet, D., Livne, M., Wilson, J. R., Mikulis, D., Nugaeva, N. & Fehlings, M. G. Characterizing the Location of Spinal and Vertebral Levels in the Human Cervical Spinal Cord. *Am. J. Neuroradiol.* **36**, 803–810 (2015).

165. Cuellar, C. A., Mendez, A. A., Islam, R., Calvert, J. S., Grahn, P. J., Knudsen, B., Pham, T., Lee, K. H. & Lavrov, I. A. The role of functional neuroanatomy of the lumbar spinal cord in effect of epidural stimulation. *Front. Neuroanat.* **11**, 82 (2017).

166. Livingston, S. C., Friedlander, D. L., Gibson, B. C. & Melvin, J. R. Motor Evoked Potential Response Latencies Demonstrate Moderate Correlations with Height and Limb Length in Healthy Young Adults. *Neurodiagnostic J.* **53**, 63–78 (2013).

167. Mynark, R. G. & Koceja, D. M. Effects of age on the spinal stretch reflex. *J. Appl. Biomech.* **17**, 188–203 (2001).

168. Beith, I. D. & Harrison, P. J. Stretch reflexes in human abdominal muscles. *Exp. Brain Res.* **159**, 206–213 (2004).

169. Myriknas, S. E., Beith, I. D. & Harrison, P. J. Stretch Reflexes in the Rectus Abdominis Muscle in Man. *Exp. Physiol.* **85**, 445–450 (2000).

170. Gerasimenko, Y. P., Lavrov, I. A., Courtine, G., Ichiyama, R. M., Dy, C. J., Zhong, H., Roy, R. R. & Edgerton, V. R. Spinal cord reflexes induced by epidural spinal cord stimulation in normal awake rats. *J. Neurosci. Methods* **157**, 253–263 (2006).

171. Lavrov, I., Gerasimenko, Y. P., Ichiyama, R. M., Courtine, G., Zhong, H., Roy, R. R. & Edgerton, V. R. Plasticity of Spinal Cord Reflexes After a Complete Transection in Adult Rats: Relationship to Stepping Ability. *J. Neurophysiol.* **96**, 1699–1710 (2006).

172. Minassian, K., Freundl, B. & Hofstoetter, U. S. Chapter 18 - The posterior root-muscle reflex. in *Neurophysiology in Neurosurgery (Second Edition)* (eds. Deletis, V., Shils, J. L., Sala, F. & Seidel, K.) 239–253 (Academic Press, 2020).

173. Lavrov, I., Dy, C. J., Fong, A. J., Gerasimenko, Y., Courtine, G., Zhong, H., Roy, R. R. & Edgerton, V. R. Epidural Stimulation Induced Modulation of Spinal Locomotor Networks in Adult Spinal Rats. *J. Neurosci.* **28**, 6022–6029 (2008).

174. Amrutha, N. & Arul, V. H. A review on noises in EMG signal and its removal. *Int. J. Sci. Res. Publ.* **7**, 23–27 (2017).

Appendices

Appendix A: Muscle and EMG Exclusions

Muscles were excluded from data analysis when the electrode was presumed to have fallen off or to have captured a movement artifact during the experimental session. An electrode that had fallen off during data collection was identified by regular oscillations in the EMG data. A motion artifact was presumed when a low-frequency response, ranging from 1 to 10 Hz[174], was detected with onset and duration that differed from a typical response. A summary of all muscle exclusions is included in Table B-1. A comparison of a typical RRA response to (1) when an electrode had fallen off and (2) a presumed motion artifact was present is shown below in Fig. A-1 and Fig. A-2, respectively.

Table A-1. Muscle exclusions: RRA = right rectus abdominis; LRA = left rectus abdominis; REO = right external oblique; RIO = right internal oblique; LEO = left external oblique; EST7 = erector spinae at T6/T7 vertebra level; and ESL3 = erector spinae at L2/L3 vertebra level.

Participant ID	Muscle(s)	Justification for Exclusion
P9	RRA	Electrode fell off
P10	LRA	Electrode fell off
P11	RRA	Movement artifact
P13	REO	Electrode fell off
P14	RIO	Movement artifact
P15	RRA, RIO	Movement artifact
P16	LEO EST7, ESL3	Electrode fell off; noise
P22	LRA, RRA	Movement artifact

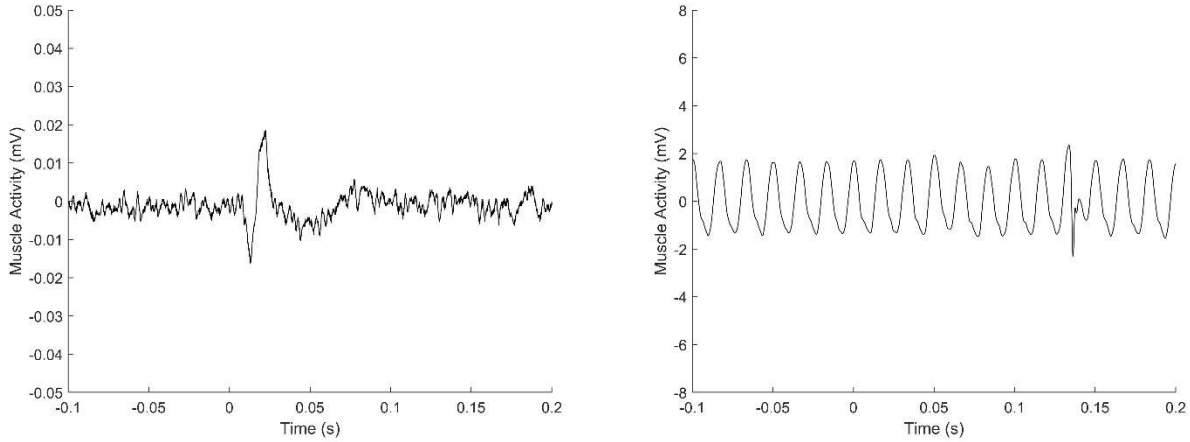

Figure A-1. A typical RRA response from P14 (left) compared to the EMG signal when the electrode fell off during experimental data collection from P9 (right). The removed electrode exhibits repeated oscillations.

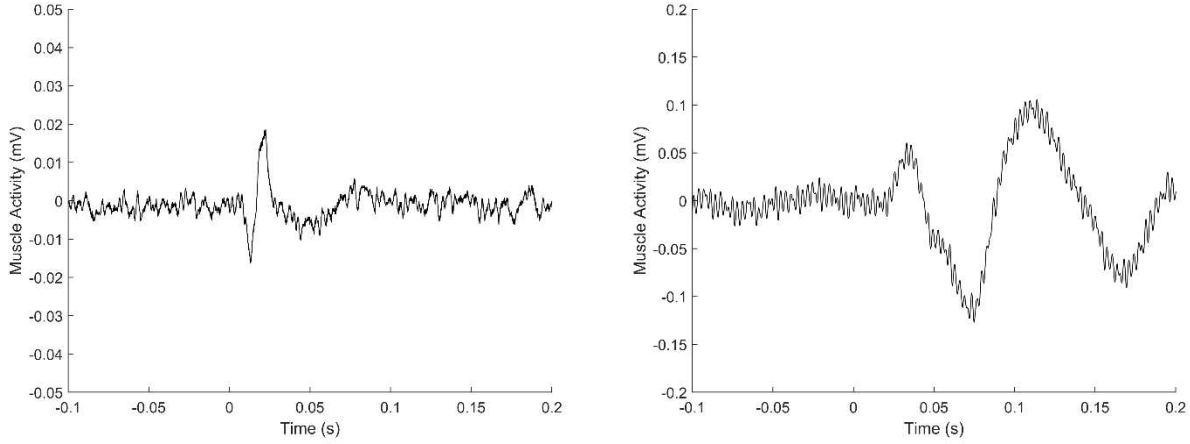

Figure A-2. A typical RRA response from P14 (left) compared to the EMG signal when a movement artifact is present in P11 (right). The movement artifact exhibits a lower frequency, ranging from 1 to 10 Hz, and atypical response amplitude and timing.

Appendix B: Onset and Duration Analysis

The three steps involved in the custom-made MATLAB algorithm for characterizing the timing of a muscle response are presented below. Applying these steps allows us to identify the time of onset and end of the muscle response. The duration of the response is then calculated as the difference between the end and onset of the response. The algorithm required manual adjustment for 15% of onset values and 22% of end values, based on visual inspections.

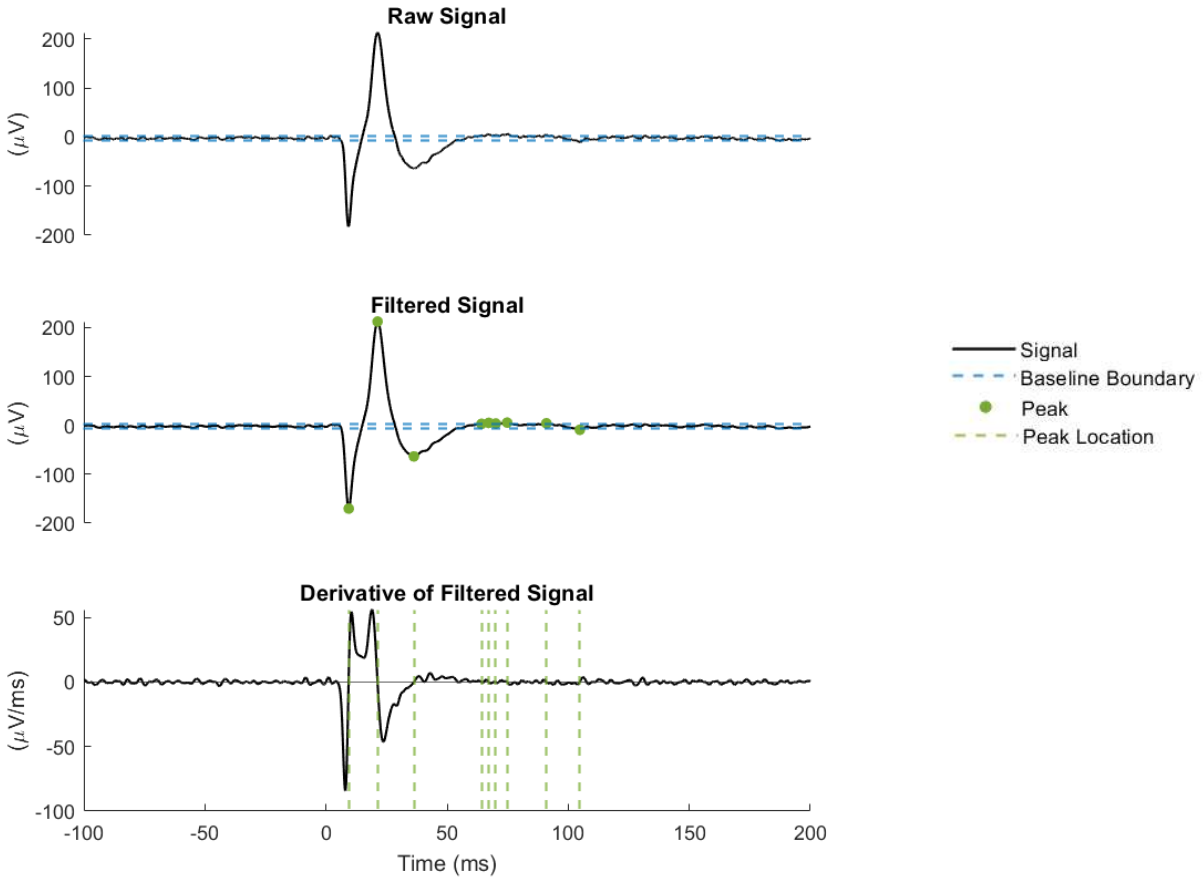

Figure B-1. Step 1: The raw signal is low-pass filtered using a fourth order, zero-phase Butterworth filter with a cut-off frequency of 300 Hz. A low-pass filter was selected to attenuate high frequency noise and obtain the overall profile of the muscle response. The derivative of the filtered data is calculated. Peaks within the filtered signal greater than the baseline band (baseline $\pm$ three times the standard deviation) are identified (green dots and lines). Baseline was calculated from the first 70 ms of the trial.

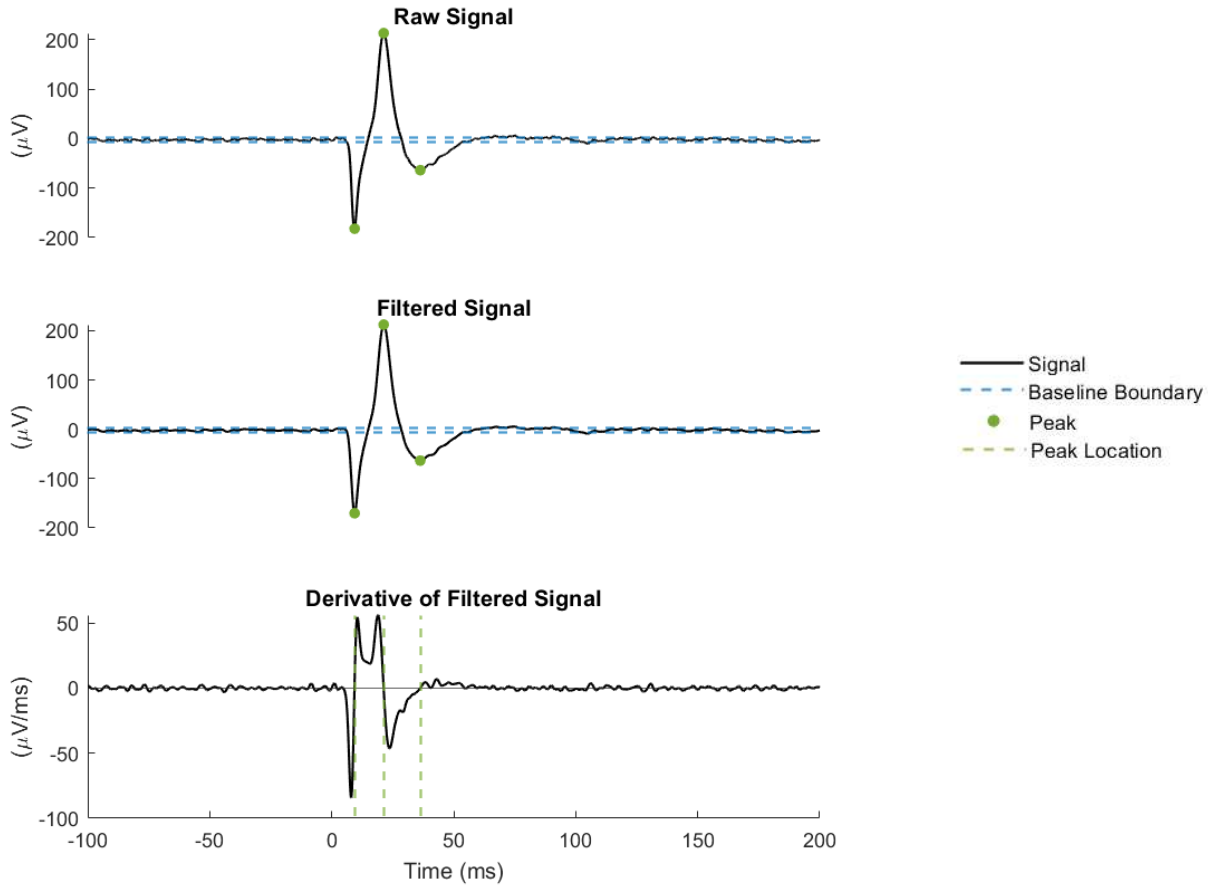

Figure B-2. Step 2: Peaks that were not part of the main response profile were removed. Beginning with the first peak, if the response derivative changed signs within the interval between the first and the second peak, the first peak was removed and the second peak became the first peak. The sign change occurring between peaks suggested that the signal is more likely random fluctuations, noise, or residual signal in tissue and therefore not part of the main response. This process was repeated until the derivative did not change signs in the interval between the first and second peak. A similar algorithm was used to determine the last peak of the main response. Starting with the last peak, if the response derivative changed signs within the interval between the last and second last peak, the last peak was removed and the second last peak became the last peak. This process was repeated until the derivative did not change signs in the interval between the last and second last peak.

Note on Step 2: Step 2 was deemed unsuccessful for trials where the incorrect number of peaks was removed. In some cases, noise in the data resulted in derivative zero crossings within the main response. In that case, peaks that were visually part of the main response were removed. In some cases, the derivative did not cross zero even when the response was no longer part of the main response. In that case, peaks that were visually not part of the main response were not removed. In such situations, the results were manually corrected.

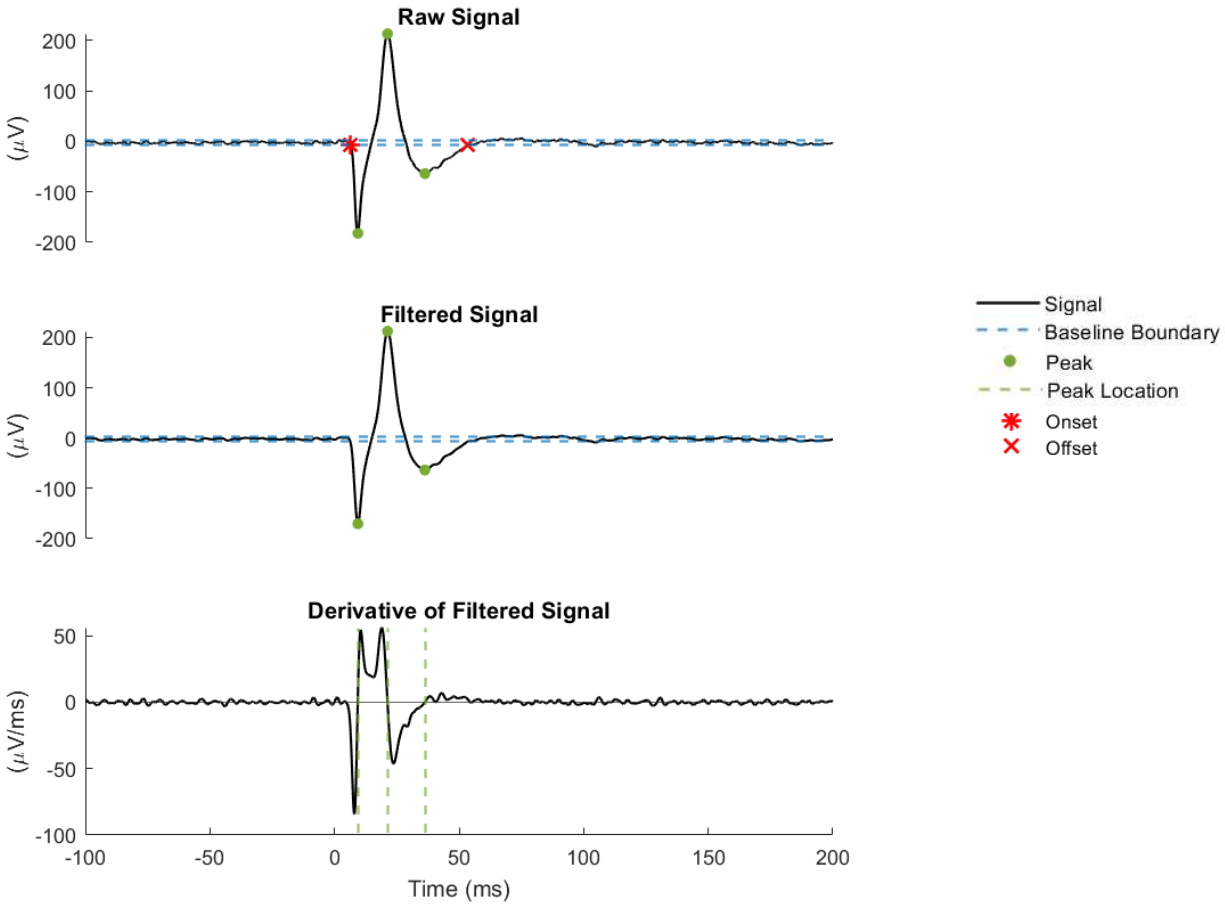

Figure B-3. Step 3: The onset of the response is identified as the last time the unfiltered signal crosses (leaves) the baseline band (baseline ± three times the standard deviation) prior to the first peak[26]. The end of the response was calculated as the first time the unfiltered response crosses (returns) into the baseline band (baseline ± three times the standard deviation) after the last peak. Response duration is the time difference between the end and onset of the response.

Note on Step 3: Step 3 was deemed unsuccessful when the incorrect response onset or end was identified. This would occur when noise allowed the signal to exit or enter the baseline band briefly, prior to when the main response profile visually exits or enters. In such situations, the results were manually corrected.

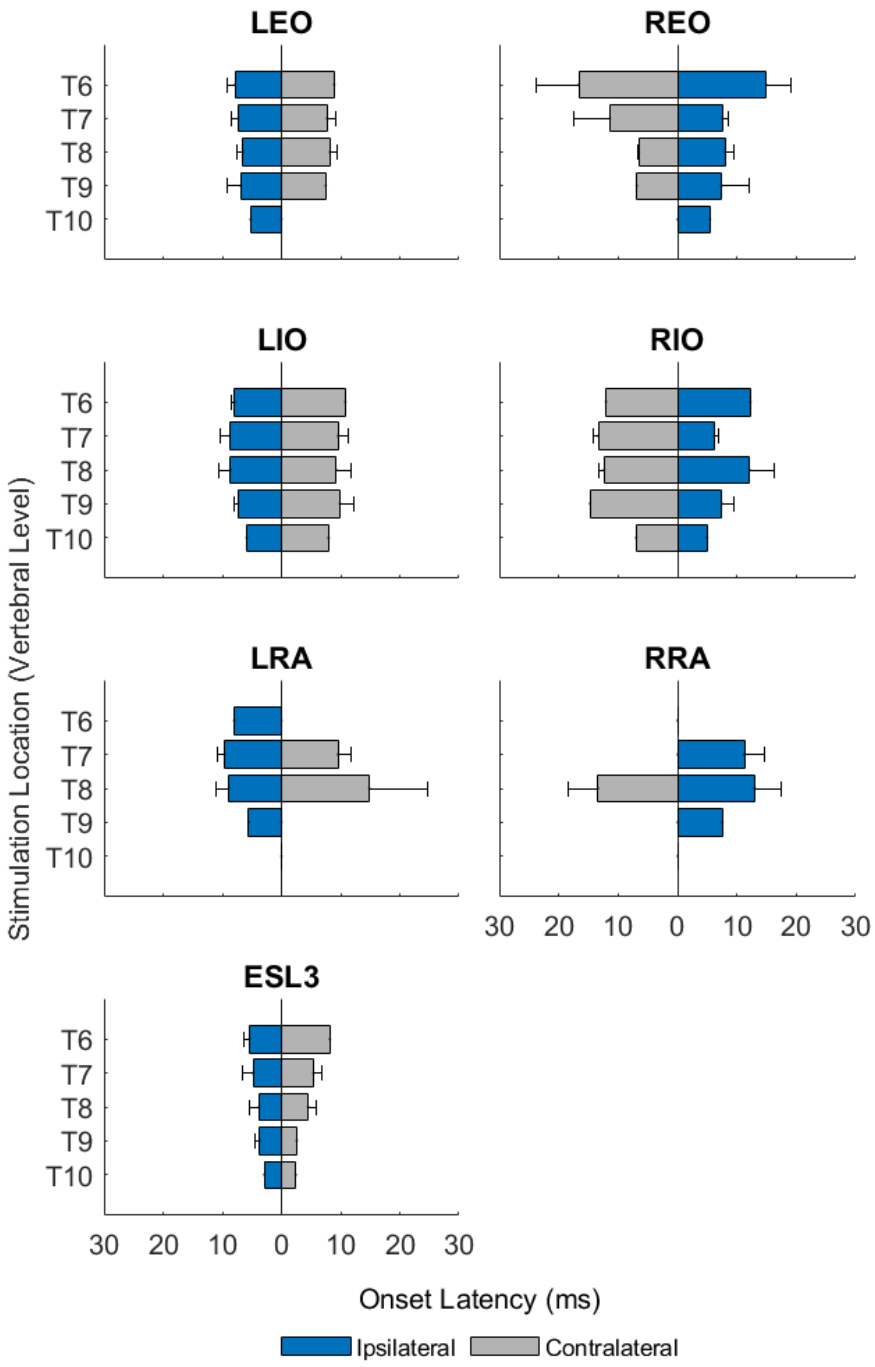

Figure B-4. Onset latency at maximum stimulation amplitude for each stimulation location along the rostrocaudal axis of the spine (vertebral levels T6 to T10) and along the mediolateral axis of the spine (left and right side of the electrode array, represented accordingly as ipsilateral and contralateral). Onset latency was calculated using a custom-made MATLAB script. Onset latency values at each stimulation location were averaged across participants (mean + one standard deviation). Non-responsive muscles were omitted.

Appendix C: Representative Evoked Potentials

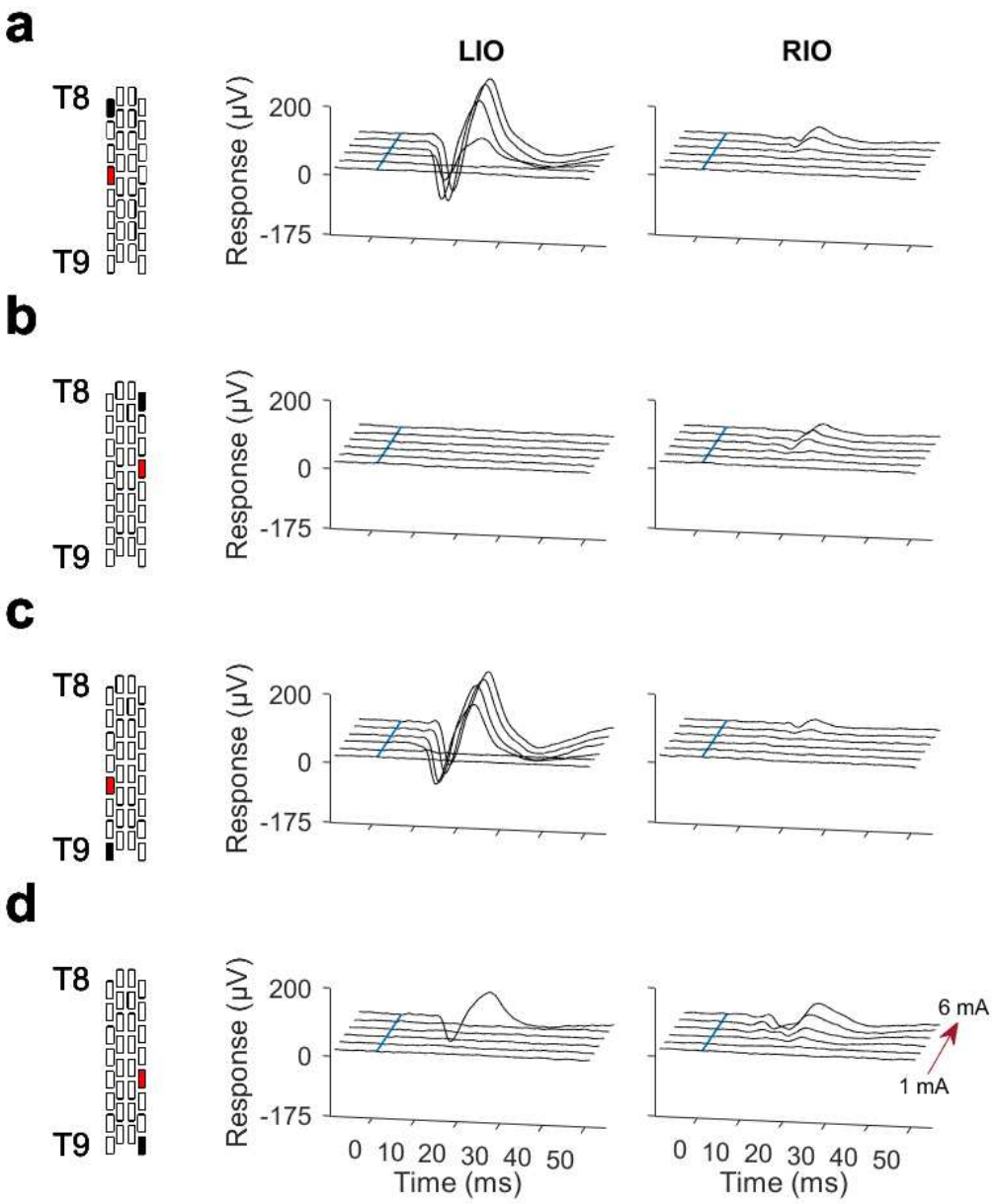

Figure C-1. Representative evoked responses from one participant (P21) for the left and right internal oblique (LIO and RIO), with electrode placement above the T8 and T9 vertebrae. The stimulating cathode is represented in black, and the anode in red. Waveforms, averaged across three trials, are depicted for increasing stimulation amplitudes (1 to 6 mA in 1 mA increments, represented by the red arrow) and when delivering stimulation above: (a) the left T8 vertebra, (b) the right T8 vertebra, (c) the left T9 vertebra, and (d) the right T9 vertebra. Stimulation occurs at zero milliseconds, represented by the blue line.

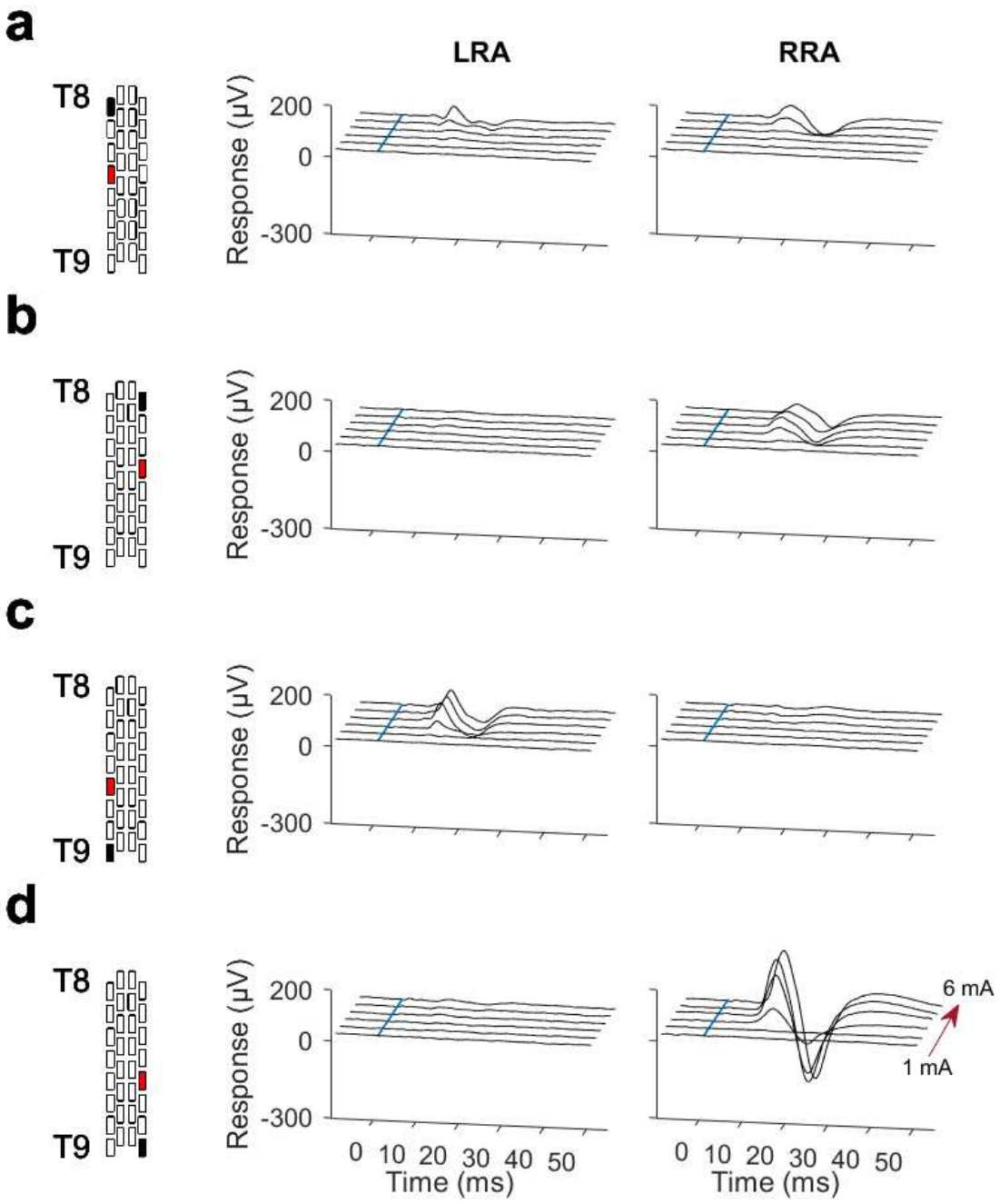

Figure C-2. Representative evoked responses from one participant (P21) for the left and right rectus abdominis (LRA and RRA), with electrode placement above the T8 and T9 vertebrae. The stimulating cathode is represented in black, and the anode in red. Waveforms, averaged across three trials, are depicted for increasing stimulation amplitudes (1 to 6 mA in 1 mA increments, represented by the red arrow) and when delivering stimulation above: (a) the left T8 vertebra, (b) the right T8 vertebra, (c) the left T9 vertebra, and (d) the right T9 vertebra. Stimulation occurs at zero milliseconds, represented by the blue line.

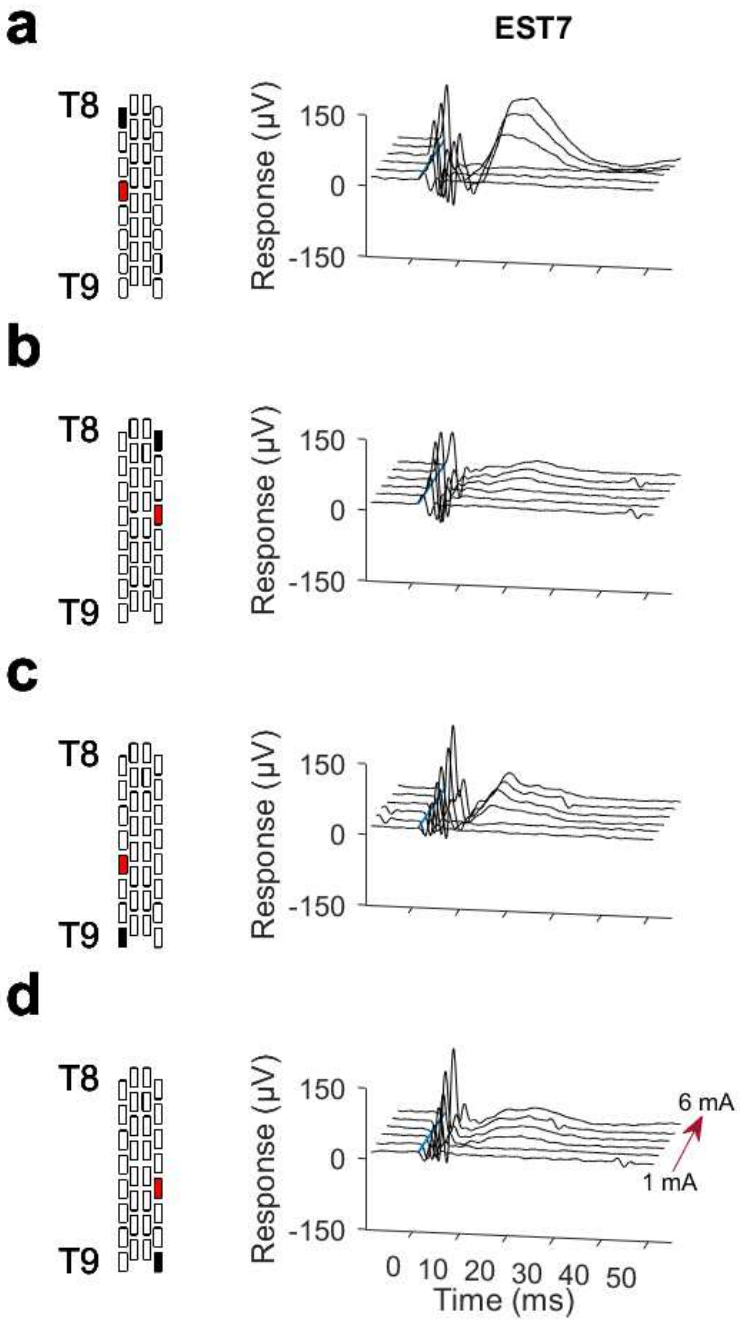

Figure C-3. Representative evoked responses from one participant (P21) for the left erector spinae at the T7 vertebra level (EST7), with electrode placement above the T8 and T9 vertebrae. The stimulating cathode is represented in black, and the anode in red. Waveforms, averaged across three trials, are depicted for increasing stimulation amplitudes (1 to 6 mA in 1 mA increments, represented by the red arrow) and when delivering stimulation above: (a) the left T8 vertebra, (b) the right T8 vertebra, (c) the left T9 vertebra, and (d) the right T9 vertebra. Stimulation occurs at zero milliseconds, represented by the blue line.

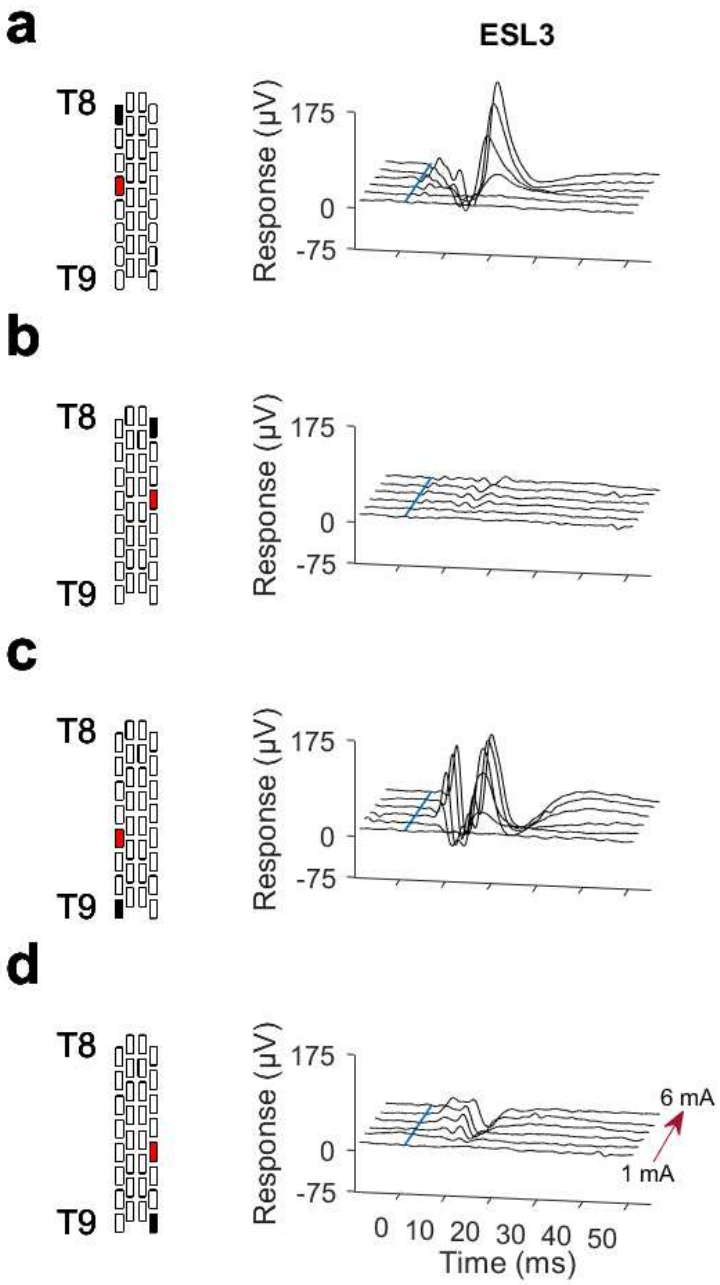

Figure C-4. Representative evoked responses from one participant (P21) for the left erector spinae at the L3 vertebra level (ESL3), with electrode placement above the T8 and T9 vertebrae. The stimulating cathode is represented in black, and the anode in red. Waveforms, averaged across three trials, are depicted for increasing stimulation amplitudes (1 to 6 mA in 1 mA increments, represented by the red arrow) and when delivering stimulation above: (a) the left T8 vertebra, (b) the right T8 vertebra, (c) the left T9 vertebra, and (d) the right T9 vertebra. Stimulation occurs at zero milliseconds, represented by the blue line.

Appendix D: Recruitment Curves

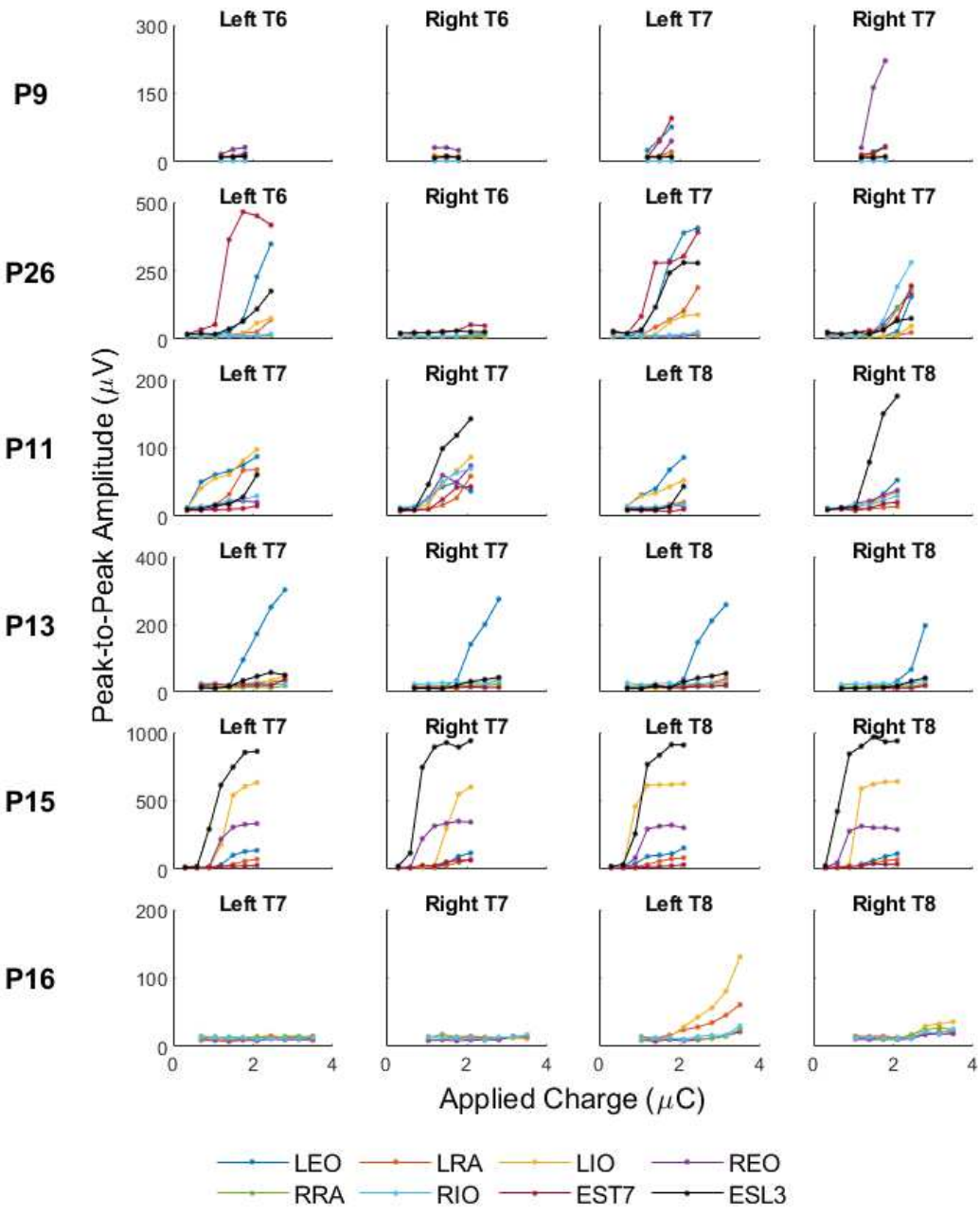

Figure D-1. Representative recruitment curves of muscle responses during stimulation above the T6 and T7 (P9 and P26), and T7 and T8 (P11, P13, P15, and P16) vertebrae. Peak-to-peak amplitudes of the left and right external obliques (LEO and REO), internal obliques (LIO and RIO), rectus abdominis (LRA and RRA), and erector spinae at the T7 and L3 vertebral levels (EST7 and ESL3) are shown in dependence of applied charge. Peak-to-peak amplitude values were averaged across three trials.

Appendix E: Onset Latency Analysis for P22

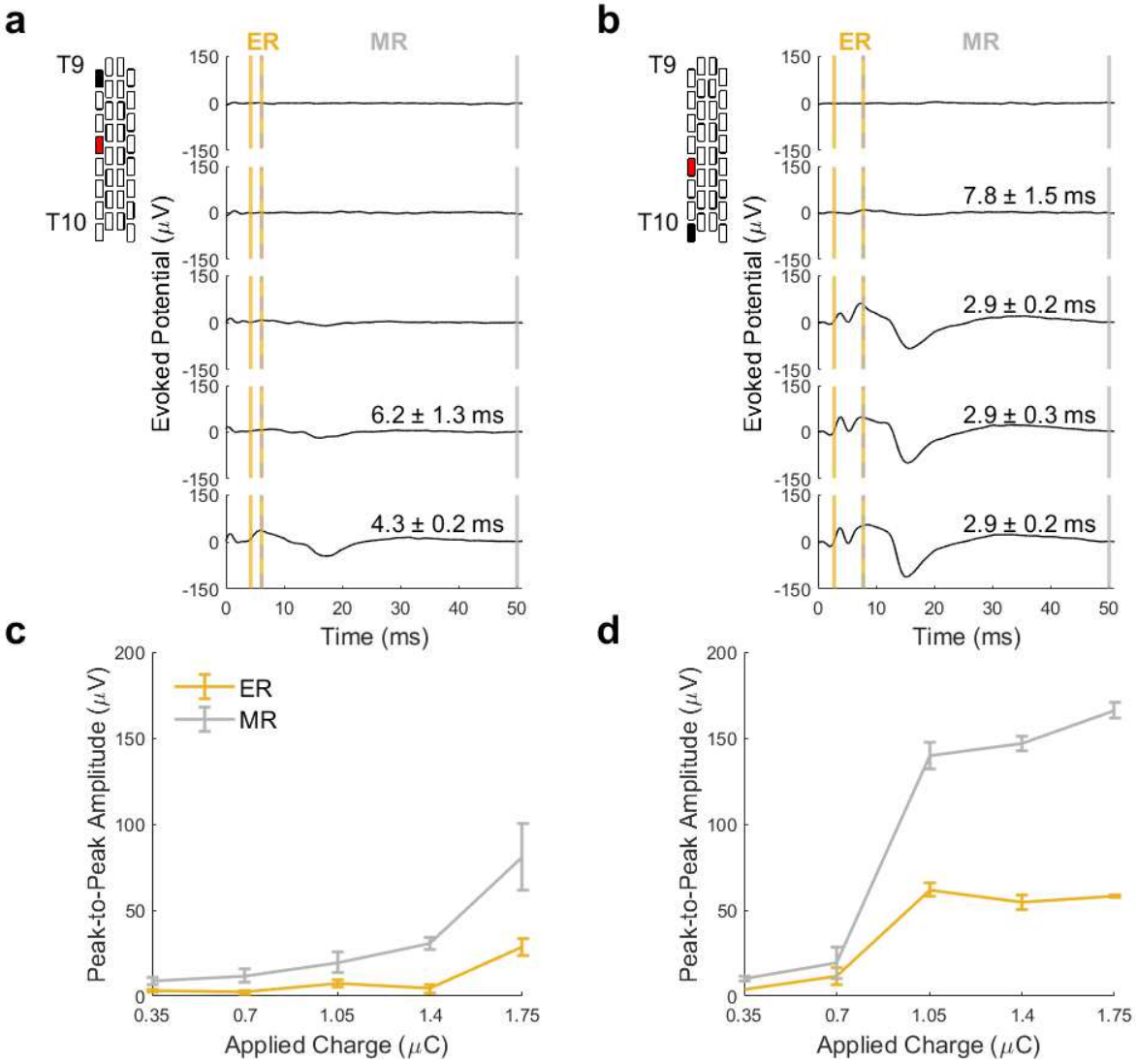

Figure E-1. Onset latency analysis for responses recorded in the ESL3 muscle for P22. Evoked responses with increasing applied charge are shown from ipsilateral stimulation above: (a) the left T9 vertebra, and (v) the left T10 vertebra. Onset latency averaged across three trials (mean ± one standard deviation stated on each waveform) decreased at higher applied charge. The start of the early latency response (ER; vertical solid yellow line) is identified as the onset latency at the highest applied charge for a given electrode configuration. The start of the medium response (MR; vertical dashed yellow and grey line) is identified as the onset latency at the lowest applied charge that evoked a response. The end of MR (vertical solid grey line) is 50 ms. In (c) and (d), the peak-to-peak amplitudes of the ER and MR components are compared when increasing applied charge. All waveforms and outputted metrics were averaged across three trials.